Imperial College London

Molecular determinants of IBDV pathogenesis and modulation of the host innate response

Department of Virology

Faculty of Medicine

Katherine Louise Dulwich

30th September 2019

Supervised by Dr Andrew Broadbent and Dr Mark Fife

(The Pirbright Institute)

Dr Mike Skinner

(Imperial College London)

Submitted for the degree of Doctor of Philosophy

Declaration of Originality

I declare the work presented in this thesis is my own, unless otherwise stated or referenced. This includes data that was generated by other sources.

Katherine Dulwich

Copyright Declaration

Abstract

Viruses are known to interact with the innate immune pathways and, in some cases, strains that differ in virulence are known to interact with these pathways in different ways. This thesis aimed to directly compare IBDV strains of differing virulence to determine key interactions with the innate immune response that may contribute to disease outcome.

Infection of chicken B cells with the very virulent s UK661 strain, suppressed type I IFN responses compared to both infection with the cell-adapted IBDV strain, D78 in primary bursal cells, and infection with the classical strain, F52/70 in DT40 cells. Birds infected with UK661 also had down-regulated type I IFN and pro-inflammatory responses in the bursa of Fabricius (BF), compared to infection with F52/70. No difference in the peak virus titres was detected in the BF or spleen, although UK661 reached higher titres in the caecal tonsils than F52/70. Increased type I IFN production following F52/70 infection coincided with a reduced mortality in these birds, indicating a protective role of this immune response. The UK661 VP4 protein was found to suppress IFNβ production *in vitro* compared to the F52/70 VP4, which instead suppressed Mx1 production, indicating that the IBDV VP4 from different strains impairs either IFN production or signalling pathways. Upon knocking out the protease function of UK661 VP4, IFNβ production remained suppressed, and multiple amino acids are likely responsible for the different phenotype between strains. This work demonstrates that UK661 and F52/70 have strain-specific differences in their interactions with the innate immune response, mediated by the VP4 protein, therefore differences in this protein between strains may contribute to virulence. This information could be useful in the development of recombinant rationally designed live attenuated IBDV vaccines, by generating a vvIBDV backbone containing a VP4 from a classical or cell-adapted strain, as a vaccine candidate.

Acknowledgements

I would like to thank my supervisors, Andrew, Mike and Mark, for all their support over the past four years. For their helpful advice and practical guidance, I will always be grateful. I want to thank all the people I have worked alongside in the lab who have offered advice, support and assistance with experiments and made me smile. Stathis Giotis, Sarah Keep, Nicole Doyle, Helena Maier and Pip Beard have been particularly patient and supportive, offering endless motivational speeches.

I would like to thank and acknowledge the support services, including the animal services and cell culture technicians, who have made the data presented in this thesis possible. Also, to thank The Pirbright Institute and BBSRC for funding my studentship, in addition to Imperial College London, The Houghton Trust and The Microbiology Society for travel grants and opportunities to network and present my work at conferences.

Last, but by no means least, I would like to thank my family, friends and partner Chris, who have provided support in so many ways in the last four years. Without this support, I have no doubt this thesis would not be in existence. Thank you for not letting me give up on myself and reminding me of the curious little girl who always loved science.

I would like to dedicate this thesis to the family members that started this journey with me and have been unable to finish it.

"For every person that believed I couldn't; for every person that knew I could"

Contents

List of Figures

List of Tables

Abbreviations

aa	Amino acid(s)
AIV	Avian influenza virus
ALV	Avian Leukosis Virus
AP-1	Activator protein-1
ATF2	Activating transcription factor 2
AWERB	Animal Welfare and Ethic Review Board
B	Base
BAFF	B cell activating factor
BF	Bursa of Fabricius
BGI	Bejing Genomics Institute
BMDC	Bone marrow-derived dendritic cell
BME	Beta-mercaptoethanol
BSA	Bovine serum albumin
BW	Body weight
caIBDV	Cell culture-adapted IBDV
CAM	Chorioallantoic membrane
CARD	Caspase activation and recruitment domains
CCL4	Chemokine (C-C motif) ligand 4
CCL5	Chemokine (C-C motif) ligand 5
CD72	Cluster of differentiation 72
CDC42	Cell division cycle protein 42
cDNA	Complimentary DNA
CEF	Chicken embryo fibroblast
chCD40L	Chicken CD40L
cIBDV	Classical IBDV
CypA	Cyclophilin A

d.p.i	Days post-infection or days post-inoculation
DAPI	4',6-Diamidino-2-Phenylindole, Dihydrochloride
DeV	Dengue virus
DF-1	Douglas Foster-1 cell
DHAV-1	Duck hepatitis A virus type 1
DMEM	Dulbecco's Modified Eagle's Medium
DNA	Deoxyribonucleic acid
dNTPs	Deoxynucleotide triphosphate
ds	Double stranded
dsRNA	Double stranded RNA
ECMV	Encephalomyocarditis virus
EDTA	Ethylenediaminetetraacetic acid
eGFP	Enhanced green fluorescent protein
ELISA	Enzyme-linked immunosorbent assay
FACS	Fluorescence-activated cell sorting
FBS	Fetal bovine serum
FDR	False discovery rate
GAF	Gamma IFN activation factor
GAS	Gamma IFN activation site
GILZ	Glucocorticoid-induced leucine zipper
GO	Gene ontology
GRAP	Grb2-related adapter protein
GRE	Glucocorticoid response element
GRIP-1	Glucocorticoid receptor interacting protein-1
GSN	Gelsolin
h.p.i	Hours post-infection or hours post-inoculation
h.p.t	Hours post-transfection
HBSS	Hanks Balanced Salt Solution
HEV	Hepatitis E virus
HIV-1	Human immunodeficiency virus 1
HP1a	Heterochromatin protein 1a

hr	Hour
HSP70	Heat shock protein 70
HSP90	Heat shock protein 90
HSV-1	Herpes Simplex Virus-1
HVR	Hypervariable region
HVT	Herpesvirus of turkeys
IBD	Infectious bursal disease
IBDV	Infectious bursal disease virus
IFIT5	IFN-induced protein with tetratricopeptide repeats 5
IFITM	IFN-induced transmembrane protein
IFN	Interferon
IgM	Immunoglobulin M
IKK	Inhibitor of nuclear factor kappa-B kinase
IL	Interleukin
IL-1R1	Interleukin 1 receptor type 1
IMDM	Iscove's Modified Dulbecco's Medium
iNOS	Nitric oxide synthase
IPNV	Infectious pancreatic necrosis virus
IRAK	Interleukin-1 receptor-associated kinases
IRF	IFN regulatory factor
ISG	IFN-stimulated gene
ISGF3	IFN-stimulated gene factor 3
ISRE	IFN-stimulated response element
ITIM	Immunoreceptor tyrosine-based inhibitory motif
JAK	Janus Kinase
Kb	Kilo base
Kbp	Kilo base pairs
kDA	Kilo Dalton
KLD	Kinase-Ligase-DpnI
LB	Lysogeny broth
LGP2	Laboratory of genetics and physiology 2

LPS	Lipopolysaccharide
MAb	Maternal antibodies
MAPK	Mitogen-activated protein kinase
MAVS	Mitochondrial antiviral-signalling protein
MDA5	Melanoma differentiation-associated protein 5
MDV	Marek's disease virus
MERS	Middle East respiratory syndrome virus
mins	Minutes
MOI	Multiplicity of infection
Mx1	IFN-induced GTP-binding protein
MyD88	Myeloid differentiation primary response 88
NDV	Newcastle's disease virus
NEMO	NF-κB essential modulator
NF-κB	Nuclear factor kappa B
NLR	Nod-like receptor
OAS	2'-5'-oligoadenylate synthetase 1
OASL	2'-5'-Oligoadenylate Synthetase Like protein
OCT	Optical coherence tomography
ORAOV1	Oral cancer overexpressed 1
ORF	Open reading frame
P	Projection
PAMP	Pattern-associated molecular pattern
PBS	Phosphate-buffered saline
PCA	Principal component analysis
PCR	Polymerase chain reaction
PEDV	Porcine Epidemic Diarrhoea Virus
pH	Potential hydrogen
pKO	Protease knock-out
PKR	Protein Kinase R
PMA	Phorbol 12-myristate 13-acetate
poly I:C	Polyinosinic: polycytidylic acid

PRD	Positive regulatory domain
preVP2	Precursor VP2
PRR	Pattern recognition receptor
PurSA	puromycin-sensitive aminopeptidase
qPCR	Quantitative PCR
RACK1	Receptor of activated protein kinase C1
RdRp	RNA dependent RNA polymerase
RIG-I	Retinoic acid-inducible gene-I
RIP1	Receptor interacting protein 1
RNA	Ribonucleic acid
RNP	Ribonucleoprotein
RPLPO	60S acidic ribosomal protein P0
RPMI-1640	Roswell Park Memorial Institute
RSAD2	Radical S-adenosyl methionine domain containing 2 or Viperin
S	Shell
secs	Seconds
SeV	Sendai Virus
SMAD3	Mothers against decapentaplegic homologue 3
SOC	Super optimal broth with catabolite repression
SOCS	Suppressor of cytokine signalling
SPF	Specific pathogen free
Ss	Single stranded
STAT	Signal transducer and activator of transcription proteins
STAU1	Staufen 1
STING	Stimulator of IFN genes
TAK1	TGF-β activated kinase 1
TANK	TRAF family member-associated NF-κB activator
TBE	Tris-borate EDTA
TBK1	TANK binding kinase-1
TBP	TATA box binding protein
$TCID_{50}$	Tissue Culture Infectious Dose 50%

TGF	Transforming growth factor
TLR	Toll-like receptor
TNFR	Tumour necrosis factor (TNF) receptor
TNFR	Tumour necrosis factor (TNF) receptor
TNFα	Tumour necrosis factor α
TPI	The Pirbright Institute
TRAF	TNF receptor-associated factor
TRAM	Translocation associated membrane protein 1
TRIF	TIR-domain-containing adapter-inducing IFNβ
TYK2	Tyrosine kinase 2
VDAC2	Voltage-dependent anion channel 2
vIBDV	Variant IBDV
VN	Virus neutralising or virus neutralisation
VP	Viral protein
vvIBDV	Very virulent IBDV
WNV	West Nile Fever virus
wt	Wild type
YAV	Yellowtail Ascites Virus
ZiV	Zika virus

1. Introduction

1.1 Birnaviruses

The *Birnavirus* family is comprised of bi-segmented, non-enveloped viruses that form icosahedral virions (Delmas *et al.* 2019). The capsid follows a T=13 *laevo* icosahedral geometry which is comprised of a single viral protein (VP), VP2, clustering in trimers (Coulibaly *et al.* 2005). Birnaviruses have a double stranded (ds) ribonucleic acid (RNA) genome that is made up of two segments, termed A and B. Segment A is 3.1-3.6 Kilo base pairs (Kbp) in length and encodes the polyprotein, preVP2-VP4-VP3, and a small open reading frame (ORF), encoding VP5, overlapping the polyprotein. Segment B is 2.8-3.3 Kbp in length and encodes the RNA-dependent RNA polymerase (RdRp), VP1 (Luque *et al* 2009a). The *Birnavirus* family has a broad host range spanning birds (*Avibirnavirus*), fish (*Aquabirnavirus* and *Blosnavirus*) and insects (*Entomobirnavirus*) (Delmas *et al.* 2019). The most extensively studied and economically important birnaviruses are Infectious Pancreatic Necrosis Virus (IPNV), which infects fish and is considered the most serious viral disease of farmed Atlantic salmon in the EU (Ariel and Olesen, 2002), and Infectious Bursal Disease Virus (IBDV), which infects chickens and poses a constant threat to the poultry industry (Alkie and Rautenschlein, 2016).

1.2 IBDV impact on the poultry industry

1.2.1 The poultry industry

Many developing countries have expanded their investment in poultry, in order to feed the growing human population (Thornton, 2010), making the need to control avian diseases more crucial. The impact of poultry diseases on the health of these birds is substantial, driving continued investment and research into vaccines for pathogens such

as avian influenza (AIV) (Spackman *et al.* 2018), Marek's disease virus (MDV) and IBDV (Gimeno and Schat, 2018).

1.2.2 Gumboro Disease

IBDV is the aetiological agent of Infectious Bursal Disease (IBD) or Gumboro disease. The first report of IBD was in Gumboro in Delaware, USA in 1962, providing the origin of its name (Cosgrove *et al.* 1962). Between 1960 and 1964, the disease spread across the USA (Lasher and Davis, 1997) and reached Europe between 1962 and 1971 (Faragher, 1972). IBD was later reported in the Middle East (Salman *et al.* 1983), Southern Africa (Onunkwo, 1975), India (Dongaonkar and Rao, 1979), the Far East (Tsukamoto *et al.* 1992) and Australia (Firth, 1974). This highly contagious disease is characterised by the destruction of lymphoid tissues, particularly the bursa of Fabricius (BF), where B lymphocytes mature and differentiate (van den Berg *et al.* 2000). As the virus primarily targets and destroys B cells, in cases where the disease itself is not fatal, birds are often immunosuppressed, which causes a greater susceptibility to secondary infections (Rosenberger and Gelb, 1976). This immunosuppression also reduces the immune response to vaccines, which are vital in the poultry industry for protection against both avian and zoonotic diseases (Giambrone, 1979; Suber *et al.* 2006; Spackman *et al.* 2018).

Typically, there is up to 100% serological conversion after infection of a flock, and morbidity rates are high. In contrast, mortality rates are much more variable and depend on the virulence of IBDV strain (van den Berg *et al.* 2000). While disease severity also depends on the age and breed of the birds, clinical signs usually include ruffled feathers, depression, diarrhoea and dehydration (Cosgrove, 1962; Ley *et al.* 1983). The BF is the main target organ for IBDV infection, as it is the primary reservoir for B cells in birds, although the virus has also been detected in other lymphoid tissues such as the spleen and thymus (Rasoli *et al.* 2015; Smith *et al.* 2015; Hussein *et al.* 2019). Birds are typically

more susceptible to infection between three and six weeks of age when the BF is at maximal development (Müller *et al.* 2003). After this developmental stage, the BF regresses as B cells enter the circulating blood (Ratcliffe, 2006). B cells are most vulnerable to infection during their immature stage, whilst they are carrying immunoglobulin M (IgM) on their surface, and this is a suggested target for the virus (Hirai *et al.* 1981; Luo *et al.* 2010; Zhao *et al.* 2016). After BF regression, healthy birds have a diverse circulating B cell population and are prepared for pathogen challenge, while birds with a history of IBDV infection have a depleted B cell population making them more vulnerable to other pathogens (Rosenberger and Gelb, 1976). The immunosuppressive nature of IBDV makes it difficult to accurately predict its impact on the poultry industry, in terms of economic loss due to IBDV as a primary pathogen and the consequential secondary infections with other viruses, bacteria and parasites (van den Berg *et al.* 2000).

1.3 IBDV genome and structure

IBDV is a non-enveloped virus with an icosahedral capsid of approximately 55-60nm diameter made up of trimers of the VP2 protein, which come together in hexameric and pentameric structures to create a T=13 lattice (Böttcher *et al.* 1997). The dsRNA bi-segmented IBDV genome is comprised of a larger segment A (3.2 Kb), encoding two partially overlapping ORFs that encode the majority of the viral proteins, and the smaller segment B, encoding VP1, which is the RdRp of the virus (Figure 1). Segment A encodes a non-structural protein, VP5, which overlaps a polyprotein precursor preVP2-VP4-VP3 (100 kDa) cleaved in *trans* by VP4 to release preVP2 (54.4 kDa) and VP3 (32 kDa) (Lejal *et al.* 2000). The VP4 protein and the cellular puromycin-sensitive aminopeptidase (PurSA), cleave the preVP2 at its C terminus to produce the intermediate preVP2 (452 residues), before further processing by VP2 itself into the mature form of the protein (Saugar *et al.* 2005; Irigoyen *et al.* 2009). VP3 acts as a scaffold protein binding dsRNA and VP1 protein (Mertens *et al.* 2015) as shown in Figure 1. VP2 and

VP3 are the main structural proteins assembling the IBDV virion with a variable amount of preVP2 present (Saugar *et al.* 2005). The final stage of VP2 processing releases peptides from the cleaved preVP2 into the virion that remain non-covalently bound to the inside of the capsid. One such peptide, pep46, contributes to cell membrane perforation in the next cell targeted by the virus (Chevalier *et al.* 2005).

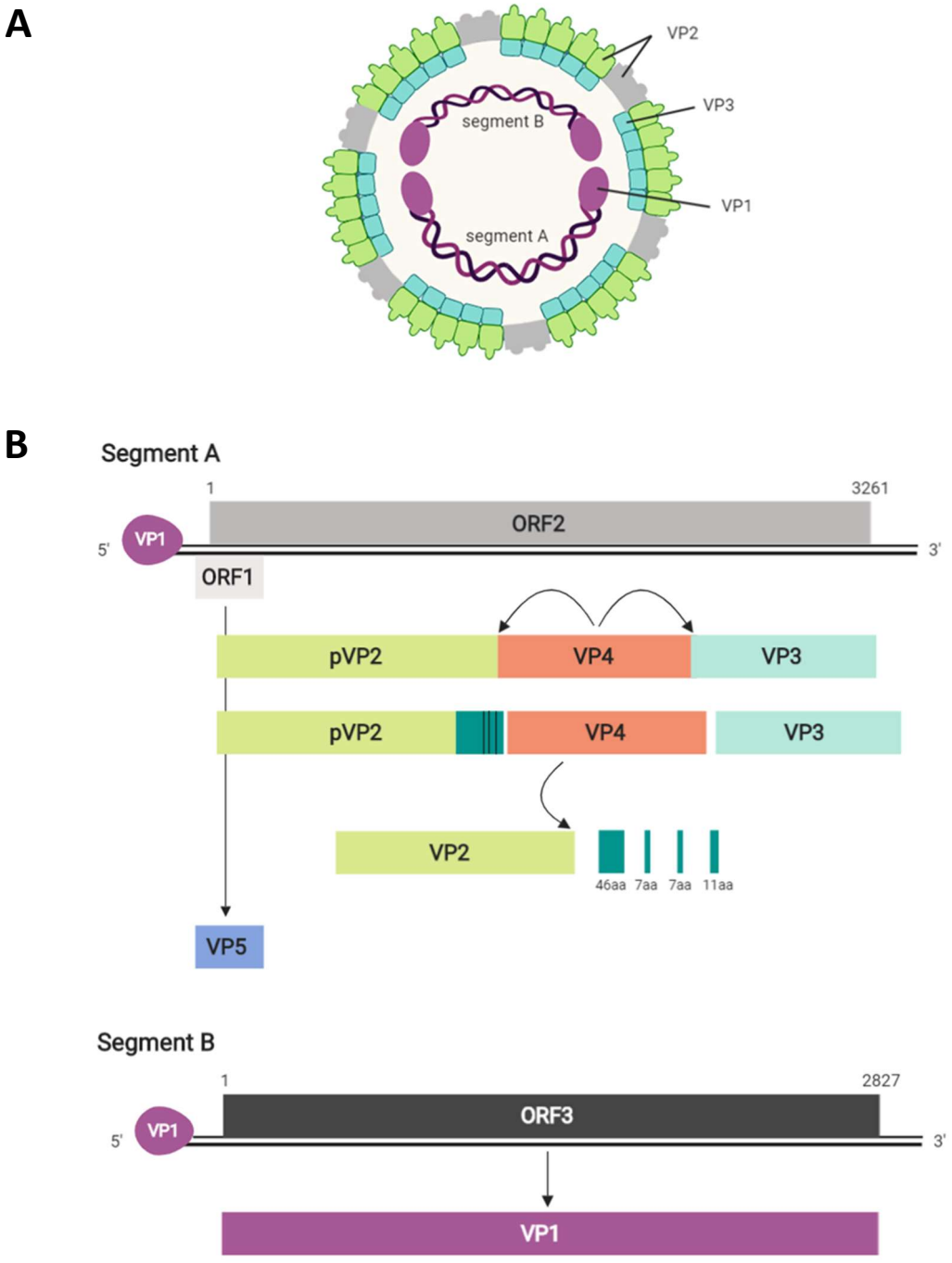

Figure 1 IBDV structure and genome arrangement.

Illustration of the structure of an IBDV virion (A). Segments A and B are encased by the capsid, which is comprised of the VP2 and VP3 proteins. The VP1 protein is attached to the termini of the dsRNA genome segments. The genome organisation and cleavage of segments A and B of IDBV (B), shows segment A is cleaved into its constituent parts by VP4, before further processing of the preVP2 into VP2 and four small peptides, including pep46. Adapted from Viral Zone (Hulo *et al.* 2011).

1.4 Viral proteins

1.4.1 VP1

Segment B contains one ORF encoding the VP1 protein (Azad *et al.* 1985). This 97 kDa protein attaches to the termini of both segments A and B (Müller and Nitschke, 1987). The primary function of VP1 is to act as the RdRp of the virus, responsible for viral genome replication and transcription during infection (Ye *et al.* 2017; Luque *et al.* 2009a). For replication to take place, VP1 requires an interaction with VP3, rather than VP2, to form ribonucleoprotein (RNP) complexes (Lombardo *et al.* 1999; Tacken *et al.* 2002; Ferrero *et al.* 2015). VP1 has also been described as a non-canonical polymerase as the RdRp domain has three motifs in a C-A-B order, rather than the A-B-C order found in the majority of other viruses. This unusual order has been associated with the ability of the polymerase to utilise $Co2^{+}$ rather than $Mg2^{+}$ or $Mn2^{+}$ which are more commonly employed by other viral polymerases (Letzel *et al.* 2007). Several studies have also demonstrated the role of VP1 in pathogenicity of the virus by identifying the key domains in VP1 responsible for virulence (Liu and Vakharia, 2004; Le Nouën *et al.* 2012). A study by He *et al.* (2016) demonstrated that reassortant viruses with the VP1 and VP2 proteins from a vvIBDV strain, and the remaining VP3, VP4 and VP5 from an intermediate strain, had more severe pathogenicity than the intermediate parental strain. Furthermore, a study by Gao *et al.* (2014) identified the triplet of amino acids (aa) 145/146/147 of the vvIBDV Gt strain contributed to its increased virulence. Several other studies have also highlighted the role of VP1 in increased IBDV virulence, however, these studies have focussed on measuring virulence by replication and mortality (Liu and Vakharia, 2004; Zierenberg *et al.* 2004; Jackwood *et al.* 2011). At present, it is unknown whether the VP1 protein interacts directly with innate immune genes during infection.

1.4.2 VP2

The IBDV VP2 protein is the main constituent of the virus capsid and consequently forms the main antigenic site, which is responsible for neutralising antibody binding (Becht *et al.* 1988; Fahey *et al.* 1989). The X-ray crystal structure of the VP2 protein revealed it has three separate domains, termed base (B), shell (S) and projection (P) (Coulibaly *et al.* 2005; Lee *et al.* 2006). The conserved N and C- terminal VP2 regions are formed by the B and S domains, while the P domain holds the hypervariable region (HVR) of VP2 (aa 206-350) (Bayliss *et al.* 1990). Within the HVR, Azad *et al.* (1987) identified two antigenic hydrophilic regions termed A (aa 212-224) and B (aa 314-325). Of these A and B regions, two loops (P_{BC} and P_{HI}) represented the outmost part of the domain, and deletion studies demonstrated the importance of these hydrophilic regions as epitopes are targeted by antibodies. Moreover, two additional loops at the top of the P domain (P_{DE} and P_{FG}) (Coulibaly *et al.* 2005) contain the aa sites 253 (glutamine), 279 (aspartic acid) and 284 (alanine) which have been shown to play an important role in cellular tropism and adaptation of field isolates to cell culture (Lim *et al.* 1999; Mundt, 1999; Brandt *et al.* 2001). Aside from this important role in cell entry, VP2 has also been shown to be an inducer of apoptosis (Fernandez-Arias *et al.* 1997). The mechanism for this interaction was unclear, until a study by Qin *et al.* (2017) identified an interaction between VP2 and oral cancer overexpressed 1 (ORAOV1). VP2 was shown to reduce the expression of ORAOV1, a protein that can act as an antiapoptotic molecule, during infection resulting in an increase in IBDV-induced apoptosis.

1.4.3 VP3

Another major structural protein, VP3, constitutes 35% of the IBDV virion, and is the C-terminal protein encoded by the large polyprotein in segment A of the virus (Luque *et al.* 2009b). The VP3 protein coats the dsRNA genome, shielding it from the pattern

recognition receptors (PRRs) such as Melanoma Differentiation-Associated protein 5 (MDA5) (Tacken *et al.* 2002; Ye *et al.* 2014; Ferrero *et al.* 2015), discussed in more detail in section 1.7.1. In addition, VP3 suppresses the activation of antiviral responses downstream of MDA5, such as the interferon (IFN) production and signalling pathways (Ye *et al.* 2014). VP3 has been shown to act as a scaffold protein, building an internal layer below the capsid's icosahedral shell which packages the viral genome into a procapsid prior to the formation of the outer VP2 capsid shell (Mata *et al.* 2018), further to its role in aiding VP1 RdRp activity.

1.4.4 VP4

The primary function of the IBDV VP4 protein is to act as a protease using a serine/lysine catalytic dyad mechanism to process the large polyprotein of Segment A from the precursor preVP2-VP4-VP3 polyprotein into preVP2, VP4 and VP3 (Birghan *et al.* 2000; Lejal *et al.* 2000; Leong *et al.* 2000). The catalytic dyad comprises of H36, D79 and S142 where mutation of the D79 or S142 result in reduced polyprotein processing, although mutating H36 to P completely abolishes this (Rodríguez-Lecompte *et al.* 2002). Aside from its function as a protease, IBDV VP4 has been associated with other functions contributing to viral pathogenesis (Wang *et al.* 2009b; Li *et al.* 2013b). Previous work by Zheng *et al.* (2015b) reported the assembling of VP4-associated type II tubules in both the cytoplasm and nucleus of infected cells. Early in infection, these tubules reduced the cytotoxic effects of the protease on the host cells and prevented premature cell death, however, the accumulation of VP4 tubules late in infection caused destruction of the host cytoskeletal and nuclear structures resulting in cell lysis (Zheng *et al.* 2015b). In addition to the VP4-host interaction via the formation of tubules, VP4 has been shown to interact with the host protein glucocorticoid-induced leucine zipper (GILZ) leading to the suppression of the type I IFN response by preventing the K48-linked ubiquitylation of GILZ, discussed in more detail in section 1.7.2 (Li *et al.* 2013b; He *et al.* 2018).

1.4.5 VP5

IBDV VP5 is a non-structural protein encoded by a small ORF overlapping the preVP2-VP4-VP3 polyprotein in segment A (Mundt *et al.* 1995). Semi-conserved across serotype I IBDV strains, VP5 has been demonstrated to play roles in virus dissemination from infected cells, and in apoptosis (Yao *et al.* 1998; Lombardo *et al.* 2000; Rodriguez-Lecompte *et al.* 2005). VP5-mediated apoptosis is initiated by an interaction between VP5, voltage-dependent anion channel 2 (VDAC2) and receptor of activated protein kinase C1 (RACK1) leading to the release of cytochrome C and activation of caspases 3 and 9 ending in apoptosis (Lin *et al.* 2015). While VP5 was initially identified as an apoptotic inhibitor, further studies reported VP5 acts an inhibitor of apoptosis at early time points (≤12 hours post-infection (h.p.i)) and inducer of apoptosis at late time points (≥24 h.p.i) during infection (Liu and Vakharia, 2006; Wei *et al.* 2011; Li *et al.* 2012; Lin *et al.* 2015). The multi-functional role of VP5 throughout the viral life cycle makes this protein an important factor supporting early virus replication and later virus release.

1.5 IBDV replication cycle

The first step in the IBDV replication cycle is the attachment of the virus to the cell plasma membrane and entry into target cells (Figure 2). Several cell surface proteins have been identified as potential receptors for the binding of the viral particles or VP2 protein (Qin and Zheng, 2017). The surface IgM was the first receptor to be reported for IBDV (Ogawa *et al.* 1998), using the immortalised B cell line, DT40, and further studies found the λ light chain can bind to the virus particles in a virulence-dependent manner, with more efficient binding to more pathogenic IBDV strains (Luo *et al.* 2010). As DT40 cells are permissive to both cell adapted (caIBDV) and field strains, unlike chicken embryo fibroblasts (CEFs) and continuous fibroblast cell lines, such as Douglas Foster-1 (DF-1) cells, this suggests IgM is involved in the binding of field strains of IBDV to target cells. Chicken heat shock protein 90 (HSP90) has also been identified as part of a receptor complex in immortalised DF-1 fibroblast cells (Lin *et al.* 2007; Chi *et al.* 2018), due to its interaction with the VP2-subviral particle. In addition, the VP2 P domain contains an Ile-Asp-Ala sequence which has been identified as a ligand of the α4β1 integrin in DF-1 cells. This integrin is also abundant in immature lymphocytes, which may partly explain the apparent tropism of IBDV infection for immature lymphocytes.

Upon entry to the cell by endocytosis or macropinocytosis (Giménez *et al.* 2012), a decrease in pH and Ca^{2+} ion concentration in the endosome causes instability of the VP2 capsid structure, allowing the exposure of a VP2-associated peptide, pep46 (Garriga *et al.* 2006; Giménez *et al.* 2012). This peptide is 46 aa in length and responsible for pore formation in the endosomal membrane (Galloux *et al.* 2007) (see Figures 1 and 2). Following this event, the IBDV genome exits the endosome through the pores and has been reported to remain associated with the cytoplasmic leaflet of the endosomal membranes and the Golgi complex where replication of the genome commences (Giménez *et al.* 2018). Following replication, studies have demonstrated two mechanisms the virus can use to exit the infected cell. The first is viral release by cell lysis where large numbers of viral particles exit the dead cell as it lyses (Méndez *et al.* 2017). The second mechanism is non-lytic egress, whereby the VP5

protein enables virus trafficking within the cell between viral factories to the extracellular milieu using the cell's vesicular network (Méndez *et al.* 2017).

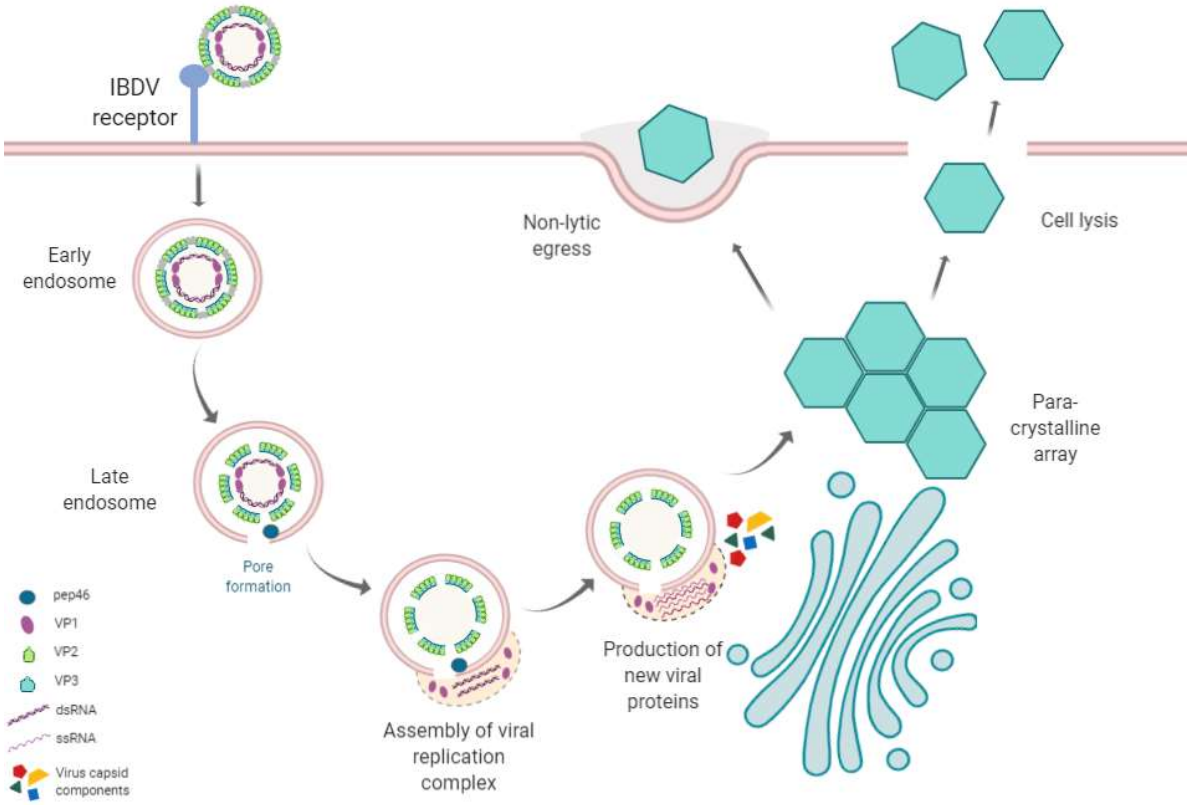

Figure 2 An illustration of the key events in the IBDV replication cycle.

An IBDV virion binds to the IBDV receptor and enters the cell by endocytosis. As the pH and Ca^{2+} levels concentration in the endosome reduce, the capsid becomes unstable releasing pep46 which is then able to form a pore in the endosome membrane. The viral genome exits the endosome, remaining associated with the outside of the endosome membrane and Golgi complex where viral replication then occurs. The viral components are then packaged forming new virions that arrange in a para-crystalline array formation prior to exit of the virus particles by non-lytic egress or cell lysis.

1.6 IBDV Virulence

1.6.1 IBDV strains

A significant obstacle to IBDV control is the constant evolution of field strains either through reassortment events due to its bi-segmented genome, or antigenic drift due to a high genetic mutation rate allowing antigenic flexibility. The original field strains circulating in the early 1960s (classical, cIBDV) had a low mortality rate of 1-2%, however this has slowly increased to ≤5% since 1987 (Figure 3) (Rosenberger and Cloud, 1986). Variant IBDV (vIBDV) strains emerged in the USA as a result of antigenic drift in vaccinated flocks. Mutations in the VP2 capsid protein were responsible for their escape from the protective immunity conferred by vaccines used during this period, inspiring the development of new 'variant' vaccines (Rosenberger and Cloud, 1986; Jackwood and Saif, 1987; Snyder *et al.* 1990). Around the same time, outbreaks occurred in Europe and later in Japan with IBDV strains that caused 50-60% mortality in laying hens and 30-40% in broilers. These viruses, termed "hypervirulent" or very virulent (vvIBDV) strains, were able to cause 100% mortality in specific-pathogen-free (SPF) chickens (van den Berg *et al.* 1991; Nunoya *et al.* 1992). Since the emergence of vvIBDV strains, reassortant viruses with combinations of A and B segments from vvIBDV, vIBDV and caIBDV vaccine strains have also been reported (Le Nouën *et al.* 2012; Lee *et al.* 2017; Pikula *et al.* 2018). The emergence of different IBDV strains is summarised in Figure 3. A new nomenclature was recently proposed for IBDV strains comprising of 7 genotypes: classic (G1); vIBDV (G2); vvIBDV (G3); distinct IBDV (dIBDV) (G4); vIBDV/ classic recombinant (G5); distinct ITA (G6) and Australian (G7) (Jackwood *et al.* 2018). This system aims to more accurately group IBDV strains to avoid differences in terminology in the literature, however, remains controversial.

Pikula *et al.* (2018) isolated a reassortant virus circulating in the field with segment A from a vvIBDV and segment B from a cIBDV attenuated strain. A mortality rate of 80% was recorded when SPF chickens were inoculated with the virus, implicating the role of segment A in determining virulence. In contrast, a study by Le Nouën *et al.* (2012) reported a chimeric virus, with segment A from a vvIBDV strain and segment B from the attenuated Cu-1 strain, had reduced pathogenicity *in vivo* compared to the parental vvIBDV strain. Having established both segments are implicated in determining virulence, He *et al.* (2016) inoculated chickens with a panel of chimeric viruses, with viral genes from either vvIBDV or vaccine caIBDV strains. The most severe pathogenicity was observed following infection with a virus containing the VP1 (segment B) and VP2 from the vv strain and the remaining VP4, VP3 and VP5 from the vaccine strain. Another chimeric virus containing the VP1 from the vv strain and the remaining viral genes from the vaccine strain, showed a reduced pathogenicity suggesting both the VP1 and VP2 proteins are involved in determining pathogenicity. These data suggest that the VP1 and VP2 proteins are the greatest contributing factors to virulence. Several studies have highlighted the importance of the VP2 protein in cell tropism (Mundt, 1999; Brandt *et al.* 2001; Qi *et al.* 2009; Ben Abdeljelil *et al.* 2014). vvIBDV and cIBDV field strains of IBDV do not infect fibroblast cell lines commonly used in the laboratory, such as DF-1 or CEF cells, without prior adaptation (van den Berg *et al.* 2000; Brandt *et al.* 2001). Several serotype I strains have been successfully adapted to tissue culture or embryos through the extensive passaging either in fibroblast cell lines (Hassan *et al.* 1996; van Loon *et al.* 2002; Raue *et al.* 2004) or in the chorioallantoic membrane (CAM) and yolk sac of embryonated eggs (Yamaguchi *et al.* 1996). Despite these successes, cell culture- or egg-adapted strains showed a reduced pathogenicity *in vivo* (Hassan *et al.* 1996; Yamaguchi *et al.* 1996) and other field isolates have failed to be adapted to cell culture (McFerran *et al.* 1980). Sequence comparison studies identified specific aa in the VP2 which allowed adaptation

of vvIBDV strains to cell culture (Mundt, 1999; Lim *et al.* 1999; Jackwood *et al.* 2008; Qi *et al.* 2013). It was first reported by Mundt in 1999, that the two aa changes Q253H and A284T were responsible for the adaptation of a BF-derived field strain to CEF cells and the quail muscle cell line, QM-7. These results were confirmed by engineering the caIBDV strain D78 to contain the H253Q and T284A mutations, resulting in a virus unable to infect tissue culture cells (van Loon *et al.* 2002). Other groups have further explored these mutations, finding both mutations were required for adaptation (Qi *et al.* 2009). The H253N performs the same function as H253Q in restoring virulence, and a D279N mutation in conjunction with the A284T mutation also adapted the field strain for *in vitro* work (Ben Abdeljelil *et al.* 2014). Further to these commonly reported VP2 mutations, mutations at R249Q and 276V have been shown to increase virulence (Qi *et al.* 2013 and Escaffre *et al.* 2013, respectively), while I256V reduced the virulence of a virulent IBDV strain (Qi *et al.* 2013). Despite VP2 being the predominant focus for identifying mutations affecting cell tropism, the study by Escaffre *et al.* (2013) identified a mutation at position A276T in the finger domain of the VP1 protein that contributed significantly to attenuation of a vvIBDV strain, although this mutation succumbed to reversion pressures *in vivo*. Another mutation in the VP1 at position 4 (V4I) was also found to attenuate a vvIBDV strain in a study by Yu *et al.* (2013).

Taken together, genome segment A determines cell tropism whereas segment B is involved in the efficiency of viral replication, while both segments contribute to virulence. Efforts to identify virulence factors associated with more pathogenic strains are still ongoing.

1.6.2 IBDV control

Control measures for IBDV are paramount due to the economic and welfare burden associated with disease and for the international poultry trade. Resistance of IBDV to

many environmental stresses, such as pH and temperature conditions, allow the virus to persist on poultry farms for long periods and compromise incoming bird populations (Alexander and Chettle, 1998; Mandeville *et al.* 2000). Many disinfectants have been tested for their ability to inactivate IBDV, including aldehyde (formaldehyde, glutaraldehyde), chlorine and iodine compounds which were successful, however their virucidial effect was greatly reduced at low temperatures (Benton *et al.* 1967; Meulemans and Halan, 1982). The pH is also important for inactivation as sodium hydroxide at a pH of 12 was effective while a pH of 2 was insufficient for virus inactivation (Benton *et al.* 1967; van den Berg, 2000). A study by Guan *et al.* (2014) combined investigating low temperatures and different disinfectants to determine the most effective disinfectant for IBDV. They managed to achieve a 5 $\log_{10}$ reduction in virus by treating viral supernatant with 2% Virkon at -20°C for 2 hours. Comparatively, in the same temperature and disinfectant Newcastle's Disease Virus (NDV) was inactivated in 5 minutes, demonstrating the increased stability of IBDV.

The persistence of IBDV in the environment means vaccines are vital in reducing the introduction of IBDV to new environments and populations in addition to biosafety measures. Chickens from breeder flocks are typically immunised in order to produce maternal antibodies (MAbs) that transfer to the embryonated egg and subsequently provide protection to the newly hatched chick. For the first few weeks after hatch, MAbs wane and chicks become vulnerable to circulating IBDV strains in the surrounding environment. The time-point of vaccination post-hatch is crucial to providing protection, as MAbs can neutralise the vaccine virus, preventing adaptive immunity to be established (Müller *et al.* 2003). Consequently, the Deventer formula is used to calculate the optimal time for vaccination and takes into consideration the vaccination age of the birds, enzyme-linked immunosorbent assay (ELISA) titre of the bird representing a certain percentage of the flock and the half-life of the antibodies (by virus neutralisation (VN)

test) in the type of chickens being sampled (Intervet, 2019). There are three types of live vaccines currently available for IBDV protection named according to the level of protection they provide (antibody levels induced): “hot” are the least attenuated and can cause lesions in the BF and immunosuppression in birds under 10 days old (8-11 VN log_2); intermediate plus/ intermediate (6-8 VN log_2) and mild vaccines which are no longer used in the commercial environment due to poor antibody response (4 VN log_2) (Intervet, 2019). An “immune complex” vaccine has also been developed, which is comprised of an intermediate vaccine virus mixed with an optimum amount of antibodies that can be used on 1 day old birds or during *in ovo* vaccination (Whitfill *et al.* 1995). The mechanism of protection remains unclear, although the immune complex may remain present on follicular dendritic cells, until after MAb levels have dropped (Jeurissen *et al.* 1998), allowing a more sustained antigen presence and the administration of the vaccine earlier, despite the presence of MAbs. Several recombinant IBD vaccines have also been developed using fowlpox virus (Bayliss *et al*. 1991; Shaw and Davison 2000), herpesvirus of turkey (HVT) (Darteil *et al*. 1995; Perozo *et al.* 2009), fowl adenovirus (Sheppard *et al*. 1998; Francois *et al*. 2001) and MDV (Tsukamoto *et al.* 1999; Li *et al.* 2017) as the vector.

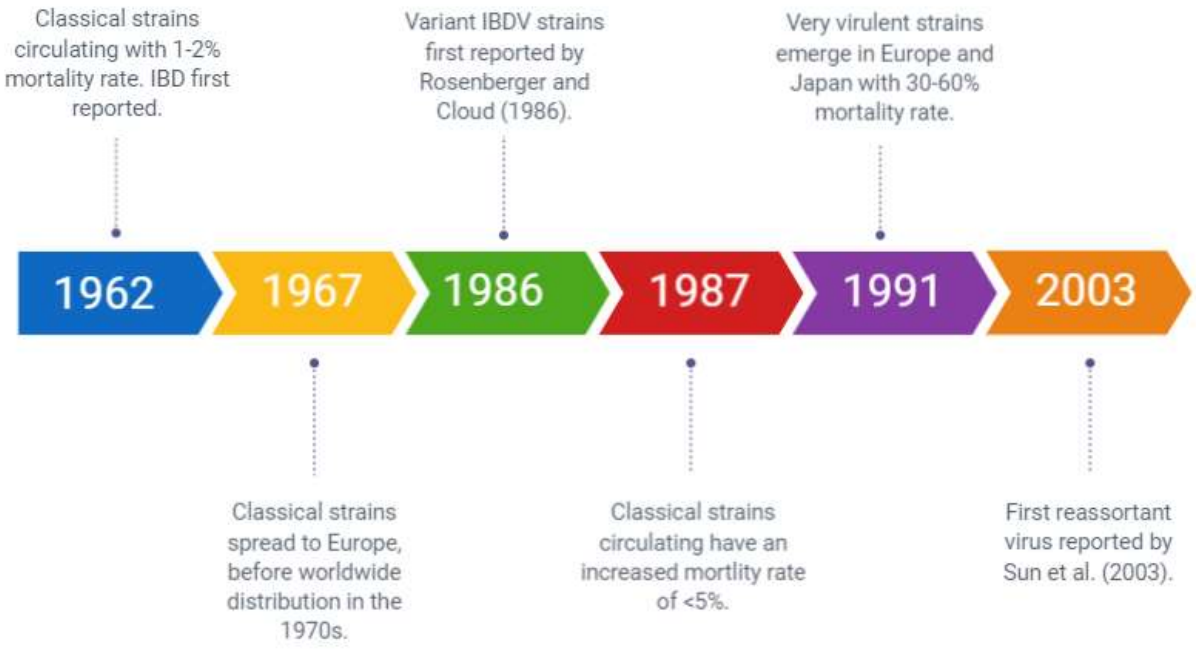

Figure 3 IBDV strain emergence since 1960s.

A timeline showing the emergence of classical (cIBDV), variant (vIBDV), very virulent (vvIBDV) and reassortant IBDV strains over time, from the first reported case of IBD reported in 1962.

1.7 Host immune responses to IBDV

1.7.1 Innate immune sensing of IBDV

The innate immune response is the first defence against invading pathogens, with detection of pathogen-associated molecular patterns (PAMPs) activating a diverse and rapid protective response in the infected and neighbouring cells (Liu *et al.* 2017b). PAMPs are detected by PRRs, including toll-like receptors (TLRs), Nod-like receptors (NLRs) and retinoic acid-inducible gene-1 (RIG-I)-like receptors (RLRs), which trigger a downstream signalling cascade of type I IFN and pro-inflammatory cytokines (Akira *et al.* 2003; Kawai and Akira, 2010). Activation of the Janus kinase/signal transducers and activators of transcription (JAK-STAT) signalling pathway by type I IFN leads to the induction of numerous IFN-stimulated genes (ISGs), establishing an antiviral response and restricting viral infection by targeting multiple stages of the virus life cycle (Platanias, 2005) (Figure 4).

In mammals, the predominant PRRs that detect non-self RNA are RIG-I, MDA5 and laboratory of genetics and physiology 2 (LGP2) and these are widely expressed across most tissue and cell types (Liu *et al.* 2017b). RIG-I primarily senses 5'triphosphorylated uncapped RNA or dsRNA akin to those produced by the virus during infection, as opposed to the capped mRNA synthesised by the host cell (Goubau *et al.* 2014). MDA5 senses long dsRNA and branched high-molecular forms sharing the same pathway as RIG-I, signalling through the mitochondrial antiviral-signalling protein (MAVS) on the mitochondrion, stimulating production of type I IFN and pro-inflammatory cytokines (Santhakumar *et al.* 2017b). LGP2 does not contain the two N-terminal caspase activation and recruitment domains (CARDs) found in RIG-I and MDA5 (Loo and Gale, 2011), and so LGP2 positively regulates MDA5 and negatively regulates RIG-I (Schlee and Hartmann, 2016; Uchikawa *et al.* 2016).

In chickens, LGP2 has previously been shown to contain features of both a MDA5-like helicase domain and RIG-I-like C-terminal domain, and LGP2 enhances MDA5 activation (Uchikawa *et al.* 2016). Despite being the most extensively studied PRR, RIG-I (DDX58) is absent in the chicken genome, although the flanking gene on chromosome Z has been identified, making it unlikely that the gene is located elsewhere in the genome (Magor *et al.* 2013). This loss of RIG-I is also found in other galliformes such as turkeys and partridges, while ducks and other anseriformes have a functioning RIG-I gene (Barber *et al.* 2010). MDA5 has been shown to compensate for this absence of RIG-I, for example, by detecting Avian Influenza Virus (AIV) in chicken cells and generating an efficient type I IFN response (Karpala *et al.* 2011; Liniger *et al.* 2012).

As previously mentioned, TLRs sense PAMPs and activate the nuclear factor kappa B (NF-κB) and type I IFN pathways (Magor *et al.* 2013). Birds have 8 TLR genes commonly found in humans: two TLR1 genes; two TLR2 genes, TLR3, TLR4, TLR5 and TLR7. In addition to these, the two non-mammalian TLR15 and TLR21 have been found to compensate, at least in part, for the loss of TLR8 and TLR9 in galliform birds (Brownlie *et al.* 2009; Brownlie and Allan, 2011; Boyd *et al.* 2012; Qi *et al,* 2016). Type I IFN is comprised of IFNα and IFNβ, and in mammals there are 13 isoforms of IFNα. In chickens, however, there are 10 isoforms of IFNα and one isoform of IFNβ (Staeheli *et al.* 2001).

Like many other RNA viruses, IBDV manipulates the innate sensors to remain undetected in the cytoplasm for enough time to replicate and release new virions. Upon entry into the cell via endocytosis, IBDV is sensed by TLR3 which activates the TIR-domain-containing adapter-inducing IFNβ (TRIF) signalling pathway resulting in an NF-κB (in particular, IL-8) and type I IFN response (Takeda and Akira, 2004). Several studies have reported the up-regulation of TLR3 at early points during IBDV infection, demonstrating its important role in the sensing of viruses of different strain virulence (Rauf *et al.* 2017;

He *et al.* 2017; Yu *et al.* 2019). Following exit from the endosome and when the dsRNA genome is still associated with the endosomal membranes, the viral genome is vulnerable to sensing by MDA5 (Giménez *et al.* 2018). Previous work by Ye *et al.* (2014) demonstrated how the VP3 protein strongly competes with MDA5 to bind the dsRNA genome, thereby blocking MDA5-dependent signalling pathways. More recently, Ye *et al.* (2019) determined the binding of the host protein Staufen1 (STAU1) to the genomic dsRNA. They found the binding of STAU1 decreased the association of MDA5 to the dsRNA genome, while not interfering with dsRNA-VP3 interaction. Together STAU1 and VP3 were shown to block MDA5 and subsequent IFNβ production (Ye *et al.* 2019).

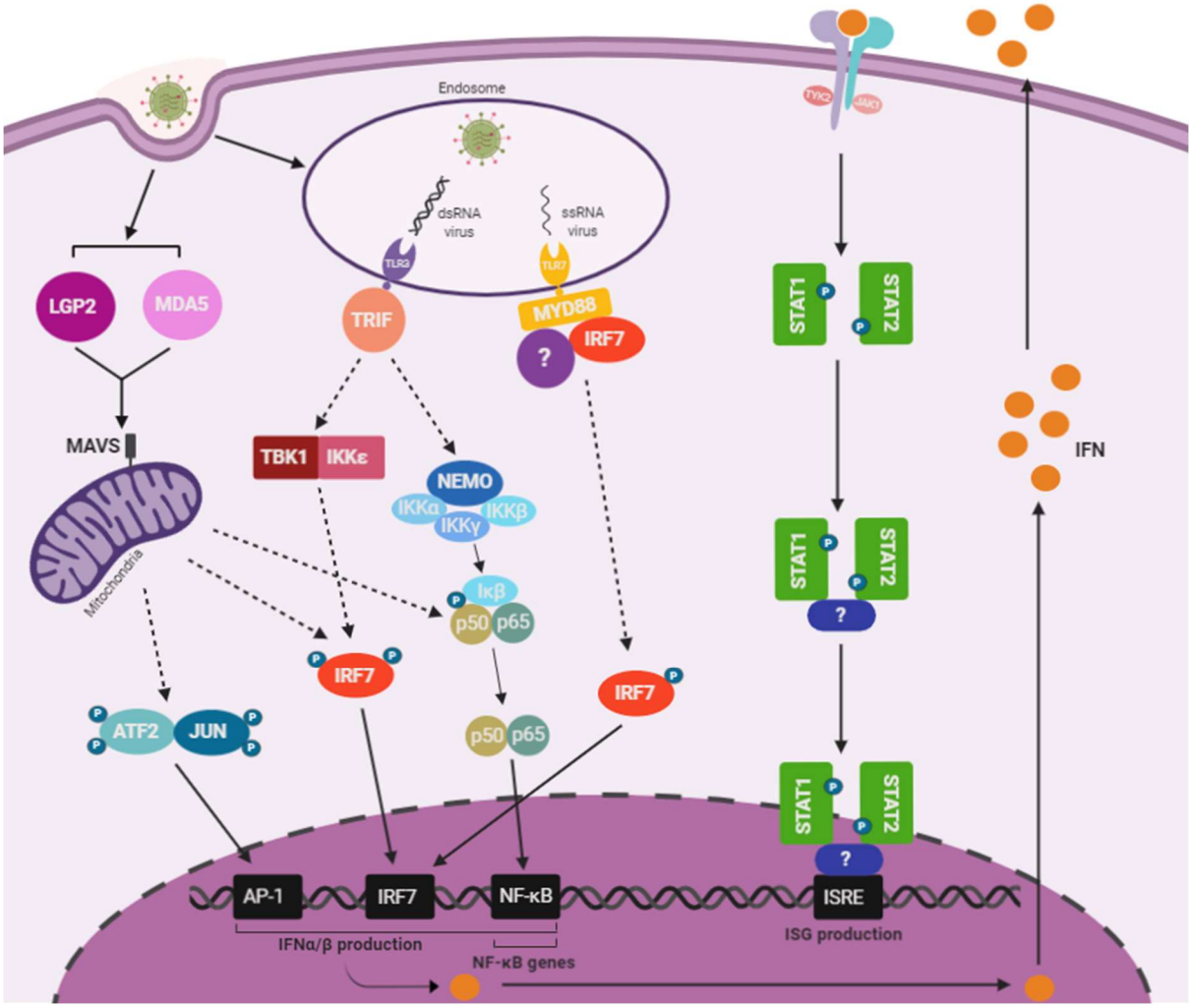

Figure 4 Chicken type I IFN production and signalling pathways.

The IFN production pathway commences with dsRNA sensing by MDA5 and LGP2 (cytoplasmic), TLR3 (endosomal) or sensing of single stranded (ss) RNA by TLR7 (endosomal). Binding to these PRRs activates downstream signalling mediated through MAVS, TRIF or MyD88, respectively. Through a series of interactions, these adaptor proteins then activate AP-1 (ATF2 and JUN), IRF7 (TBK1 and IKKε) and NF-κB (NEMO, IKKs, p50 and p65). Upon activation, AP-1, IRF7 and NF-κB translocate to the nucleus and stimulate the transcription of antiviral genes including type I IFN. Secreted type I IFN can act both in an autocrine and paracrine manner to stimulate the JAK-STAT pathway via the binding of IFN to the IFN receptor. Activation of JAK-STAT leads to the phosphorylation of STAT1 and STAT2, along with other factors, form the ISGF3 complex. This complex binds to the ISRE and initiate the transcription of hundreds of ISGs to establish an antiviral state in the cell. "P" represents the phosphorylation of this protein, "?" indicates other proteins are thought to be involved in this interaction/ complex but this is currently unknown in chickens. Dotted lines indicate intermediate steps are involved that have not been depicted in this diagram or are unknown at the time of submission.

1.7.2 IBDV evasion and antagonism of type I IFN production

Stimulation of the type I IFN production pathway commences with the sensing of the virus by MDA5 and LGP2, as established in the previous section (1.7.1). MDA5 undergoes a conformational change revealing its two CARDs, allowing the N-terminal CARD of MAVS to bind (Seth *et al.* 2005). This binding interaction mediates the downstream signalling of three innate immune pathways, ultimately leading to the activation of activator protein-1 (AP-1), IFN regulatory factor 7 (IRF7) and NF-κB (Figure 4). Recently, IRF7 was shown to be the primary IRF involved with MAVS- and stimulator of IFN genes (STING)-mediated IFNβ regulation in response to infection (Cheng *et al.* 2019), with previous studies having reported the absence of IRF3 in the chicken genome (Cormican *et al.* 2009; Huang *et al.* 2010). TANK binding kinase 1 (TBK1) was also found to be indispensable for STING-mediated activation of IRF7. AP-1 is activated by the phosphorylation of activating transcription factor 2 (ATF2) and JUN allowing AP-1 binding to the positive regulatory domain (PRD) IV, activating transcription of inflammatory factors such as IL-1, IL-6 and tumour necrosis factor α (TNFα) (Fan *et al.* 2015; Intayoung *et al.* 2016), and has been linked with bursal atrophy in chickens following Lipopolysaccharide (LPS) treatment (Ansari *et al.* 2017). IRF7 activation can occur through TLR3 (dsRNA) or TLR7 (ssRNA) signalling via TRIF or myeloid differentiation primary response gene (MyD88), respectively (O'Neill and Bowie, 2007). TLR3 is induced by the binding of dsRNA to its surface, stimulating a downstream TRIF-dependent signalling pathway resulting in the expression of type I IFN (Yamamoto *et al*. 2003; Keestra *et al.* 2013). In mammals, the induction of type I IFN depends on TNF receptor-associate factor (TRAF) 3 (Hacker *et al.* 2006; Oganesyan *et al.* 2006) which recruits TRAF family member-associated NF-κB activator (TANK), TBK1 and inhibitor of nuclear factor kappa-B kinase (IKK)ε to mediate downstream signalling (Guo and Cheng, 2007; Oganesyan *et al.* 2006). Previous studies have suggested chickens lack a functional LPS-specific translocation associated

membrane protein1 (TRAM)-TRIF signalling pathway (Adler and DaMassa, 1979; Keestra and van Putten, 2008), although further investigation identified the presence of MyD88 and TRIF and absence of the TRAM orthologue (Lynn *et al.* 2003). While the up-regulation of TRIF and IFNβ following LPS treatment has been demonstrated, indicative of a functional TRAM/TRIF pathway, it remains unknown whether LPS-TLR4 signalling induces an effective type II IFN (IFNγ) response in chickens (Barjesteh *et al.* 2015; Karnati *et al.* 2015). TRIF signalling can also lead to NF-κB activation through the IKK complex-p50/p65 pathway which concludes with the phosphorylation of p50 and p65 before their translocation into the nucleus. NF-κB can consequently bind to the PRD II domain and induce pro-inflammatory cytokines, such as IL-1β and IL-6 (Kim and Zhou, 2015; Santhakumar *et al.* 2017b).

There are two well-documented strategies used by IBDV to evade activation of the type I IFN response. Firstly, the competitive binding of IBDV VP3 and the host protein STAU1 with the dsRNA genome shielding the viral genome from MDA5 detection (Ye *et al.* 2019), described previously in section 1.7.1. Secondly, the VP4 protein from a vvIBDV strain has been shown to act as a type I IFN antagonist. HEK293T or DF-1 cells transfected with IBDV VP4 showed a suppression of type I IFN and pro-inflammatory cytokines following infection with Sendai Virus (SeV) (Li *et al.* 2013b; He *et al.* 2018). These studies identified an interaction between VP4 and the host protein GILZ, whereby VP4 inhibits the degradation of GILZ which is required for NF-κB regulation. In uninfected cells, GILZ binds to a proline-rich region of p65 preventing translocation to the nucleus (Di Marco *et al.* 2007). As VP4 leads to accumulation of GILZ in the cytoplasm, NF-κB signalling and consequential type I IFN response is inhibited. Conversely, the host protein cyclophilin A (CypA) has been found to target VP4 resulting in the inhibition of viral replication (Wang *et al.* 2015b). In mammalian cells, CypA targets RIG-I, MDA5 and MAVS leading to stimulation of the RIG-I and MDA5 signalling pathways (Liu *et al.* 2017a). While little is

known on the role of cyclophilin in the avian host, we can speculate it may have a similar function. Many studies have reported the induction of type I IFN following IBDV infection, however, the specific host-virus interactions involved remain poorly understood.

1.7.3 IFN signalling and ISG production following IBDV infection

In mammals, IFNs form a large family of cytokines comprising of type I (IFNα, IFNβ, IFNκ, IFNε, IFNδ, IFNω, IFNτ), type II (IFNγ) and type III (λ1-4) IFNs (Santhakumar *et al.* 2017b). In contrast, only IFNα, IFNβ, IFNγ and IFNλ have been identified in chickens at present, since the first IFN identified by Isaacs and Lindenmann (1957). Another type I IFN, IFNκ, was also recently identified in the chicken genome (Santhakumar *et al.* 2017a; Gao *et al.* 2018).

Following production, type I and II IFNs cause the up-regulation of ISGs by binding to the IFN receptors, IFNAR1 or IFNAR2, and initiating either autocrine or paracrine signalling (Randall and Goodbourn, 2008). Recognition of IFN by the IFNARs causes the phosphorylation of signal transducer and activator of transcription 1/2 (STAT1 and STAT2) by Janus kinase 1 (JAK1) and tyrosine kinase 2 (TYK2). Phosphorylated STAT1 and STAT2 proteins together form the ISG- factor 3 (ISGF3) complex with a currently unknown protein in chickens (IRF9 in mammals) (Kessler *et al.* 1990; Randall and Goodbourn, 2008). Type II IFNs initiate the formation of a STAT1-STAT1 homodimer assembling gamma IFN activation factor (GAF) independent of IRF9 or a similar protein. Both ISGF3 and GAF translocate into the nucleus and bind to IFN-stimulated response elements (ISREs) or gamma IFN activation site (GAS) element, respectively (Decker *et al.* 1997). Binding of ISGF3 to the ISREs leads to the activation and up-regulation of hundreds of ISGs in order to establish an antiviral state in the cell. Activation of the GAS element by GAF results in the expression of pro-inflammatory cytokines including IL-6 and IL-12 (Decker *et al.* 1997;

Piaszyk-Borychowska *et al.* 2019). Several protein phosphatases and suppressors of cytokine signalling (SOCS), including SOCS1 and SOCS3, have been implicated in the negative regulation of STATs phosphorylation, allowing the positive and negative feedback mechanisms to be controlled by the cell (Yasukawa *et al.* 1999; Santhakumar *et al.* 2017b).

Out of the vast number of ISGs stimulated by the JAK-STAT pathway, IBDV has been shown to inhibit many of these ISGs including IFN-induced GTP-binding protein (Mx1), Protein Kinase R (PKR) and 2'-5'-oligoadenylate synthetase 1 (OAS) (Smith *et al.* 2015; Ouyang *et al.* 2017). The effect of IBDV on ISG expression is discussed in detail in section 1.8. Several mammalian viruses have also been shown to manipulate IFN signalling by down-regulating key proteins involved in the JAK-STAT pathway. For example, the NS5 protein of yellow fever virus binds to STAT2 when exposed to IFN to prevent binding of the ISGF3 to the ISRE (Laurent-Rolle *et al.* 2014). STAT1 and STAT2 are often inhibited through binding with viral proteins such as the V and W proteins of paramyxoviruses (Rodriguez *et al.* 2002; Shaw *et al.* 2004), the Vif protein of Human immunodeficiency virus-1 (HIV-1) (Gargan *et al.* 2018), the P protein of rabies virus (Vidy *et al.* 2005) or the NS5 protein of Dengue virus and Zika virus (Grant *et al.* 2016). Ebola virus has also been shown to target this pathway by inhibiting JAK1 by the binding of its VP40 protein (Valmas *et al.* 2010) and the VP24 protein competes with STAT1 to prevent its nuclear translocation and downstream induction of ISGs (Guito *et al.* 2017).

1.7.4 IBDV and NF-κB signalling

The NF-κB family is comprised of five related transcription factors: p50, p52, p65, c-Rel and RelB. In mammalian cells, activation of the canonical NF-κB pathway is initiated by the detection of viral RNA by TLRs and RIG-I (as previously described in section 1.7.1),

tumour necrosis factor (TNF) receptor (TNFR), and interleukin 1 receptor type 1 (IL-1R1). These detectors transmit signals to their adaptor proteins: TLRs to MyD88 (TLR7) or TRIF (TLR3), RIG-I to MAVS, TNFR1 to receptor interacting protein 1 (RIP1) and IL-1R to MyD88 (Deng *et al.* 2018). Following this, MyD88 activates interleukin-1 receptor-associated kinases (IRAKs) and TRAF6, MAVS interacts with TRAF6, and TRIF interacts with RIP1. Both TRAF6 and RIP1 can then activate the transforming growth factor (TGF)-β-activated kinase 1 (TAK1) complex (Chattopadhyay *et al.* 2010). Activation of this complex in turn stimulates the IKKs, resulting in the phosphorylation and degradation of IκBα and consequential release of p50/p65. Translocation of p50/p65 into the nucleus and binding to NF-κB activation sites induces the expression of pro-inflammatory cytokines and IFN (Zou *et al.* 2017).

While many key immune genes in the mammalian NF-κB pathway are also consistent in avian species, the absence of RIG-I, TLR8, TLR9 and IRF9 alters the pathway described above (Magor *et al.* 2013; Santhakumar *et al.* 2017b). As chickens still have functionally active MDA5, MAVS and STING these genes are believed to compensate although the underlying mechanisms remain unclear (Cheng *et al.* 2015).

A major contributor to the burden of IBDV infection is the lasting immunosuppression that affects surviving birds due to the destruction of the B cell population by apoptosis (Cubas-Gaona *et al.* 2018). Both the VP3 and VP4 proteins have been identified as suppressors of the innate immune response (see section 1.7.2), however VP2 and VP5 have been demonstrated to regulate apoptosis during infection (Qin and Zheng, 2017). The PKR pathway has also been implicated as the target of VP2 and VP3 (Fernandez-Arias *et al.* 1997; Busnadiego *et al.* 2012; Cubas-Gaona *et al.* 2018), while there is evidence to suggest VP5 acts as an inhibitor of apoptosis at early time points (≤12 h.p.i, Liu and Vakharia, 2006; Wei *et al.* 2011) and an apoptotic inducer later in infection (≥24 h.p.i, Li *et al.* 2012; Lin *et al.* 2015). The mechanism for VP5-mediated apoptosis involves

interactions with VDAC2 and RACK1. VDAC2 was found to be required for the release of cytochrome C and activation of caspases 3 or 9, resulting in apoptosis, while RACK1 acts as an antiviral protein (Lin *et al.* 2015).

1.7.5 Adaptive immunity during IBDV infection

The HVR of the VP2 capsid protein is the main target for efficient neutralisation of virus particles, resulting in protection against IBDV (Oppling *et al.* 1991). As protective levels of MAbs drop, birds 2-3 weeks of age become most vulnerable to IBDV infection (Li *et al.* 2017). The timing of vaccination is therefore vital to providing protection, as the levels of the MAbs present at the time of vaccination are inversely linked with the efficacy of the vaccine (Block *et al.* 2007; Gimeno and Schat, 2018). If administered too early, high levels of MAbs will have an inhibitory effect on the vaccine, and an adaptive immune response cannot be successfully mounted (Müller *et al.* 2003). If given too late, inadequate protection means birds will become infected with wild-type (wt) strains that can undergo antigenic drift, driving the evolution of more diverse and potentially more pathogenic viruses (Müller *et al.* 2003). Moreover, previous work has demonstrated vaccine failure in the field can lead to more pathogenic reassortant viruses emerging in commercial bird populations (Chen *et al.* 2018). The co-existence of field and vaccine strains in one environment can also lead to reassortment events as viruses continue to evolve side-by-side (Pikula *et al.* 2018). Reassortant viruses with segment A from vvIBDV and the segment B from cIBDV or vaccine strains were able to cause higher morbidity and mortality rates than viruses with both segments from the parent cIBDV or vaccine strain (Jackwood *et al.* 2016; Pikula *et al.* 2018). As these viruses can break through higher Mab titres, the vaccines currently used may not adequately protect against these reassortant strains (Jackwood *et al.* 2016).

Although the primary target of IBDV is IgM^+ B cells, macrophages, dendritic cells and heterophils have also been shown to be susceptible to infection (Lam, 1998; Khatri *et al.* 2005; Khatri and Sharma, 2007; Liang *et al.* 2015; Yasmin *et al.* 2019). A recent study by Jahromi *et al.* (2018) detected IBDV by quantitative polymerase chain reaction (qPCR) in $CD3^-/28.4^+$ intraepithelial lymphocytes (natural killer cells extracted from the duodenum of infected birds), however, the virus copy number didn't change over time and imaging of histopathology sections showed the virus was instead outside of these cells. Therefore, there remains no evidence to support that T cells are targeted by the virus. In healthy chickens, the BF is made up of approximately 98% B cells with few resident T cells, macrophages and dendritic cells (Ko *et al.* 2018; Ribatti *et al.* 2019). Previous studies have demonstrated the influx of immune cells into the BF due to IBDV replication in this target organ (Khatri and Sharma, 2007; Liang *et al.* 2015). Rautenschlein *et al.* (2002) demonstrated that T cells are instrumental in the production of protective antibodies against IBDV, as only 9% of T cell-compromised chickens were protected following challenge with a virulent strain, compared to 91% of T cell-competent chickens. The accumulation of T cells in the BF has been linked with viral replication and the up-regulation of IFNγ in this tissue, which also correlated to infection with more pathogenic strains (Rautenschlein *et al.* 2003). It is thought that a robust T cell response is responsible for clearance of IBDV infection and recovery from disease, by direct lysis of infected cells by cytotoxic CD8-positive T cells, and by providing CD4-T cell help to macrophages and dendritic cells. While T regulatory cell subsets have recently been identified (Gurung *et al.* 2017), the role of these cells in IBDV infection remains poorly understood.

1.8 IBDV host transcriptomics

1.8.1 *In vitro* studies

There are several studies in the literature that have investigated the gene expression in different cell types following IBDV infection with a range of strains *in vitro.* By studying host gene expression the key pathways activated by the host or targeted by the virus can shed light on the course of disease and how infection leads to morbidity and mortality. The 'cytokine storm' previously reported in chickens following IBDV infection (Ingrao *et al.* 2013), and that the IFN and pro-inflammatory responses intending to protect the host and clear the virus may contribute significantly to BF damage during infection with less pathogenic strains. More pathogenic vvIBDV strains have been shown to suppress these pathways to facilitate viral replication and transmission, which highlights contributions of both the host and the virus on the outcome of disease.

The cell types most commonly used in host gene expression studies have been DF-1 (Lee *et al.* 2014; Hui and Leung, 2015), CEF (Li *et al.* 2007; Wong *et al.* 2007), DT40 (Quan *et al.* 2017), HD11 (Lee *et al.* 2015) and bone marrow-derived dendric cells cultured *ex vivo* and infected *in vitro* (Yasmin *et al.* 2015). Two such studies conducted in DF-1 cells found many innate immune genes were up-regulated in response to IBDV infection, including Mx1, OAS, PKR (EIF2AK2) and IFNβ. However, the conclusions of these studies are limited by the choice of cell type and IBDV strains used. Immortalised fibroblast cells are not the target cell type for IBDV infection naturally occurring in the field, and as such field strains do not replicate in these cells without prior adaptation and subsequent attenuation (Mundt, 1999; van Loon *et al.* 2002; Escaffre *et al.* 2013; Yu *et al.* 2013). As caIBDV strains were the necessary choice for these studies, their reduced pathogenicity compared to c- and vvIBDV field strains would suggest their gene expression profiles would limit the conclusions that can be drawn. Li *et al.* (2007) and Wong *et al.* (2007) used primary CEF

cells for their gene expression studies. As these are primary cells, the results may be more relevant than in immortalised cells, however, field strains of virus are still unable to be used in these cells as they are fibroblasts, thus limiting the relevance of their findings.

One previous study used the immortalised B cell line DT40 to study gene expression in the target cell for IBDV (Quan *et al.* 2017). This study found pro-inflammatory cytokines were up-regulated, upon vvIBDV infection, causing apoptosis of infected cells. It has previously been shown *in vivo* that pro-inflammatory cytokines (e.g. IL-6, IL-8 and IL-1β) are up-regulated following the arrival of macrophages and that these cytokines contribute to the BF lesions following infection with vvIBDV (Palmquist *et al.* 2006). These cytokines were also up-regulated in a study using the HD11 macrophage cell line to study caIBDV infection (Lee *et al.* 2015). Other than being able to infect these cells with field strains of IBDV, a significant benefit to using the DT40 cell line is the ability to study IBDV-B cell interactions in the lab without requiring their extraction during *in ovo* or *in vivo* studies. However, the main drawback for using this cell line for investigating gene expression is their immortalisation using the oncogenic retrovirus avian leukosis virus (ALV), which makes it difficult to determine the effect of IBDV alone on gene expression.

Macrophages and dendritic cells are secondary targets of IBDV infection and are thought to be the first cells infected in the bird before the virus reaches the BF. Consequently, the gene expression of these cells upon infection has been investigated. Yasmin *et al.* (2015) prepared bone marrow-derived dendritic cells and infected them *in vitro* with a vvIBDV strain before comparing gene expression in infected and mock-infected cells. A range of pro-inflammatory cytokines were up-regulated in these cells including IL-1β, IL-8 and IFNγ, consistent with the results reported in Lee *et al.* (2015). A different approach was taken by Lin *et al.* (2016) where the birds were inoculated with a caIBDV strain, and the bone marrow-derived dendritic cells were prepared following infection. In this study,

the greatest differences in gene expression compared to dendritic cells prepared from mock-infected birds was in the JAK-STAT and mitogen-activated protein kinase (MAPK) signalling pathways. However, the benefit of infecting primary cells *in vitro* is the controlled conditions such as set time points, calculated multiplicities of infection and study of a single cell type compared to a whole tissue in the context of *in vivo* infection.

1.8.2 *In vivo* studies

IBDV has been studied more extensively *in vivo* than *in vitro,* with many papers comparing gene expression between strains of differing virulence, immune cell populations and timings during infection.

The immune response of different cell types during IBDV infection has been explored *in vivo* in macrophages (Khatri *et al.* 2005; Rasoli *et al.* 2015), $CD4^+$ $CD8^+$ T cells (Tippenhauer *et al.* 2013) and lymphocyte natural killer cells ($CD3^-$ 28.4^+) (Jahromi *et al.* 2018). In a study by Rasoli *et al.* (2015), the number of macrophages in the spleen of birds inoculated with a vvIBDV strain was higher than the BF earlier during infection at day 2 compared to day 4 post-inoculation. This correlated with the up-regulation of pro-inflammatory cytokines earlier during infection in the spleen compared to the BF. Another study by Khatri *et al.* (2005) found that IL-6, IL-1β and nitric oxide synthase (iNOS) were not induced before day 3 post-inoculation in the BF, supporting the conclusion made by Rasoli *et al.* (2015) that there is a delayed pro-inflammatory response in the BF following IBDV infection. Both the virulence of the IBDV strain and the host genotype have also been demonstrated to influence the T cell response to IBDV infection (Tippenhauer *et al.* 2013; Jahromi *et al.* 2018). CD3- 28.4+ Natural Killer cells up-regulated the expression of CD69, BLec and NK-lysin, cell surface receptors associated with cell activation, at day 3 post-inoculation with a vaccine strain (Jahromi *et al.* 2018). Conversely, when these cells were infected with a vvIBDV strain, the expression of these genes was suppressed as early

as day 1 post-infection. Tippenhauer *et al.* (2013) concluded from their investigations that a more highly stimulated cytokine response resulted in the faster development of BF lesions and clinical disease, and ultimately mortality in more susceptible birds. This susceptibility was linked to host genotype with layer-type breeds more vulnerable to vvIBDV infection.

As mentioned in the previous section, the timing of the innate immune response following inoculation and host genotype has been shown to be important by several groups (Ruby *et al.* 2006; Smith *et al.* 2015; Ou *et al.* 2017). Ruby *et al.* (2006) studied the immune response in different chicken lines either resistant or susceptible to IBDV infection. In resistant birds inoculated with a cIBDV strain, they found the IFN and pro-inflammatory responses were up-regulated earlier following inoculation than in susceptible chicken lines, supporting the conclusions made by Tippenhauer *et al.* (2013). Another study by Smith *et al.* (2015), found key differences in the gene expression levels in mock-inoculated resistant and susceptible chicken lines, in addition to differences following inoculation with a cIBDV strain. In susceptible birds, chemokine (C-C motif) ligand 5 (CCL5), IL-6 and IFN-induced transmembrane proteins (IFITM) 1, 3 and 5 were among the genes more highly expressed. Ou *et al.* (2017) showed the expression of immune genes was higher early during infection at day 1 post-inoculation although as the virus peaked in virus titre at day 3 post-inoculation. As metabolic pathways are activated at day 3 post-inoculation, the act of cell repair may support further replication of the virus.

In studies comparing innate immune responses to different IBDV strains, several groups have found cIBDV, vIBDV and vaccine strains induce a strong innate immune response, predominantly by up-regulating type I IFN and pro-inflammatory cytokines including IFNα, IFNβ, IL-6, IL-8 and IL-1β (Guo *et al.* 2012; Carballeda *et al.* 2014). One the contrary,

a study by Rauf *et al.* (2011) found key differences between cIBDV and vIBDV strains, whereby more pronounced BF damage, inflammatory response and infiltration of T cells was detected following cIBDV infection. This heightened response to the cIBDV may have been due to increased virus titres in the BF compared to the vIBDV strain.

Other studies have compared vvIBDV to caIBDV strains *in vivo* (Liu *et al.* 2010; Yu *et al.* 2015), reporting the up-regulation of a vast number of Th1 (IFNγ, IL-2) and Th2 (IL-4, IL-5 and IL-10) cytokines in birds inoculated with the vvIBDV compared to the cell adapted IBDV strain. However, in the Liu *et al.* (2010) study the replication of the cell adapted strain was greatly reduced compared to the vvIBDV strain, which would make the reduced immune response to infection unsurprising due to the lower virus titres. Virus replication in the Yu *et al.* (2015) study was lower for the vvIBDV strain, although the virus stock was diluted prior to inoculation, unlike the cell adapted strain. Also, this study compared the up-regulation of innate immune genes during infection with each virus to the mock phosphate-buffered saline (PBS) control, rather than to the other virus, increasing the statistical significance and drawing conclusions not completely supported by the data. Higher replication of vvIBDV strains was reported in a study by He *et al.* (2017) where they concluded TLR3, IFNβ and IL-8 expression correlated with the more virulent strain (in this case a vvIBDV strain).

A study by Eldaghayes *et al.* (2006) found more differences in the type I IFN response during infection with a vv- compared to a cIBDV strain, than in the regulation of pro-inflammatory genes. The vvIBDV down-regulated type I IFN, whereas the cIBDV appeared not to induce this pathway early during infection, suggesting these viruses have different approaches to modulating the host immune response. The main limitations of this conclusion were that different starting inoculum titres were used for each virus and that these viruses were not studied *in vivo* in the same experiment, as they were carried out

on separate occasions. Therefore, the study design should be improved in order to support these conclusions.

As chicken primary B cells could not be cultured *ex vivo* and would not survive for long once removed from the BF (Schermuly *et al.* 2015), it has previously been difficult to conduct an in-depth analysis of IBDV- B cell interactions with different field strains of IBDV. Several groups have performed *in vivo* studies which reported an increase in the expression of genes associated with type I IFN production and signalling, pro-inflammatory cytokines and apoptosis during infection with IBDV (Guo *et al.* 2012; Rasoli *et al.* 2015; Smith *et al.* 2015; Ou *et al.* 2017). Some studies found an up-regulation of pro-inflammatory cytokines including IL-6, IL-1β, IFN-γ and IRF1 (Guo *et al.* 2012; Smith *et al.* 2015), with Rasoli *et al.* (2015) also describing increased iNOS mRNA expression levels resulting in oxidative stress and cell apoptosis. The up-regulation of IFNα, IFNβ, Mx1 and Radical S-adenosyl methionine domain containing 2 (RSAD2) during infection *in vivo* identifies the type I IFN pathways as playing a key role in host-virus interactions.

While these studies provide a good insight into the effect of infection on the BF tissue, there are multiple cell types present in the population such as macrophages and dendritic cells, which also contribute to the gene expression profiles described in these studies (Lee *et al.* 2015; Lin *et al.* 2016). Identifying the direct interactions between IBDV and infected B cells is therefore difficult to tease apart from those produced by other bystander cells in response to infection. To overcome this limitation, several research groups have characterised the transcriptional response of cells infected with IBDV *in vitro* (Li *et al.* 2007; Wong *et al.* 2007; Lin *et al.* 2016; Quan *et al.* 2017).

1.9 Thesis aims and objectives

The principal aim of this thesis was to identify molecular determinants of IBDV pathogenesis, and their modulation of the host innate immune response. The following objectives were derived to test this hypothesis:

Hypothesis: Very virulent IBDV strains differentially modulate the innate immune response compared to less virulent IBDV strains

Objective 1: Use a chicken primary bursal cell *ex vivo* culture model to characterise interactions between IBDV and its target cell.

A. Optimise and validate the primary bursal cell *ex vivo* culture system for use with caIBDV and field isolates of IBDV.
B. Use bioinformatics to determine differences in B cell gene expression following infection with different IBDV strains.

Objective 2: Investigate differences in gene expression between c- and vvIBDV infection *in vitro* and *in vivo.*

A. Compare viral replication kinetics and the expression of type I IFN and pro-inflammatory genes following infection with c- and vvIBDV strains *in vitro.*
B. Study the replication kinetics, host gene expression and dissemination of c- and vvIBDV strains during infection *in vivo.*

Objective 3: Determine the role of VP4 in IBDV virulence *in vitro* and *in vivo*.

A. Characterise the IFN antagonistic role of VP4 and determine whether this function has a strain-specific phenotype.

B. Compare the interactions between the type I IFN response and IBDV VP4 from strains of different virulence *in vitro* and *in vivo.*

2. Materials and Methods

2.1 Cell lines and media

All cells were maintained at 5% CO_2 and 37°C, unless otherwise stated, and their media constituents are detailed below as final concentrations.

2.1.1 DF-1 cells

DF-1 cells are a continuous chicken fibroblast cell line originating from the spontaneous transformation of fibroblasts from 10-day-old embryos of East Lansing line chickens (Himly *et al.* 1998). Cells were grown in Dulbecco's Modified Eagle's Medium (DMEM) with high glucose and L-Glutamine (Merck) supplemented with 10% fetal bovine serum (FBS) (Gibco) and 1% sodium pyruvate (Gibco).

2.1.2 DT40 cells

DT40 cells are a continuous chicken B lymphoblast cell line derived from ALV-induced bursal lymphoma in the Hyline SC chicken line (Baba *et al.* 1985). Cells were cultured in Roswell Park Memorial Institute (RPMI) 1640 medium supplemented with 10% FBS (Gibco), 10% tryptose phosphate broth (Merck), 1% sodium pyruvate (Gibco) and 0.1% beta-mercaptoethanol (BME) (Gibco).

2.1.3 Chicken primary bursal cells

The BF was harvested from 3-week-old Rhode Island Red chickens at The Pirbright Institute (TPI) and washed in 70% ethanol followed by several washes in sterile PBS. An enzyme solution containing 8mg/mL collagenase D (Merck), 1x Hanks Balanced Salt Solution (HBSS) with calcium (Gibco) and 7.5% sodium carbonate was used to digest the BF tissue. Once digested, the tissue was passed through a 100µm Falcon™ cell strainer (Fisher Scientific) into cell medium containing 1x HBSS without calcium (Gibco), 7.5% sodium carbonate and 500mM

Ethylenediaminetetraacetic acid (EDTA) (Merck), before centrifugation at 1200 rpm for 10 mins to pellet the cells. Pelleted cells were resuspended in Iscove's Modified Dulbecco's Medium (IMDM) supplemented with 8% FBS, 2% chicken serum (Merck), insulin transferrin selenium (100µL/L, Gibco), 50mM BME (Gibco), penicillin/streptomycin (1ml/L, Gibco) and nystatin (5ml/L, Gibco), as previously described (Kothlow *et al.* 2008), so called "B cell medium" before mononuclear cells were separated by a density gradient centrifugation at 2000 rpm for 20 mins at 4°C over Histopaque 1083 (Merck). Bursal cells were washed in PBS three times, before resuspending in B cell medium in the presence of chicken CD40L (chCD40L) to enable B cell proliferation.

2.1.4 Human Embryo Kidney (HEK)-293T cells expressing msCD8- chCD40L

HEK-293T cells stably expressing a mouse CD8- chCD40L construct were generated in the lab of Dr John Young (Insititute of Animal Health, now TPI). The CD8-chCD40L construct was made by fusing the extra-cellular domains of mouse CD8α and chCD40L, before protein purification and the expression of the construct in HEK-293T cells. Cells were cultured in RPMI-1640 supplemented with L-glutamine, sodium bicarbonate (Merck), 10% FBS (Merck) and 1µg/mL puromycin (Gibco).

2.1.5 chCD40L harvest, concentration and titration

Supernatant from HEK-293T cells stably expressing the msCD8- chCD40L construct was harvested and concentrated using Pierce™ Protein Concentrators PES, 10K MWCO (ThermoFisher Scientific) at 4000 rpm for 1 hr. Concentrated chCD40L was sterilised by passing through a 0.22µM Millex-GP Syringe Filter (Merck) and stored at 4°C prior to use. In order to titrate the chCD40L, to determine the optimal concentration to use, primary bursal cells were seeded in 96 well U-bottomed plates (Fisher Scientific) and the chCD40L was added in a 10-fold series dilution. Cells were counted and viability recorded using trypan blue solution (Merck) and a TC20™ Automated Cell Counter (Bio-Rad) at 2-, 4- and 6-days post-treatment with chCD40L.

2.2 Virus techniques

2.2.1 IBDV strains

UK661: A vvIBDV strain of IBDV originally isolated by Dr Mike Skinner (Imperial College London) (Brown and Skinner, 1996) was kindly gifted by Dr Nicolas Eteradossi (ANSES, France). Virus stock was generated by inoculation and harvest of virus from the BF of 3-week-old Rhode Island Red chickens at TPI. BF tissues harvested from birds at each time point were pooled and resulting virus stocks were generated by homogenisation of the tissue (as described later in section 2.4.1) in piperazine-N,N'-bis(2-ethanesulfonic acid) (PES) buffer, comprising of 150mM sodium chloride, 20mM calcium chloride, and 25mM PIPES at a final pH of 6.2. Ultracentrifugation at 20000 rpm for 2hrs was used to for virus purification.

F52/70: A cIBDV strain of IBDV kindly donated by Dr Nicolas Eterradossi (ANSES, France), virus stocks were generated by inoculation and harvest of virus from the BF of 3-week-old Rhode Island Red chickens at TPI. Virus stocks were prepared and purified consistent with UK661 virus stocks.

D78: A caIBDV vaccine strain kindly donated by Dr Nicolas Eterradossi (ANSES, France). Virus stocks were generated by inoculating flasks of CEF cells and harvesting the supernatant upon observation of cytopathic effect. These stocks were purified by ultracentrifugation at 20000 rpm for 2hrs.

PBG98: A caIBDV vaccine strain kindly donated by Dr Mike Skinner (Imperial College London). Virus stocks were generated by inoculating flasks of CEF cells and harvesting the supernatant once cytopathic effect was observed. These stocks were purified by ultracentrifugation at 20000 rpm for 2hrs.

2.2.2 IBDV titration by tissue culture infectious dose 50% ($TCID_{50}$)

For virus titration, a 96 well U-bottomed plate (Thermo Scientific) was seeded with DT40 cells at a seeding density of $1x10^4$ cells in 180µL media. A ten-fold serial dilution was set up from 10^{-1} to 10^{-10} and 20µL of virus dilutions added to each well. Each dilution had four replicates and was incubated at 37°C for five days. Cells were then stained according to the protocol described in section 2.5.1 and wells were imaged by immunofluorescence microscopy and scored positive or negative. $TCID_{50}$/mL was calculated by the Reed and Muench method (Reed and Muench, 1938).

2.2.3 IBDV infection

For infection of cells with IBDV, DF-1 cells were seeded into plates at the seeding densities indicated in Table 1 and incubated at 37°C and 5% CO_2 overnight to allow adhesion. As DT40 and primary bursal cells are in suspension, numbers were counted and distributed into 15 or 50ml Falcon tubes for infection before centrifugation at 1100 rpm to pellet cells. Virus stocks were diluted in media to the appropriate multiplicity of infection (MOI) and added to cells either in plates or tubes, prior to incubation for an hr at 37°C and 5% CO_2. After incubation, suspension cells were centrifuged at 1100 rpm, washed with fresh media, centrifuged at 1100 rpm and suspended in fresh media before being seeded in plates. Virus media was removed from adherent cells before washing in fresh media and final addition of fresh media. All cell types were then incubated at 37°C until the chosen time points.

Table 1 Seeding densities for DF-1, DT40 and primary bursal cell cultures.

Cell	Plate well number	Seeding density (cells per well)
DF-1	12	$3.0x10^5$
	24	$1.5x10^5$
	96	$3.0x10^3$
DT40	12	$2x10^6$
	24	$1x10^6$
	96	$0.5x10^6$
Primary bursal cell	12	$2x10^7$
	24	$1x10^7$
	96	$0.5x10^7$

2.3 DNA techniques

2.3.1 Polymerase chain reaction (PCR)

Polymerase chain reaction (PCR) was performed using 1 unit of *Taq* DNA polymerase (Invitrogen) in a reaction also containing 0.2 mM of each deoxyribonucleic triphosphate (dNTPs) (Invitrogen), 0.5µM of both forward and reverse primers, 200ng DNA template, 1x PCR buffer (Invitrogen), 1.5mM $MgCl_2$ and RNase free water (Merck) added to a total reaction volume of 25µL. The cycling method was as follows: 95°C for 2 mins, 30 cycles of 95°C for 30 secs, 56°C for 30 secs, 72°C for 2 mins and 72°C for 10 mins final extension.

High fidelity PCR was performed using 0.02 units of Q5® High-Fidelity DNA polymerase (New England Biolabs (NEB)) in a reaction also containing 0.2mM of each dNTPs (Invitrogen), 0.5µM of both forward and reverse primers, 200ng of DNA template, 1X Q5® buffer (NEB) and RNase free water (Merck) added to a total reaction volume of 50µL. The cycling method was as follows: 98°C for 30 secs, 30 cycles of 98°C for 10 secs, 55°C for 30 secs and 72°C for 2 mins and 72°C for 2 mins final extension.

For detection by PCR and sequencing, oligonucleotides were designed to amplify the region of the VP4 on segment A of the virus (Table 2). All oligonucleotides were purchased from Merck.

Table 2 Primers for PCR amplification and DNA sequencing.

Name	Sequence (5’-3’)
F1676A	GGTACGAGGTAGTCGCGAATC
R1916A	CTTTGAGATGGAGGTTGGAG
R2516A	CCATTCTCTTCCAGCCACAT

2.3.2 Site-directed mutagenesis

IBDV VP4 expression plasmids tagged at the 5' end with enhanced green fluorescent protein (eGFP) were generated in the pcDNA3.1(-) vector. For single base mutagenesis of pcDNA3.1_eGFP+UK661_VP4 and pcDNA3.1_eGFP+F5270_VP4 plasmids (Table 3), NEBaseChanger v1.2.8 was used to design primers containing the desired base change (Table 4). The Q5 Site-Directed Mutagenesis Kit (NEB) was used to perform the mutagenesis starting with a PCR step, to amplify the template with the mutagenic primers, which was set up as follows: 1X Q5 Hot Start High-Fidelity Master Mix; 0.5µM forward primer; 0.5µM reverse primer; 25ng of template DNA and nuclease-free water added to a total of 25µL. Cycling conditions were performed as follows: 98°C of 30 secs; 25 cycles of 98°C of 10 secs, 68°C for 20 secs and 72°C for 30 secs; final extension at 72°C for 2 mins. The PCR product was then added to a Kinase-Ligase-DpnI (KLD) mix for circularisation and removal of template DNA, carried out as follows: 1µL of PCR product; 1X KLD Reaction Buffer; 1X KLD Enzyme Mix and nuclease-free water added to a total of 10µL. This reaction mixture was incubated at room temperature for 5 mins before 5µL of the KLD mixture was added to chemically-competent cells for transformation as previously described in section 2.3.7.

Table 3 Plasmids used in this study.

Plasmid	Expression	Tag/promoter	Source
pcDNA3.1(-)	-	-/CMV	Invitrogen
rPBG98 Segment A	Segment A from PBG98 IBDV strain	-/CAG	GeneArt, Thermofisher Scientific
rPBG98 Segment B	Segment B from PBG98 IBDV strain	-/CAG	GeneArt, Thermofisher Scientific
pcDNA3.1_eGFP	eGFP	eGFP/CMV	Designed in this study
pcDNA3.1_eGFP+UK661_VP4	eGFP-tagged UK661 VP4 protein	eGFP/CMV	Designed in this study
pcDNA3.1_eGFP+F52/70_VP4	eGFP-tagged F52/70 VP4 protein	eGFP/CMV	Designed in this study
pcDNA3.1_eGFP+UK661_VP4_KO	eGFP-tagged UK661 VP4 protein with protease function knocked out (KO)	eGFP/CMV	Designed in this study
pcDNA3.1_eGFP+F52/70_VP4_KO	eGFP-tagged UK661 VP4 protein with protease function knocked out (KO)	eGFP/CMV	Designed in this study
pcDNA3.1_eGFP+5'UK_3'F52	eGFP-tagged chimeric protein with 1-460 UK661 VP4 and 461-729 F52/70 VP4	eGFP/CMV	Designed in this study
pcDNA3.1_eGFP+5'F52_3'UK	eGFP-tagged chimeric protein with 1-460 F52/70 VP4 and 461-729 UK661 VP4	eGFP/CMV	Designed in this study
pGL3_IFNβ luciferase	Luciferase and IFNβ	-/ luciferase	Prof Steve Goodbourn, St George's, London
pGL3_Mx1 luciferase	Luciferase and Mx1	-/ luciferase	Prof Steve Goodbourn, St George's, London

Table 4 Primers designed for site-directed mutagenesis using the NEBaseChanger (NEB).

Primer name	Primer sequence (5'-3')	Plasmid template	Purpose
Q5SDM_UK/F52/KO_F	CCGCGGTGCACCGAACCTCGACT	pcDNA3.1_eGFP+UK661_VP4 pcDNA3.1_eGFP+F52/70_VP4	Knock-out protease function
Q5SDM_UK/KO_R	AGTATCCCGGGTGAAGCG	pcDNA3.1_eGFP+UK661_VP4	Knock-out protease function
Q5SDM_F52/KO_R	AGTACCCCAGGTGAAGCAAG	pcDNA3.1_eGFP+F52/70_VP4	Knock-out protease function

2.3.3 Gel electrophoresis

To separate and visualise DNA fragments by gel electrophoresis, 1% agarose (Merck) solution was prepared using 1x Tris-borate EDTA (TBE) buffer (Invitrogen) and 1x SYBR Safe (Invitrogen). The gel was submerged in 1x TBE buffer and an equal volume of GeneRuler 1Kb Plus DNA Ladder (Thermo Scientific) and DNA samples containing DNA loading buffer (Thermo Scientific) were loaded. Gels were run at 100V for approximately 1 hr and visualised using a Gel Doc EZ Gel Documentation System (Bio-Rad).

2.3.4 Gel extraction/ PCR purification

DNA products from PCR or digested fragments were purified using the Monarch PCR & DNA Cleanup Kit (NEB) according to manufacturer's instructions and eluted into a total volume of 10µL of elution buffer (NEB). DNA products were excised form the gel using a scalpel and the DNA extracted using the Monarch DNA Gel Extraction Kit (NEB) according to manufacturer's instructions also eluted into 10µL of elution buffer (NEB).

2.3.5 Restriction digest

Restriction digests were performed as double-digests with restriction enzymes from NEB selected using the NEBcutter 2.0 tool (Vincze *et al.* 2003). Reactions were set up as standard using 1 unit of each restriction enzyme, 1x NEBuffer, 1µg of template complimentary DNA (cDNA) and RNase-free water to a total volume of 25µL, before incubation for 1 hr at 37°C. Enzymes were selected based on 100% buffer compatibility. Digested DNA plasmids were then gel purified according to sections 2.3.3 and 2.3.4, and DNA inserts were purified as detailed in section 2.3.4.

2.3.6 Ligation

DNA constructs were ligated into the desired vector using T4 DNA ligase (NEB) according to manufacturer's instructions. Ligation was performed with 1 unit of T4 DNA ligase, 2µL 1x DNA ligase buffer (NEB), an insert: vector molar ratio of 3:1 or 5:1 and nuclease-free water (Merck)

to a final volume of 20µL. The reaction was incubated at room temperature for 10 mins or at 16°C overnight.

2.3.7 Transformation

The ligation mixture was transformed into NEB® Turbo Competent *E. coli* (High Efficiency) cells (NEB) by adding 5µL ligation mixture to 45µL cells and incubating on ice for 30 mins. Cells were then heat-shocked at 42°C for 30 secs before incubation on ice for 2 mins. Super optimal broth with catabolite repression (SOC) media (NEB) was added to the cells and the mixture was incubated at 37°C for 1 hr while shaking at 200 rpm. The transformation mix was applied to Lysogeny Broth (LB) agar plates containing ampicillin (100µg/mL, Merck) or kanamycin (50µg/mL, Merck) as appropriate. Plates were incubated for 16 hrs overnight at 37°C.

2.3.8 Plasmid Miniprep

Bacterial colonies grown on agar plates were picked and cultured overnight at 37°C in a shaking incubator in 2mL LB broth and either 100µg/mL ampicillin or 50µg/mL kanamycin as appropriate. The bacterial culture was purified using the Monarch Plasmid Miniprep Kit (NEB) according to manufacturer's instructions. A colony PCR was performed with *Taq* polymerase (Invitrogen) on the plasmids, as detailed in 2.3.1, and positive PCR products were sequenced by Sanger sequencing.

2.3.9 Plasmid Maxiprep

Colonies were picked and grown in 2mL LB containing 20mg/mL of ampicillin or 25mg/mL of kanamycin for 6-8 hrs at 37°C in a bacterial shaker. Cultures were then transferred to 150mL of LB containing the same antibiotic and incubated overnight at 37°C in a shaking incubator. Glycerol stocks were made for each colony by mixing 150µL glycerol and 850µL bacterial culture and stored at -80°C. Plasmids were extracted and purified using the Plasmid DNA Maxiprep Kit (Qiagen) according to manufacturer's instructions. Plasmids were reconstituted in 100µL of

RNase-free water (Merck) and DNA concentration determined by NanoDrop Lite spectrophotometer (Thermo Scientific). Plasmids were sequenced by Sanger sequencing.

2.3.10 DNA sequencing

Plasmids and PCR products were sequenced by Eurofins-GATC. Reactions contained 5uL of primer at 5pmol/µL and 5µL of DNA product at 50-100ng/µL. Primers used for sequencing are listed in table 2.

2.4 Transcriptional analysis

2.4.1 RNA extraction from cells and animal tissues

Cells were lysed in RLT buffer (NEB) and RNA was extracted using a Monarch Total RNA Miniprep Kit (NEB) according to manufacturer's instructions including the optional RNase-free DNase on-column digestion. RNA was eluted into 30µL RNase Free Water (NEB) and quantified on a NanoDrop Lite spectrophotometer (Thermo Scientific).

For the extraction of RNA from BF tissue, 600uL RLT buffer was added to 30mg of tissue in a 2mL round-bottomed tube (Eppendorf) containing a 5mm stainless steel bead (Qiagen) and homogenised for 4 mins at 20Hz using a TissueLyser II (Qiagen). The remaining steps of the method was carried out using the Monarch Total RNA Miniprep Kit (NEB) according to manufacturer's instructions and eluted as detailed previously.

2.4.2 Reverse transcription

Complementary DNA (cDNA) was generated using SuperScript III Reverse Transcriptase (Invitrogen), starting with between 100ng and 500ng RNA. The reaction was set up with 0.5mM of dNTPs, 10ng/µL of Random primer (10uM) and nuclease free water to a total of 13µL before a thermocycling step of 65°C for 5 mins. After this step, 1X First Strand Buffer, 0.1M of DTT, 40U/µL of RNAseOUT and 200U/µL of Superscript III Reverse Transcriptase was added to the reaction and thermocycling resumed with the following conditions: 25°C for 10 mins, 50°C for 60 mins and 70°C for 15 mins. The resulting cDNA was then diluted 1:10 prior to downstream applications.

2.4.3 Taqman qPCR

Quantitative PCR (qPCR) was performed using 1X TaqMan™ Universal qPCR Master Mix (Applied Biosystems) according to manufacturer's instructions; with 0.2µM each primer and 0.25µM probe in a 10µL reaction containing 100ng cDNA. Amplification and detection of targeted genes

was performed with a QuantStudio™ 5 qPCR machine (Applied Biosystems) with the following cycling conditions: 50°C for 5 mins, 95°C for 2 mins, 40°C cycles of 95°C for 3 secs and 60°C for 30 secs.

Table 5 Primers used in this study for qPCR.

TPI= The Pirbright Institute

Name	Sequence (5'-3')			Source
	Forward	Reverse	Probe	
IBDV	GAGGTGGCCGACCTCAACT	GCCCGGATTATGTCTTTGAAG	FAM-CCCCTGAAGATTGCAGGAGCATT-TAMRA	Dr Andrew Broadbent, TPI
IL-6	AACATGCGTCAGCTCCTGAAT	TCTGCTAGGAACTTCT CCATTGAA	SYBR Green	Dr Joe James, TPI
IL-1β	GCTCTACATGTCGTGTGTGATGAG	TGTCGATGTCCCGCATGA	SYBR Green	Dr Joe James, TPI
IL-8	GCCCTCCTCCTGGTTTCAG	TGGCACCGCAGCTCATT	SYBR Green	Dr Joe James, TPI
Mx1	CACACCCAACTGTCAGCGAT	ATGTCCGAAACTCTCTGCGG	SYBR Green	Giotis *et al.* 2017
IFNα	CCACCGCTACACCCAGCACC	ATGGTGAGGTGAAGGTTGCGA	SYBR Green	Giotis *et al.* 2017
IFNβ	CAGTCTCCAGGGATGCACAG	GAGAAGGTGGTGGTGAGAGC	SYBR Green	Giotis *et al.* 2017
GAPDH	GGTGGTGCTAAGCGTGTTA	CCCTCCACAATGCCAA	SYBR Green	Staines *et al.* 2016
RPLP0	TTGGGCATCACCACAAAGATT	CCCACTTTGTCTCCGGTCTTAA	SYBR Green	Staines *et al.* 2016
TBP	CTTCGTGCCCGAAATGCT	GCGCAGTAGTACGTGGTTCTCTT	SYBR Green	Staines *et al.* 2016
RPL13	TCGTGCTGGCAGAGGATTC	TCGTCCGAGCAAACCTTTTG	SYBR Green	Staines *et al.* 2016
B2M	AAGGAGCCGCAGGTCTAC	CTTGCTCTTTGCCGTCATAC	SYBR Green	Staines *et al.* 2016
ALAS1	GGTGGACAGGAAAGGTAAAGA	ACTGGTCATACTGGAAGGTG	SYBR Green	Li *et al.* 2013a
GNB2L1	GCAGCAACCCCATCATTGTC	ATTCAGGTCCCACAGCATGG	SYBR Green	Zhang *et al.* 2015
ACTB	CAGGTCATCACCATTGGCAAT	GCATACAGATCCTTACGGATATCCA	SYBR Green	Staines *et al.* 2016
PGK1	GTTTATGTCAATGATGCTTTTGGAA	GCCTTTGCAAAATAATCCAGTTCT	SYBR Green	Staines *et al.* 2016
HMBS	GGTTGAGATGCTCCGTGAGTTT	GGCTCTTCTCCCCAATCTTAGAA	SYBR Green	Staines *et al.* 2016
HPRT1	TGGTCAAAAGAACTCCTCGAAGT	TGTAATCGAGGGCGTATCCAA	SYBR Green	Staines *et al.* 2016

2.4.4 SYBRgreen qPCR

The SYBRgreen qPCR was performed using Luna® Universal qPCR mix (NEB) according to manufacturer's instructions; with 0.25µM each primer in a 10µL reaction containing 100ng cDNA. Amplification and detection of targeted genes was performed with the QuantStudio™ 5 qPCR machine (Applied Biosystems) with the following cycling conditions: 95°C for 20 secs, 40 cycles of 95°C for 1 sec and 60°C for 20 secs, then a melt curve step at 95°C for 1 sec, 60°C for 20 secs and 95°C for 1 sec.

2.4.5 GeNorm

In order to select the most appropriate reference genes for qPCR data normalisation, a GeNorm analysis was performed. Briefly, the C_T values for each candidate reference gene tested across a subset of samples was calculated using the QuantStudio™ Design & Analysis Software v1.3.1 (Applied Biosystems). Raw Cq values were exported as xls. Files were imported into the qbase+ real-time qPCR software version 3.0 (Biogazelle). The software uses the geNorm algorithm (Vandesompele *et al.* 2002) to calculate the geNorm M and V values representing the stability of each reference gene and the optimal number of reference genes to ensure stability, respectively.

2.4.6 qPCR analysis

To calculate the fold change in gene expression sample C_T values were first normalised to the housekeeping genes identified as the most stable by the GeNorm analysis, as per the $2^{-\Delta Ct}$ method. Data were then expressed relative to the mock control samples as per the $2^{-\Delta\Delta CT}$ method.

2.5 Immunostaining

2.5.1 Fluorescence and confocal microscopy

Cells were fixed in 4% paraformaldehyde (Merck) for 30 mins at room temperature and transferred to U-bottomed 96-well plates (Thermo Fisher Scientific). Cells were permeabilised using 0.5% Triton X-100 (Merck) for 30 mins at room temperature, blocked with 4% bovine serum albumin (BSA) (Merck) for 30 mins at room temperature on a rotating platform and then stained with a primary monoclonal antibody diluted in BSA and incubated for 1 hr at room temperature, alongside with stained with 4',6-Diamidino-2-Phenylindole, Dihydrochloride (DAPI). Information on the antibodies is given in Table 6. After three washes in PBS, the cells were incubated for 1 hr with the secondary antibody in the dark. Suspension cells were pelleted by centrifugation at 1100 rpm for 5 mins between each step, and the supernatant removed. Stained cells were viewed with a Leica SP5 confocal microscope.

Table 6 Antibodies and dyes used in this study for immunofluorescence (IF).

Antibody	Primary or secondary	Target	Application	Dilution	Source
Anti-VP2	Primary	IBDV VP2	IF	1:400	Clone JF7-PD5 (Wark, 2000)
Alexa Fluor® 488 Goat anti-Mouse IgG	Secondary	Mouse IgG Fc	IF	1:200	Invitrogen
DAPI stain	-	dsRNA	IF	1:20000	Merck
Trypan blue	-	-	Live cell counting	-	Merck

2.6 Cellular pathway methods

2.6.1 Transfection

DF-1 cells were seeded into a 24 well plate at a density of $1.5x10^5$ cells/well and incubated for 24 hrs at 37°C and 5% CO_2 for cell adhesion until 80% confluency. Cells were transfected with expression plasmids using Lipofectamine™ 2000 (Invitrogen). For the transfection mixture, 50µL of Opti-MEM (Gibco) was mixed with 2.5µL of Lipofectamine ™ 2000 in one tube and 50µL Opti-MEM was mixed with 500ng plasmid in another tube, before their separate incubation for 5 mins at room temperature. These two mixtures were then combined in one tube and incubated together at room temperature for 20-25 mins. Following incubation, 450µL of fresh DMEM was added to cells before the addition of 50µL/well of transfection mixture. Cells were incubated at 37°C until the appropriate time point.

2.6.2 IFN reporter assay

To measure type I IFN production and signalling, pGL3 Luciferase reporter plasmids were used containing the promoter regions for either IFNβ or Mx1 upstream of a Firefly luciferase gene. Cells were transfected in triplicate according to section 2.6.1 with 40ng Renilla luciferase pCAGGs expression plasmid and 80ng IFNβ or Mx1 luciferase reporter plasmid. To stimulate IFNβ production, polyinosinic: polycytidylic acid (poly I:C) was transfected, according to section 2.6.1, 24 hrs after luciferase transfection. Recombinant IFNα produced as described in Laidlaw *et al.* (2013) and Buttigieg *et al.* (2013) (gift from Dr Stathis Giotis) was used to stimulate Mx1 expression. Recombinant IFNα was transfected, according to section 2.6.1, 24 hrs after luciferase transfection. Cells were lysed 6 hrs after poly I:C or IFNα transfection using 100µL 1X passive lysis buffer (Promega). Plates were frozen for 30 mins at -80°C and thawed before reading on the GloMax Multi plate reader (Promega). Once thawed, 10µL sample was added in triplicate to a 96 well opaque white plate (Pierce) and analysed on the plate reader using Stop and Glo reagents (Promega) according to manufacturer's instructions. Firefly and Renilla values

were recorded and Firefly luciferase values were normalised to Renilla values. The effect of the viral VP4 gene on IFN production and signalling was determined by co-transfecting 500ng expression plasmids expressing eGFP-tagged VP4 and eGFP controls, along with the IFNβ and Mx1 reporter plasmids as described in the relevant results chapter.

2.7 *In vivo* techniques

2.7.1 Ethics statement

Chickens of the Rhode Island Red line were provided by the National Avian Research Facility (NARF) for *in vivo* studies and for extraction of tissues for cell isolation. Briefly, embryonated eggs were shipped from NARF to TPI and birds were hatched and reared in an SPF facility at TPI. All animal procedures conformed to the United Kingdom Animal (Scientific Procedures) Act 1986 under Home Office Establishment, Personal and Project licences, following approval of the internal Animal Welfare and Ethic Review Board (AWERB) at TPI.

2.7.2 *In vivo* infection model

For the *in vivo* study in chapter 4, chickens were randomly allocated into three groups, two with 18 birds and one with 6 birds, before wing-tagging at one week old. At three weeks old, one group of birds was inoculated with 100µL PBS, one group was inoculated with F52/70 and one group was inoculated with UK661. A dose of $1.8x10^3$ $TCID_{50}$/ bird, was delivered intranasally with approximately 50µL inhaled by each nostril. Clinical scores were measured twice daily according to a semi-cumulative points-based scoring system that characterised disease as mild (0-7), moderate (8-11) or severe (12-17) (Appendix A). Six birds from both infected groups were humanely culled by cervical dislocation at 24, 48 and 72 hrs post-inoculation, and all six birds from the mock-infected group were culled at 72 hrs post-inoculation. Tissues were harvested at post-mortem for downstream analysis. Buccal and cloacal swabs were obtained at 24, 48 and 72 hrs post-inoculation to quantify virus shedding with sterile polyester tipped swabs (Fisher Scientific) and stored in the media described in section 2.1.2.

The second *in vivo* study found in chapter 5 was performed with minimal changes to the study described above. This study comprised of four infection and one mock group each containing 18 birds, with 6 birds to be culled at each time point. These birds were also wing-tagged at one week old. At three weeks old, the four infection groups were inoculated intranasally with

$1.8x10^3$ $TCID_{50}$/ bird of either the PBG98, PBG+F52/70 VP4, PBG+UK661 VP4 or UK661 viruses, while the mock group were inoculated with 100µL PBS. The clinical scores of these birds were measured twice daily according to the points-based scoring system described above (Appendix A). Six birds from each group were culled at days 2, 4 and 14 post-inoculation by cervical dislocation and these birds were bled for downstream serology analysis.

2.7.3 Processing and storage of infected tissues

At post-mortem tissues were harvested and stored for downstream processing. For B cell isolation and *ex vivo* culture, the birds were culled by cervical dislocation and head removal with scissors to allow for bleeding. BF tissues were stored in PBS at 4°C and transported quickly to the lab for the cell extraction. These BF tissues were pooled prior to downstream processing (section 2.1.3) and the B cell population cultured from these tissues were therefore from multiple birds. BFs harvested during the *in vivo* study were separated equally into three sampling tubes: one in RNAlater for RNA extraction; one snap frozen for $TCID_{50}$ and the remaining stored in 20% sucrose overnight at 4°C before being snap frozen in optical coherence tomography (OCT) compound for cryosectioning and immunohistochemistry. Caecal tonsil contents removed from the tissue and spleens were also stored in RNAlater at -80°C for RNA extraction at a later date (see section 2.4.1).

2.8 Bioinformatics

2.8.1 Sequence analysis

Sequence alignments were performed using Clustal Omega© and managed in the SSE v1.2 bioinformatics program. This program was also used to design primers and construct plasmids.

2.8.2 Microarray

2.8.2.1 Microarray preparation

Microarray data were generated and analysed by Dr Stathis Giotis at Imperial College London. Briefly, the microarray was carried out using the GeneChip 3' IVT Express Kit (Affymetrix) according to manufacturer's instructions. Hybridisation of RNA to chips and scanning of the arrays was carried out by the Medical Research Council's Clinical Sciences Centre (CSC) Genomics Laboratory, Hammersmith Hospital, London, UK. RNA was hybridised to GeneChip Chicken Genome Array chips (Affymetrix) in a GeneChip Hybridisation Oven (Affymetrix) for 16 hrs at 45°C and 60 rpm, before staining and washing of the chips on a GeneChip Fluidics Station 450 (Affymetrix). Arrays were scanned in a GeneChip Scanner 3000 7G with autoladder (Affymetrix). Gene-level expression signal estimates were derived from CEL files generated from raw data using the multi-array analysis (RMA) algorithm implemented from the Affymetrix GeneChip Command Console Software v3.0.1.

2.8.2.2 Data analysis

Processing and filtering of the data was done using the Partek Genomics Suite software v6.6. This included RMA background correction, quantile normalisation across all chips in the experiment, $\log_2$ transformation and median polish summarisation. For the data analysis a one-way ANOVA adjusted with the Benjamini-Hochberg multiple-testing correction (false discovery rate (FDR) of $P<0.05$) (Benjamini and Hochberg, 1995) was performed with the Partek Genomics Suite v6.6 across all samples. Principal Component Analysis (PCA), also performed with the

Partek Genomics Suite (v6.6), confirmed the lack of variability among infected samples. Comparisons were conducted between virus- and mock-infected samples and a fold change of $\geq\pm1.5$ and P value of ≤0.05 were used as the cut-off criteria for analysis. The Affymetrix chicken genome arrays contain probe sets for detecting IBDV in addition to 16 other avian viruses, thus enabling the confirmation of viral infection. The original microarray data produced during this study was deposited in the public database ArrayExpress (http://www.ebi.ac.uk/microarray-as/ae/), with the accession number E-MTAB-5947, according to MIAME guidelines. Data mining and enrichment analysis was performed using the MetaCore software suite (Clarivate Analytics, https://clarivate.com/products/metacore/). Enrichment analysis involved mapping gene IDs of datasets onto gene IDs of human orthologues in entities of built-in functional ontologies represented in MetaCore by pathway maps and process networks. Statistical significance was measured according to the number of genes mapping onto a given pathway and were calculated based on P value, based on hypergeometric distribution (a built-in feature of Metacore).

2.8.2.3 Microarray validation

A two-step RT-qPCR was performed on RNA samples to validate the microarray data, as described in sections 2.3.1 and 2.4.2. RNA was first reverse-transcribed into cDNA using the QuantiTect Reverse Transcription Kit (Qiagen) according to manufacturer's instructions. Resulting cDNA was used to carry out a qPCR in a 384-well plate with an ABI-7900HT Fast qPCR system (Applied Biosystems). The reactions were set up with 5µL of Mesa Green qPCR MasterMix (Eurogentec) and 2µL of sample cDNA, before amplification conditions of 95°C for 15 secs; 40 cycles of 95°C for 15 secs, 57°C for 20 secs and 72°C for 20 secs; 95°C for 15 secs, 60°C for 15 secs; and 95°C for 15 secs. Output Ct values were analysed using SDS v2.3 and RQ Manager v1.2 (Applied Biosystems). Gene expression data were normalised against the housekeeping gene GAPDH and compared to the mock controls using the $2^{-\Delta\Delta CT}$ method. All samples were loaded in triplicate.

2.8.3 Next generation sequencing

2.8.3.1 Library construction

Library construction was carried out by Beijing Genomics Institute (BGI) where they performed the following instructions. The workflow started with the purification of poly-A containing mRNA molecules using poly-T oligo-attached magnetic beads (NEB). After this step, the mRNA was fragmented (RNA fragmentation reagents kit, Ambion) into shorter mRNA using divalent cations under an elevated temperature. Reverse transcriptase and random primers (both Invitrogen) were then used to synthesise first strand cDNA from the cleaved RNA fragments generated in the previous step. The second strand cDNA synthesis used DNA Polymerase I (NEB) and RNase H (Invitrogen), and removed the RNA template synthesising a replacement strand switching dUTP to dTTP for the generation of ds cDNA. The incorporation of dUTP reduced the amount of available second strand during amplification, as the polymerase does not incorporate the sequence past this nucleotide. The cDNA fragments produced during the previous step had the addition of a single 'A' base and subsequent ligation of the adapter. Finally, the products were purified and enriched by PCR before purification with the MinElute PCR Purification Kit (Qiagen) and eluted in EB buffer (Qiagen). These purified PCR products were the cDNA library used in later RNA-seq stages.

2.8.3.2 RNA-seq and bioinformatics analysis

RNA-seq read processing was performed by BGI on the Illumina HiSeq2500. Following sequencing, initial analysis was conducted by BGI using SOAPnuke software (v1.5.5) to filter the sequence reads with the following parameters: *-n 0.1 -l 20 -q 0.4 -i -A 0.25 -Q 2 -G --seqType 1*. Reads with adaptors were removed, as were reads with unknown bases at a frequency of >0.1%. Reads comprising of over 40% of bases with a quality score for each individual base of less than 20, were determined as low quality and these reads were removed. The remaining reads were defined as 'clean reads' and stored in FASTQ format. FASTQ files were imported into CLC bio's

Genomics Workbench (CLC bio, Qiagen Bioinformatics, Aarhus, Denmark), quality-controlled and processed from this point using CLC bio v10.1.1. Downstream analysis including pathway analysis and the generation of Venn diagrams was performed by Dr Mike Skinner (Imperial College London). Following quality control, reads were subjected to quality trimming before mapping to ENSEMBL galGal5 assembly annotated genes (release 89) for quantitative analysis of expression. Fold change and False Discovery Rates (Bonferroni) were calculated using CLC bio's Differential Expression for RNA-Seq tool (v0.1). Data mining and enrichment analysis was conducted using Genego, which is part of the MetaCore software suite (Clarivate Analytics). For the enrichment analysis, chicken gene IDs were mapped from the datasets onto the gene IDs of human orthologues as entities of built-in functional ontologies, represented in MetaCore by pathway maps and process networks. The statistical significance was measured by the number of genes that map onto a given pathway, and was calculated using the p-value, based on hypergeometric distribution (a built-in feature of MetaCore). Full enrichment analysis included enrichment by gene ontology (GO) processes, process networks, pathway maps and protein function. This analysis was performed using the MetaCore transcription regulation algorithm.

2.8.4 Statistical analysis

All statistics in this study, unless otherwise stated, were performed using the statistical function on Minitab v19 or GraphPad Prism v7. Statistical tests included a two-tailed unpaired student's t-test, one-way and two-way ANOVAs with a Tukey's multiple comparison test, Kruskal-Wallis and Dunn's multiple comparisons test, and Shapiro-Wilk normality test to check the normal distribution of data sets. P values <0.05 were considered significant ($*P \leq 0.05$, $**P \leq 0.01$, $***P \leq 0.001$, $****P \leq 0.0001$) and values >0.05 were considered not significant (NS).

3. Developing an *ex vivo* IBDV infection model

The work presented in this chapter has been peer-reviewed and published in "Differential gene expression in chicken primary B cells infected ex vivo with attenuated and very virulent strains of infectious bursal disease virus (IBDV)" Dulwich and Giotis et al. Journal of General Virology, 2017.

3.1 Background

An *ex vivo* B cell culture system was recently developed, where B cells were cultured in the presence of soluble chCD40L allowing proliferation of B cells rather than apoptosis. chCD40L is required for B cell proliferation, therefore the identification of chCD40L in the lab of John Youngs (Tregaskes *et al.* 2005), enabled the development of a soluble chCD40L construct that could support the proliferation of B cells *in vitro* (Kothlow *et al.* 2008). This system was consequently used for the study of MDV replication by Schermuly *et al.* (2015). As the chicken B cell is essential to studying IBDV pathogenesis, this B cell culture system was optimised for IBDV infection. Studying IBDV in primary B cells would identify host-virus interactions during natural infection that previous *in vitro* and *in vivo* studies may have missed. Furthermore, the insights provided could be exploited to develop novel strategies for controlling IBDV.

3.2 Chapter Aims

The focus of this chapter was to use the chicken primary bursal cell *ex vivo* culture model to characterise interactions between IBDV and its preferred target cell. The primary bursal cells were cultured in the presence of chCD40L and infected with the vvIBDV strain UK661 and caIBDV vaccine

D78 strain, before transcriptional analysis to identify key differences in the gene expression of cells infected with these two viruses.

3.3 Results

3.3.1 Chicken primary B cells can be cultured in the presence of chCD40L

To validate and optimise the B cell *ex vivo* culture system previously described by Schermuly *et al.* (2015) and Kothlow *et al.* (2008), a soluble chCD40L construct (generated in the lab of Dr John Young, then Institute of Animal Health, now TPI) was supplemented to growth media and the number of live cells and the cell viability was determined daily for 6 days post-treatment (methods section 2.1.5). Mock-treated cells showed no increase in the number of live cells or cell viability for the duration of the experiment by trypan blue staining (Figure 5). Primary B cells treated with chCD40L showed an increase in both number and viability of live cells, with more than a 3-fold increase in live cells compared to mock-treated cells at 3 days post-treatment ($P<0.05$). These data suggest the treatment of primary B cells with chCD40L stimulates their proliferation, leading to a higher number of live cells and steady cell viability.

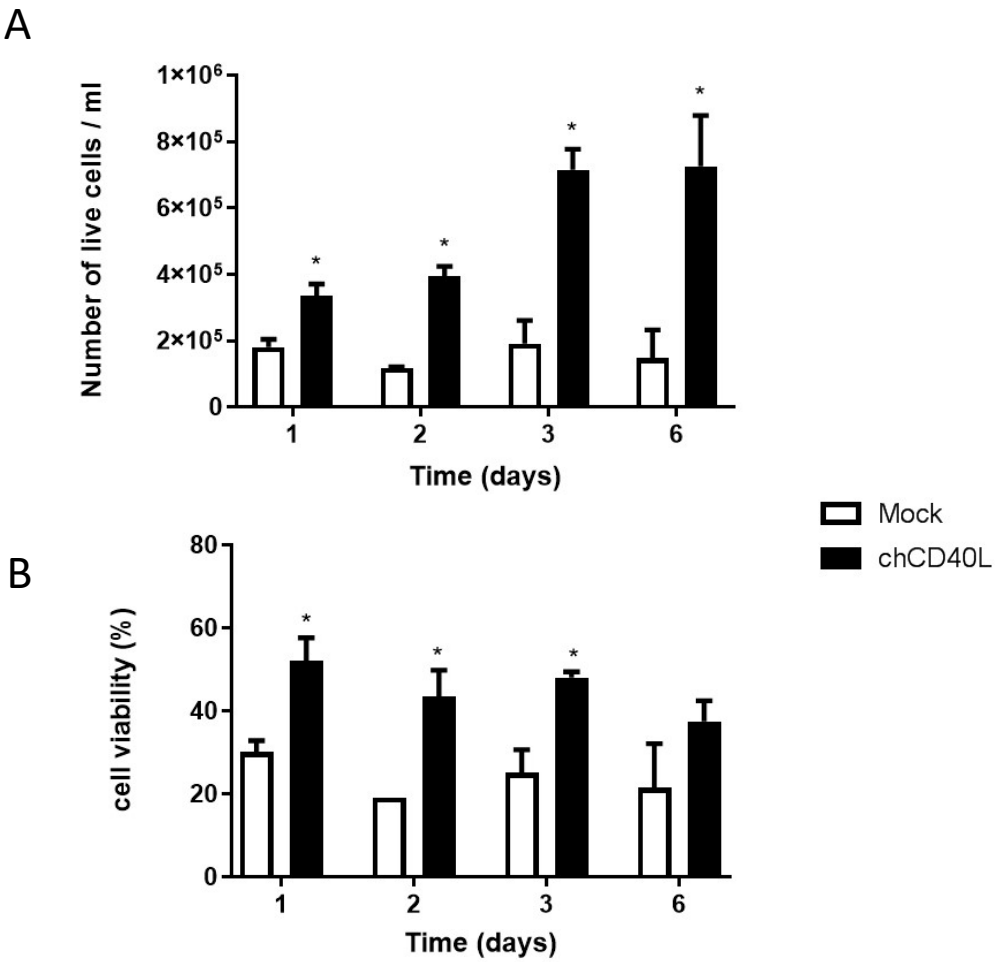

Figure 5 Chicken primary B cells cultured in media supplemented with chCD40L.

Primary B cells were cultured in the presence (black bars) or absence (white bars) of chCD40L, the number of live cells (A) and percentage of viable cells (B) were subsequently recorded at the indicated time points. Data shown are representative of at least three replicate experiments, with error bars representing the standard deviation of the mean as calculated by a two-tailed unpaired Student's t-test at each time point, *P<0.05.

3.3.2 Chicken primary B cells can support the replication of both caIBDV and vvIBDV strains

To validate this model for studying IBDV pathogenesis, primary B cells were infected with either the caIBDV D78 or vvIBDV UK661 strains at a MOI of 3 on day 3 post-BF extraction. A sample from each infected or mock-infected culture was fixed, labelled with an antibody against the IBDV VP2 protein and imaged by confocal microscopy to identify infected cells (methods section 2.5.1). Visualisation of the labelled cells revealed the presence of infected cells in the D78- and UK661-infected cultures (Figure 6A). A 'ring' of green fluorescence was observed surrounding the nucleus which indicates the presence of virus in the cytoplasm.

RNA was extracted from remaining cells before reverse transcription and amplification of viral transcripts by qPCR (methods section 2.4.2-2.4.3). Compared to mock-infected cells, the fold change in viral RNA in both D78- and UK661-infected cells was increased at all four indicated time points (Figure 6B). While D78 initially replicated more than UK661 at 5 and 8 h.p.i, there was no significant difference in replication between the strains by 24 h.p.i (*$P<0.05$, ***$P<0.001$). These data demonstrate primary B cells cultured *ex vivo* can be successfully infected with both caIBDV and vvIBDV strains, this is in contrast to CEF cells or the immortalised fibroblast chicken cell line DF-1, which do not support replication of vvIBDV strains. Therefore, these cells could be used to study the transcriptional response to infection with different strains of IBDV.

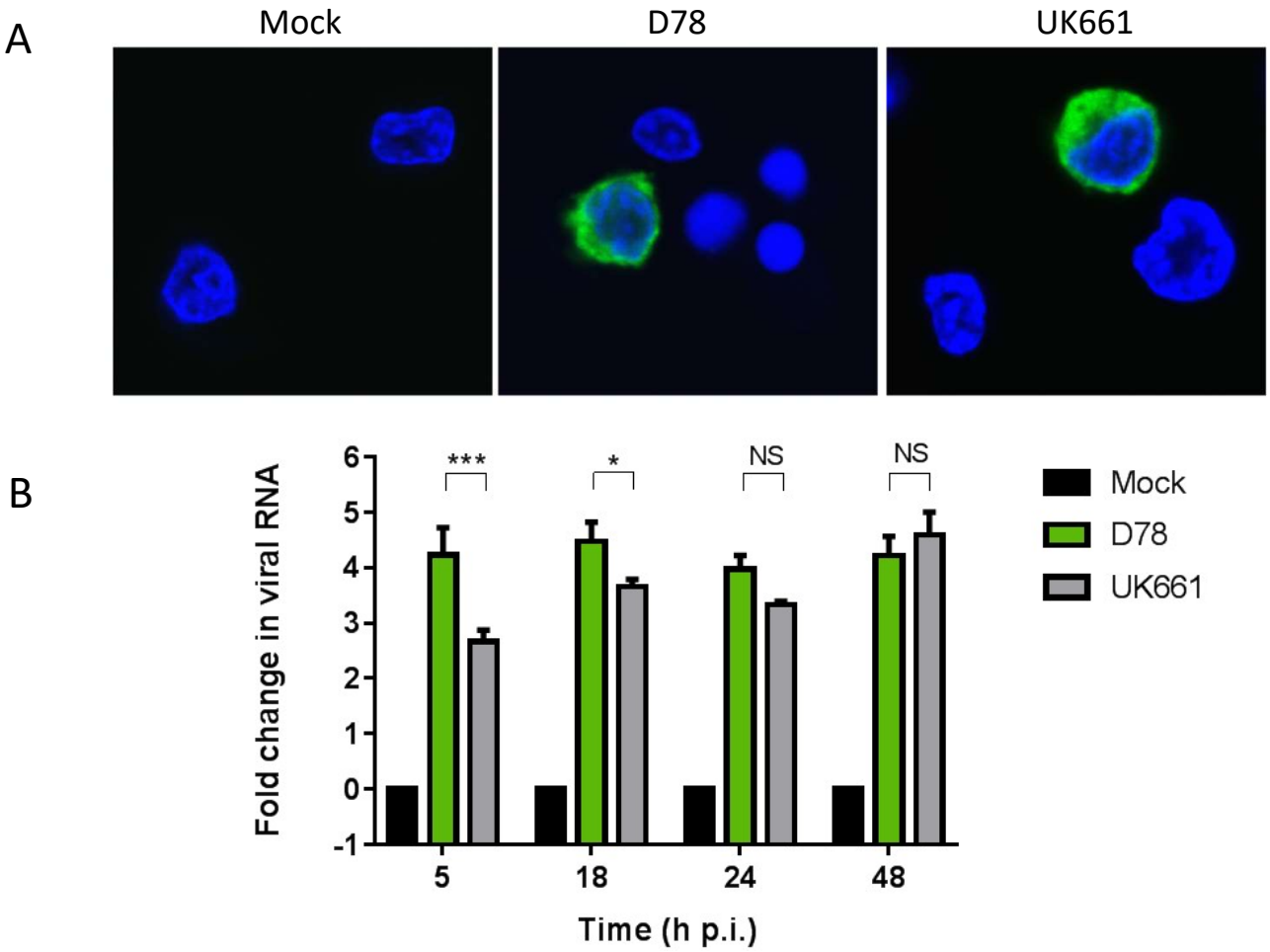

Figure 6 Chicken primary B cells can support the replication of caIBDV and vvIBDV strains.

B cells were either mock- (black), D78- (green) or UK661-infected (grey), and a sample from each infection was fixed, labelled and imaged: IBDV VP2, green; nuclei, blue (A). RNA was extracted from cells at the indicated time points post-infection, reverse transcribed and a conserved section of the VP4 gene was amplified by qPCR (B). VP4 gene Ct values were normalised to the TBP housekeeping gene as per the $2^{-\Delta CT}$ method and subsequently passed a Shapiro-Wilk normality test before being analysed using 2-way ANOVA and a Tukey's multiple comparison test (NS, not significant; *P<0.05; ***P<0.001). Data were expressed as $\log_{10}$-fold change in VP4 RNA relative to mock-infected samples as per the $2^{-\Delta\Delta CT}$ method. Data shown are representative of at least three replicate experiments, and error bars indicate the standard deviation of the mean.

3.3.3 Chicken primary B cells infected with caIBDV D78 and vvIBDV UK661 show a differential gene expression profile

Having shown that primary B cells can support the replication of ca- and vvIBDV, the differential gene expression in cells infected with D78 and UK661 was assessed by qPCR and microarray to identify key differences in B cell-virus interactions. The cDNA generated from infected cells in section 3.3.2 was used to measure the gene expression of IFNβ and IFIT5 in cells infected with either D78 or UK661. Compared to mock-infected cells and the housekeeping gene TATA box binding protein (TBP), expression of IFNβ was significantly higher in D78- than UK661-infected cells at 18, 24 and 48 h.p.i (****P<0.0001) (Figure 7A). In D78-infected cells, IFNβ expression peaked at 24 h.p.i while expression was consistently low in UK661-infected cells over all time points, with no significant difference to mock-infected cells. IFIT5 expression followed a trend consistent with IFNβ, as infection with the D78 virus induced a greater IFIT5 expression than UK661 at 18, 24 and 48 h.p.i (***P<0.001, ****P<0.0001 and *P<0.05, respectively) (Figure 7B). This gene expression analysis indicates that UK661 infection is associated with reduced expression of IFNβ and IFIT5, and so may dampen innate immune responses in B cells.

Following on from the qPCR data, we used a microarray targeting transcripts from the chicken genome. This method allowed us to conduct a screen of the infected cells 18 h.p.i as virus titres were high for both viruses at this time point but there was still a significant difference in replication. We identified pathways significantly altered by each of these viruses. Data were analysed to identify individual genes (Partek Genomics Suite) and pathways (MetaCore) that were up- or down-regulated during infection with each virus. Using PCA, mock-, D78- and UK661-infected individual samples mapped closely to each other in a cluster, meaning there were minor variations within replicates of each

infection sample group. In contrast to this, sample groups mapped separately to each other, indicating their transcriptional distinctiveness from one another.

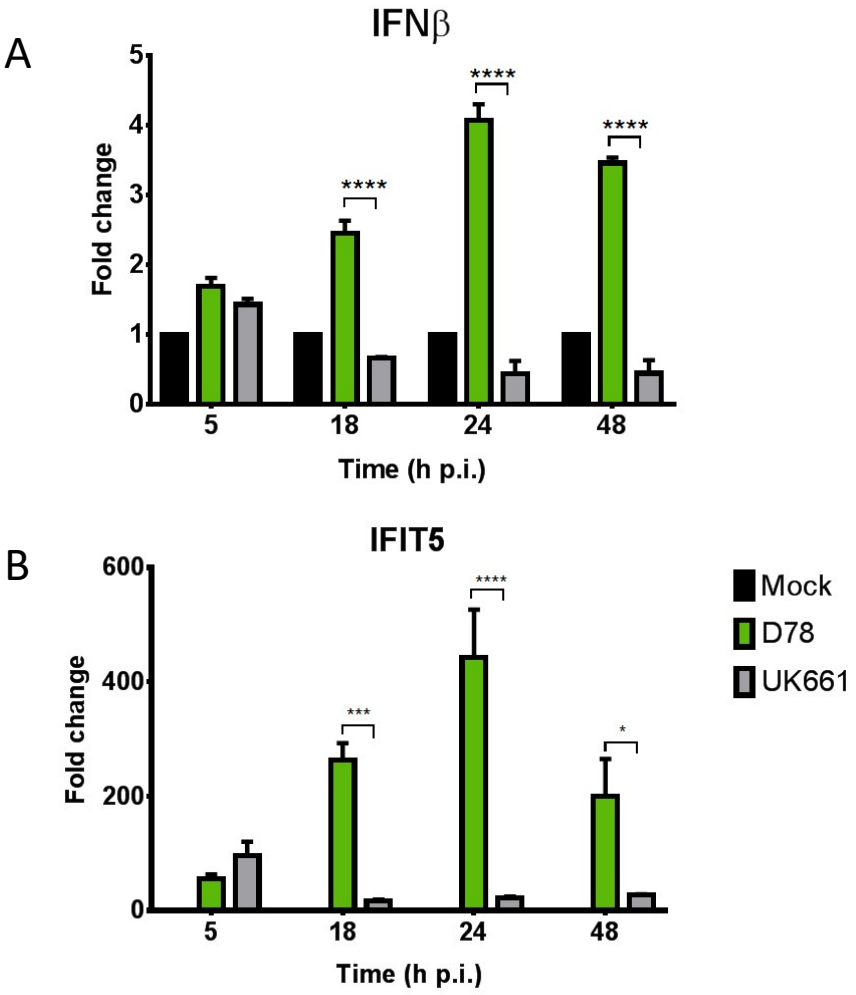

Figure 7 IFNβ and IFIT5 expression in primary bursal cells infected with D78 or UK661.

RNA was extracted from mock-, D78- and UK661- infected cells at the indicated time points post-infection, reverse transcribed and the chicken IFNβ (A) and IFIT5 (B) genes were amplified by qPCR. Ct values were normalised to the Ct values of a housekeeping gene as per the $2^{-\Delta CT}$ method and passed a Shapiro-Wilk normality test before being analysed using a 2-way ANOVA and Tukey's multiple comparison test (*P<0.05, ***P<0.001, ****P<0.0001). Data were then expressed as fold change in IFNβ and IFIT5 RNA relative to mock-infected samples as per the $2^{-\Delta\Delta CT}$ method. Error bars represent the standard deviation of the mean and experiments were carried out on at least three separate occasions.

Analysis of the microarray data revealed 69 genes were up- or down-regulated relative to mock infected cells following infection with D78 ($P<0.05$, fold change cut-off 1.5), and 12 of these genes were also differentially regulated in UK661 infected cells compared to mock (Figure 8A). During D78 infection, 53 of the total 69 genes were up-regulated, and 16 were down-regulated. Following UK661 infection, all 12 genes differentially expressed relative to mock were up-regulated and no genes down-regulated in these samples were found to be significant. By directly comparing gene expression of D78- and UK661-infected samples, 37 differentially expressed genes were identified, with 27 up-regulated and 10 down-regulated genes in D78- compared to UK661-infected cells. Two up-regulated genes (HBG2 and HSP25) and two down-regulated genes (LOC422305 and MCOLN2) had not been previously identified by comparing infected to mock-infected cells.

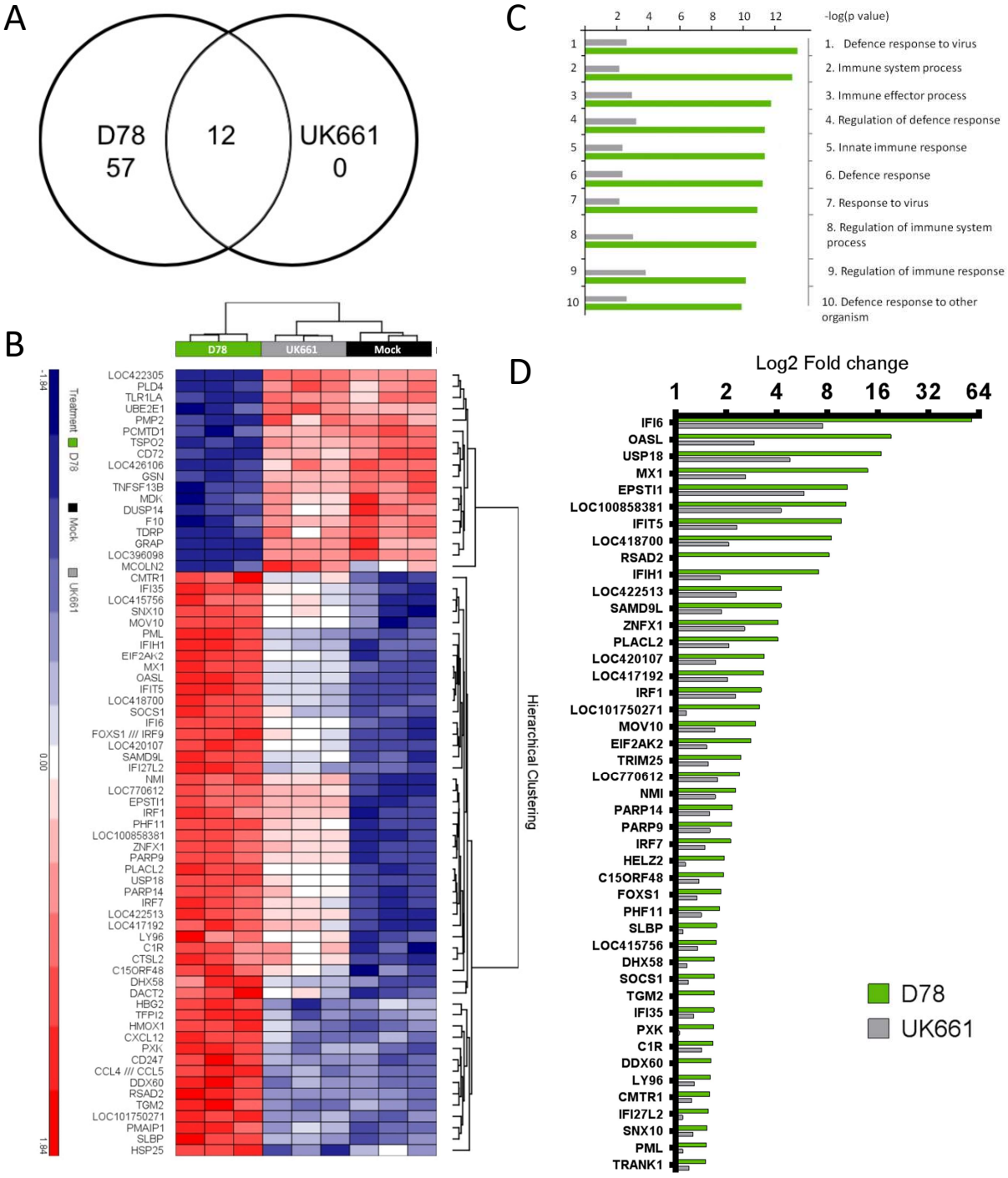
A
D78
57
12
UK661
0
B
D78
UK661
Mock
Treatment
D78
Mock
UK661
Hierarchical Clustering
C
-log(p value)
1. Defence response to virus
2. Immune system process
3. Immune effector process
4. Regulation of defence response
5. Innate immune response
6. Defence response
7. Response to virus
8. Regulation of immune system process
9. Regulation of immune response
10. Defence response to other organism
D
Log2 Fold change
D78
UK661

Figure 8 Differential gene expression in primary bursal cells infected with D78 or UK661 by microarray.

RNA was extracted from mock-, D78- and UK661-infected cells at 18 h.p.i and subjected to microarray analysis. (A) Venn diagram showing the overlap in differentially expressed genes induced by D78 and UK661 infection compared to mock-infected cells. (B) Hierarchical clustering heat map of 69 transcripts found to be significantly up- or down-regulated in at least one of the study's microarray gene expression comparisons using Partek v6.6 software: D78 vs mock (green), UK661 vs mock (grey) and D78 vs UK661 (black). Each column represents a sample and each row represents mRNA quantification of the indicated transcript. The default settings of Euclidian dissimilarity were used for each row (log2-transformed and median-centred transcripts). The vertical legend shows the colours that correspond to expression intensity values in the heat map (red, up-regulated; dark blue, down-regulated). (C) Distribution histogram of GO process term enrichment analysis using the MetaCore enrichment analysis tool. The 10 most enriched GO process terms in the microarray comparisons D78 (green) and UK661 (grey) were plotted relative to mock, sorted by 'statistically significant maps', which list terms in decreasing order of the standard deviation of the –log (p-value) between the two comparisons. (D) Comparisons of the relative expression of known chicken ISGs between B cells infected with D78 (green) and UK661 (grey).

Unsupervised hierarchical clustering analysis of the significantly differentially regulated genes confirmed more transcripts were up-regulated following infection with D78 than UK661 (Figure 8B+C). From this analysis genes could be separated into four groups: the first group included the 16 genes transcribed at lower levels in D78- compared to mock-infected samples. These genes were involved in B cell activation and signalling (TNFSF13B, which encodes BAFF, CD72, GRAP), immune processes (TLR1LA, DUSP14, PLD4, MDK, PMP2, F10, GSN) and other processes including cholesterol transport and binding (TSPO2) and protein ubiquitination (UBE2E1). LOC422305 and MCOLN2 were also added to this group as they were found to be significantly down-regulated in D78- relative to UK661-infected cells. The other three groups contained the 53 genes that were transcribed at a higher level in D78- relative to mock-infected cells, in addition to the two genes (HBG2 and HSP25) significantly up-regulated during D78 relative to UK661 infection. These genes were involved in innate immune responses (IFI6, SAMD9L, NMI, IRF7, LGP2, IFI35, HMOX1, LY96, SOCS1 and others), antiviral responses (OASL, Mx1, IFIT5, RSAD2, IFIH1, IRF1, EIF2AK2 or PKR, TRIM25, IRF7, PMAIP1, LGP2, DDX60 and PML), TGFβ signalling (DACT2, PML), inflammation (Chemokine (C-C motif) ligand 4 (CCL4), CCL5) and apoptosis (PMAIP1, PML).

Enrichment analysis was performed using MetaCore (Clarivate) by matching differentially regulated genes based on functional Gene Ontologies (GO) and biological processes. The highest ranking GO processes from this analysis were ‘defence response to virus’ and ‘immune system processes’ (Figure 8C). Although gene expression in UK661-infected cells was up-regulated relative to mock, the magnitude of expression was reduced compared to D78-infected cells. Furthermore, RSAD2, TGM2 and DDX60 were not induced during UK661 infection. Analysis of the differentially regulated genes previously identified to function as ISGs in chickens, confirmed the down-regulation of the type I IFN responses following infection of the bursal cells with UK661 compared to the D78 virus (Figure 8D).

3.3.4 Confirmation of microarray data for selected genes by qPCR

Microarray results were validated by measuring the expression of a panel of genes (IFIT5, IFI6, OASL, Mx1, RSAD2, IFIH1, IFNα and IFNβ) by qPCR. Data was plotted as log_{10} fold changes by microarray (x-axis) and qPCR (y-axis) (Figure 9). The mean Spearman correlation coefficient (Spearman's *ρ*) of gene expression by microarray vs qPCR was 0.90, indicating the level of differential gene expression by each method was highly correlative.

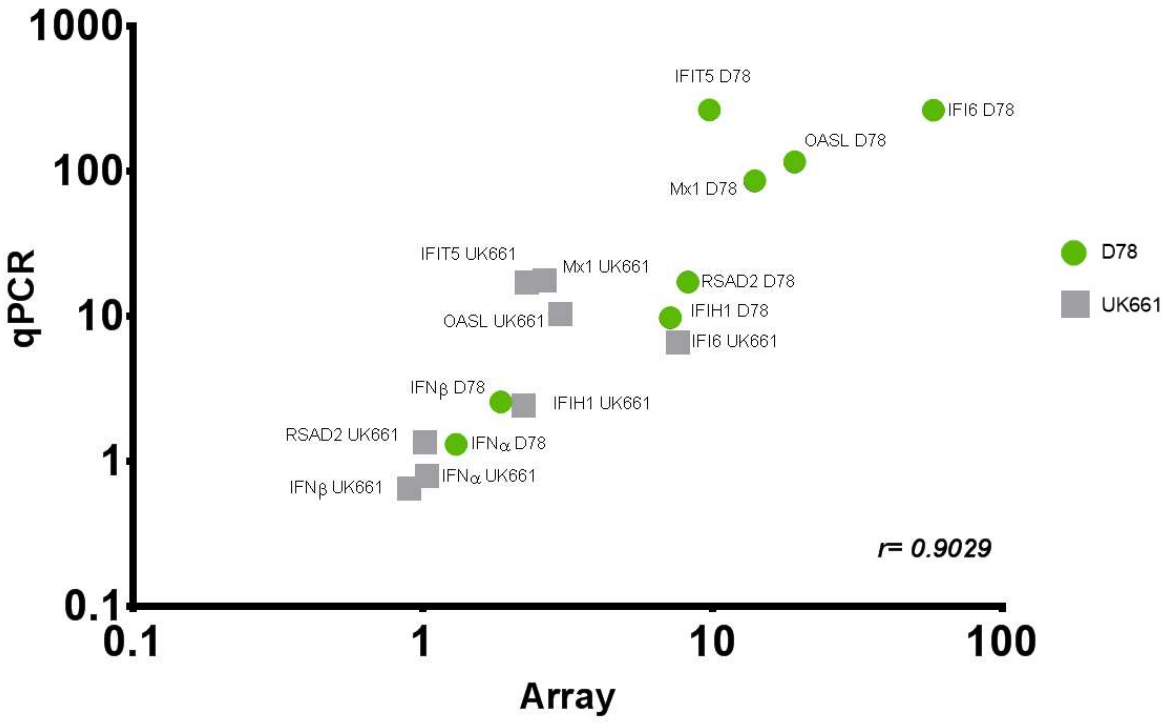

Figure 9 Validation of the microarray results by qPCR

The fold change values for a panel of innate immune genes (IFIT5, IFI6, OASL, Mx1, RSAD2, IFIH1, IFNα and IFNβ), determined by microarray and qRPCR, were normalised by $\log_{10}$ transformation and plotted against one another for cells infected with D78 (green) and UK661 (grey). GraphPad Prism v7.0a was used to calculate the mean Spearman correlation coefficient (r).

3.4 Conclusions

- Primary B cells can be cultured in the presence of chCD40L enabling their culture *ex vivo*.
- Primary B cells can support the replication of cell-culture adapted and vvIBDV strains.
- Key genes involved in B cell activation and proliferation (BAFF, CD72 and GRAP) were down-regulated during infection.
- Primary B cells infected with a vvIBDV strain express innate immune genes to a lesser extent than a cell-culture adapted virus.

3.5 Discussion

The main objective of this chapter was to use the chicken primary B cell *ex vivo* culture model to characterise host-virus interactions between ca- and vvIBDV strains. By comparing the differential gene expression in primary B cells, key differences in host-virus interactions between ca- and vv strains of IBDV were revealed for the first time, to our knowledge, in the primary B cell.

The primary B cell *ex vivo* culture model previously described in this chapter (Schermuly *et al.* 2015) was able to support IBDV infection of both ca- and vvIBDV strains. In addition to the control over MOI and time points, this primary B cell culture can be used to compare IBDV strains of different virulence as well as field isolates not supported by *in vitro* systems. This culture method is a valuable tool for studying IBDV-host interactions in its target cell population without the complication of other immune cells contributing to the gene expression of the total population, as with *in vivo* studies. Taking advantage of the primarily B cell population means we were able to study the transcriptional response of chicken bursal cells infected *ex vivo* for the first time. Moreover, since this work was conducted, another study by Soubies *et al.* (2017) compliments these findings, adding that phorbol 12-myristate 13-acetate (PMA) can also simulate B cell proliferation instead of chCD40L.

From the transcriptional data in this chapter, we found 35 of the 57 genes differentially expressed in the D78- compared to mock-infected cells had previously been reported as differentially expressed *in vivo* (Guo *et al.* 2012; Smith *et al.* 2015; Ou *et al.* 2017). For example, the Guo *et al.* (2012) study reported the differential expression of LY96, IRF1, IRF7, CCL4, CCL5 and SOCS1 in 4-week-old SPF birds inoculated with a cIBDV IBDV strain. Mx1 and RSAD2 were also previously reported to be differentially expressed in 3-week-old birds infected with different cIBDV IBDV strains (Smith *et al.* 2015; Ou *et al.* 2017, respectively), as was CCL4. These studies demonstrate similarities in the transcriptional response observed in the primary B cell cultures compared to *in vivo* studies and highlights the benefits of studying a primary bursal cell population without the infiltration of circulating immune cells. As 18 of the 57 genes were differentially expressed between D78- and mock-infected cells, this highlights some of the benefits of using this *ex vivo* system to find novel IBDV-host interactions which may have been difficult to observe *in vitro*. We found one inconsistency with the literature, in that GSN which codes for Gelsolin was down-regulated in our study but up-regulated in the Smith *et al.* (2015) study. Gelsolin regulates actin assembly and there is some evidence in the literature is has also been associated with apoptosis (Korte *et al.* 2012). The reason for this difference is unknown, although one possible explanation is that gene expression in this study was characterised at 18 h.p.i compared to the 3- and 4- days post-inoculation (d.p.i) time points studied in the Smith *et al.* (2015) study. Another explanation is the use of different chicken breeds in the experiments, as this has previously been shown to influence the transcriptional response in other studies (Psifidi *et al.* 2016). Furthermore, we used the attenuated vaccine strain D78 whereas they used a cIBDV field strain so there may be differences in gene expression between IBDV strains of varying attenuation.

Studying the transcriptional response of infected B cells, identified key genes involved in B cell activation and proliferation that were down-regulated during infection with both D78 and UK661. These genes included TNFSF13B, CD72 and GRAP which are also down-regulated during *in vivo* infection with the cIBDV strain F52/70 in two previous studies (Ruby *et al.* 2006; Smith *et al.* 2015), and CD72 that was down-regulated during an *in vitro* study in DT40 cells with the vvIBDV strain Lx

(Quan *et al.* 2017). TNFSF13B encodes the B cell activating factor (BAFF) which is fundamental for the survival of B cells. BAFF is a transmembrane protein with three known receptors expressed on B cells to varying amounts. Expression levels are dependent on the maturation of the cell and BAFF-induced signalling, which stimulates B cells to proliferate, replenishing the population following apoptosis (Mackay and Browning, 2002). BAFF also increases expression of the B cell co-receptor cluster of differentiation 72 (CD72), which can mediate positive and negative signalling of the B cell receptor due to immunoreceptor tyrosine-based inhibitory motifs (ITIMs), ITIM1 and ITIM2 (Wu and Bondada *et al.* 2009). Some evidence suggests positive signalling occurs through the Grb2-Sos-Ras pathway, as ligation of CD72 has been shown to induce proliferation of both resting and activated B cells (Wu and Bondada *et al.* 2009). Grb2 and Grb2-related adapter protein (GRAP) are members of the adapter protein family that couple signals from receptor tyrosine kinases to the Ras pathway (Feng *et al.* 1996). A study by Fujiwara *et al.* (2006) found Grb2 proteins can interact with the ITIM2 motif of the avian CD72 homologue in the DT40 cell line, thereby attenuating negative signals from the ITIM1 motif and permitting positive signalling. As BAFF is involved in the up-regulation of CD72, and its positive signalling via Grb2-like proteins, the combination of BAFF, CD72 and GRAP causes activation and proliferation of B cells. In this study, we found all three of these proteins to be down-regulated during infection with both IBDV strains. This pathway may therefore be a target for the virus in order to prevent the replenishing of B cells following infection, resulting in the immunosuppression associated with IBD. This observation should be followed up in future studies.

Transcriptional analysis revealed a group of genes the more significantly down-regulated in B cells infected with the UK661 virus compared to D78 virus. Some of these genes, such as OASL (Masuda *et al.* 2012), Mx1 (Benfield *et al.* 2010) and RSAD2 (Goossens *et al.* 2015), have previously been identified as IFN-stimulated genes (ISGs) whereby they are upregulated upon IFN stimulation to establish an antiviral state in the infected cell. The ISG function of 2'-5'-oligoadenylate synthase-like (OASL) is stimulated by dsRNA, resulting in its binding to RNase L. This interaction between OAS and RNase L leads to the dimerization and activation of RNAse L, which subsequently cleaves viral and host RNA

transcripts (Masuda *et al.* 2012). In mammalian hosts, OASL has demonstrated antiviral activity against many RNA viruses mediated through its interaction with RIG-I leading to its increased sensitivity to viral RNA (Ghosh *et al.* 2019). As chickens do not have the RIG-I gene, OASL may have a similar interaction with MDA5 although this interaction is poorly understood. Mx1 plays a critical role in resistance to a wide range of viruses in mammalian hosts, including mice and humans, for example influenza virus (Benfield *et al.* 2010) by inhibiting the replication of the viral genome. Originally, chicken Mx1 was found to have no detectable antiviral activity (Bernasconi *et al.* 1995), however its polymorphic nature was determined to be the reason for this earlier conclusion. More recent studies have demonstrated its role as an antiviral against other avian diseases such as duck hepatitis A virus type 1 (DHAV-1) and NDV (Schilling *et al.* 2018; Xie *et al.* 2019). Furthermore, some studies have suggested Mx1, along with some other ISGs, could provide an antiviral defense in the absence of an induced IFN response (Paludan *et al.* 2016; Xu *et al.* 2017). Viperin (RSAD2) is a well-established and highly conserved ISG across mammalian species and its function in inhibiting the trafficking of viral proteins has also been demonstrated in chickens. Upon infection with a cIBDV strain of IBDV or an H5N1 AIV strain, viperin was upregulated significantly in the BF and lung, respectively (Goossens *et al.* 2015). IFN-induced protein with tetratricopeptide repeats, IFIT5, was found to interact with RIG-1 and MAVS in 293T cells following SeV stimulation or infection with NDV, thus causing a down-regulation in IFNβ production (Zhang *et al.* 2013). This function as an ISG has also been confirmed in chickens, however only IFIT5 has been identified in the chicken genome, so IFIT5 may have other unknown additional functions (Santhakumar *et al.* 2018).

Several host genes contributing to NF-κB regulation and downstream apoptosis were also down-regulated, further to the down-regulation of ISGs in primary B cells infected with the UK661 virus compared to the D78 virus. Included in this subset of genes was CCL4 and CCL5, involved in attraction and proliferation of T cells (Gao *et al.* 2019); CXCL12, up-regulation of IL-6 by P13K/AKT pathway activation (Liu *et al.* 2019) as well as IFIT5, a positive regulator of IKK phosphorylation and NF-κB activation (Zheng *et al.* 2015a). EIF2AK2, IF127L2 and PMAIP1 also have roles in NF-κB signalling and

apoptosis. As these genes were down-regulated during UK661 infection of B cells compared to D78 infection, apoptosis and immune cell recruitment may be impeded during UK661 infection.

In summary, the application of soluble chCD40L has enabled the characterisation of the gene expression profiles of primary B cells during infection with ca- and vvIBDV strains for the first time. The data presented in this chapter demonstrates some key differences in IFN production and signalling between IBDV strains of differing virulence. As the vvIBDV strain UK661 induced lower levels of expression of ISGs, the vvIBDV strain may be able to suppress antiviral responses to a greater extent than the caIBDV strain. This may, in part, contribute to its increased virulence. However, it is necessary to test hypothesis further.

4. Comparing the host immune response to cIBDV and vvIBDV strains *in vitro* and *in vivo*

4.1 Introduction

A better understanding of how different strains of IBDV lead to different disease outcomes is important for surveillance and vaccine development, however, there are currently no known genetic signatures of high and low virulence in IBDV strains. By identifying genetic signatures of high virulence, it would aid the surveillance of IBDV, and by identifying genetic signatures of low virulence, it might be possible to engineer a rationally designed live vaccine.

A study by Zierenberg *et al.* (2004) demonstrated that both segments of a reassortant serotype I/serotype 2 IBDV strain were important for pathogenicity, where segment A determines the cell tropism (the BF in non-cell-culture-adapted strains) and segment B is involved in the efficiency of viral replication. Moreover, in subsequent studies, some specific VP2 residues were identified as useful molecular determinants for virulence, cell tropism and pathogenic phenotype of vvIBDV, following *in vivo,* sequencing and phylogenetic studies (Yamaguchi *et al.* 1996; Brandt *et al.* 2001). However, a study by Boot *et al.* (2000) investigated the virulence of chimeric viruses with exchanged VP2 genes between cIBDV and vvIBDV strains and concluded the VP2 is not exclusively responsible for virulence.

Tissue tropism, viral replication and interactions with the host immune response have all been shown to contribute to increased virulence of IBDV strains. A study by Yasmin *et al.* (2015) evaluated the role of spleen-derived dendritic cells during infection with either a vaccine or vvIBDV strain *in vivo*. A higher mortality rate and more severe BF scoring was reported for the vvIBDV compared to the vaccine IBDV strain. The vvIBDV strain was detected in the BF from day 1 post-inoculation and was detected in the

spleen at day 2. However, in contrast, the vaccine strain wasn't detected in the BF until day 3 although virus was detected in the spleen prior to this at day 2 post-inoculation. The viral load detected in either spleen or BF was greater for the vvIBDV strain compared to the vaccine strain at all time points (1, 2, 3 and 5 post-inoculation). This study provided a good insight into the differences in tissue tropism and histopathology between vaccine and vv IBDV strains in the BF and spleen, however, the gene expression analysis was only performed on the dendritic cells extracted from the spleen, which are not the primary target cell for IBDV. Another limitation to this study is the use of a vaccine strain for comparison to vvIBDV infection, as vaccine strains have previously been shown to interact differently with the host immune response (Yasmin *et al.* 2015; Jahromi *et al.* 2018). Targeting of the spleen and BF by vvIBDV strains was also investigated in a study by Rasoli and colleagues where they evaluated the role of macrophages in these lymphoid tissues (Rasoli *et al.* 2015). They determined that gene expression of pro-inflammatory cytokines was higher in the spleen earlier in infection and higher in the BF later during infection, suggesting a migration of macrophages from the spleen to the BF. Despite this insight into macrophage involvement in vvIBDV infection, macrophages are not the primary target cell for IBDV and are a minority of the total cell population in both spleen and BF.

Some studies have focused on the differences between field strains of IBDV during infection *in vivo.* A study by He *et al.* (2017) compared the Chinese vaccine B87 and vv NN1172 strains *in vivo* to identify the role of TLR3 in virulence of IBDV strains. During infection with the NN1172 virus, TLR3, IFNβ and IL-8 were significantly up-regulated at day 3 post-inoculation, while B87 significantly down-regulated the same three genes at day 1 post-inoculation. Despite this reported difference in gene expression, at days 1 and 2 post-inoculation the NN1172 virus down-regulated IFNβ although it didn't reach statistical significance. Also, the down-regulation of IFNβ at earlier time points may have contributed to a higher NN1172 virus titre compared to B87 at day 3 post-inoculation and subsequently the up-regulation in expression of these genes at the same time point. The innate immune regulation and pathology of infection was explored by Rauf and colleagues (2011) during infection with cIBDV and vIBDV strains. They reported more severe BF damage and up-regulation of pro-inflammatory

cytokines at day 3 in birds inoculated with the cIBDV strain compared to the vIBDV strain. Comparing the response to these viruses with that of vvIBDV strains *in vivo* would improve our understanding of the fundamentals of IBDV virulence. A study by Liu *et al.* (2010) also described higher expression of pro-inflammatory cytokines in response in vvIBDV infection when they compared this to infection with a caIBDV strain *in vivo*. They found IL-2, IL-12 and IFN-γ peaked between day 3 and 5 in birds inoculated with the vvIBDV strain, in contrast there was very low induction of any of these genes in birds inoculated with the caIBDV strain. Virus titre in the BF peaked at day 3 in the vvIBDV-inoculated birds, while this peak was later in the birds inoculated with the caIBDV strain. In another study using the same viruses (Zhang *et al.* 2002), there were differences in the virus distribution throughout the tissues of infected birds. The vv strain was detected in the liver, kidney and spleen early in the first 4 h.p.i, then in the thymus, caecal tonsil and thigh muscle at 8 h.p.i. In contrast the caIBDV strain was detected in all of these tissues from 4 h.p.i. The vv strain was detected in the BF from 8 h.p.i whereas this was later at between 8 and 16 h.p.i for birds inoculated with the caIBDV strain, consistent with the Li *et al.* (2010) study.

Work previously described in Chapter 3 identified the lower expression of type I IFN and ISGs during infection of primary B cells with the vvIBDV strain UK661 and the attenuated vaccine strain D78. The expression of genes involved in the type I IFN responses were lower in cells infected with the UK661 strain compared to the D78 strain, and it was hypothesised that this reduced expression during vvIBDV infection may, in part, explain their enhanced virulence. Following on from these conclusions, the vvIBDV UK661 strain was compared to a more pathogenic field strain with a classical virulence type, F52/70 to investigate whether the type I IFN responses were reduced during infection with the vvIBDV virus to a greater extent than during infection with a cIBDV strain. Moreover, in order to rule out whether the phenotypes observed in Chapter 3 were due to the use of the primary bursal cell system, gene expression was also compared *in vitro* and *in vivo*. Investigating these host-virus interactions with the type I IFN response can contribute to the field of IBDV pathogenesis and shed light on the

mechanism responsible for the large variation in mortality rates between birds infected with cIBDV and vvIBDV strains.

4.2 Chapter Aims

The research objective for this chapter was to determine key differences in cIBDV F52/70 and vvIBDV UK661 infection *in vitro* and *in vivo,* comparing gene expression data from DT40 cells infected with the F52/70 or UK661 virus *in vitro* to gene expression following infection *in vivo*. Birds inoculated with either the viral F52/70 or UK661 virus were assessed for clinical scores, viral replication kinetics, tissue tropism and host gene expression in infected tissues.

4.3 Results

4.3.1 Replication of IBDV strains in DT40 cells

To determine the replication kinetics of IBDV strains of different virulence *in vitro,* the immortalised B cell line DT40 was infected with the vvIBDV strain UK661 and the cIBDV strain F52/70 at an MOI of 0.1 to study kinetics over multiple replication cycles. Extracted RNA was reverse transcribed and a region of the VP4 gene amplified to quantify fold change in viral RNA, compared to mock-infected cells. The replication of F52/70 was reduced compared to UK661 at all four time points (*P<0.0001) (Figure 10).

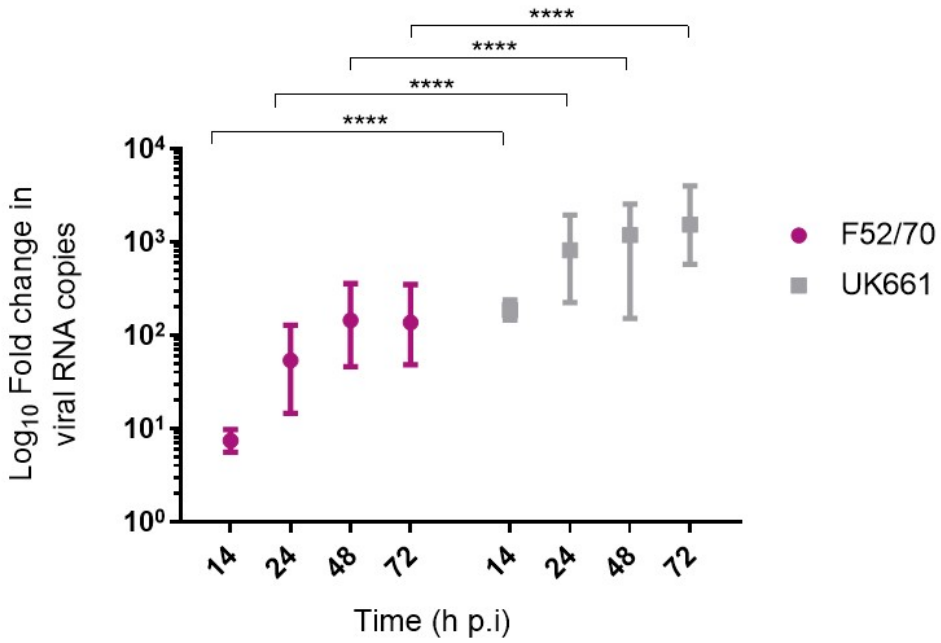

Figure 10 Replication of F52/70 and UK661 viruses in DT40 cells.

Cells were infected at an MOI of 0.1, before RNA extraction from cells at the indicated time points. RNA was reverse transcribed and a conserved section of the VP4 gene was amplified by qPCR. VP4 gene Ct values were normalised to the RPLP0 housekeeping gene as per the $2^{-\Delta CT}$ method and subsequently passed a Shapiro-Wilk normality test before being analysed using a one-way ANOVA and a Tukey's multiple comparison test (****P<0.0001). Data were expressed as log_{10}-fold change in VP4 RNA relative to mock-infected samples as per the $2^{-\Delta\Delta CT}$ method. Data shown are representative of at least three replicate experiments, and error bars indicate the standard deviation of the mean.

4.3.2 Differential gene expression in DT40 cells infected with IBDV strains

To compare the host-virus interactions during infection with either F52/70 or UK661, IFNα, IFNβ and Mx1 were selected for qPCR using cDNA from infected samples which were then normalised to the housekeeping gene, 60S acidic ribosomal protein P0 (RPLP0), and then mock-infected cells. Despite replicating to a lower titre, F52/70-infected cells showed higher expression of IFNα, IFNβ and Mx1 compared to UK661 at 14, 48 and 72 h.p.i (***P<0.001, ***P<0.001 and *P<0.05, respectively) (Figure 11). During UK661 infection, all three host genes measured had a fold change of less than -2 prior to 72 h.p.i as compared to mock-infected cells.

A panel of pro-inflammatory cytokines (IL-6, IL-8 and IL-1β) was also chosen for qPCR with the same cDNA samples. Despite replicating to a lower titre, expression of IL-6 was higher in F52/70- compared to UK661-infected cells at 14, 48 and 72 h.p.i (Figure 12A), while for IL-1β this was the case for three of the time points (***P<0.001) (Figure 12C). IL-8 expression during UK661 infection was higher than in F52/70-infected cells at 48 h.p.i, although this was not statistically significant (Figure 12B).

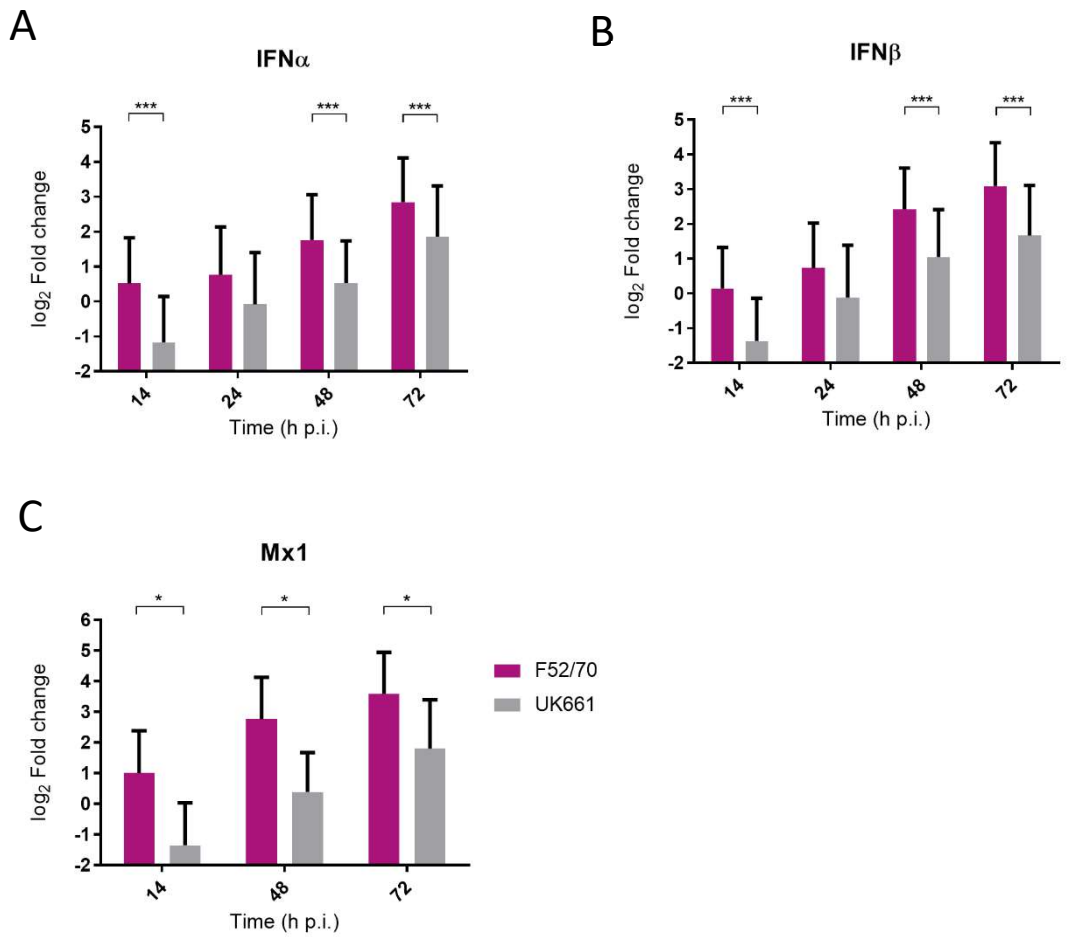

Figure 11 qRT-PCR analysis of type I IFN-related genes in F52/70- and UK661- infected DT40 cells.

Extracted RNA from F52/70- (pink), UK661- (grey) and mock-infected cells collected at 14, 24, 48 and 72 h.p.i were reverse transcribed and amplified by qPCR using specific primer sets for IFNα (A), IFNβ (B) and Mx1 (C). The Ct values of infected samples were then normalised to the housekeeping gene, RPLP0, and mock-infected samples using the $2^{-\Delta\Delta CT}$ method. Data are representative of at least three replicate experiments and passed a Shapiro-Wilk normality test before analysis using a one-way ANOVA and a Tukey's multiple comparison test (*P<0.05, ***P<0.0001).

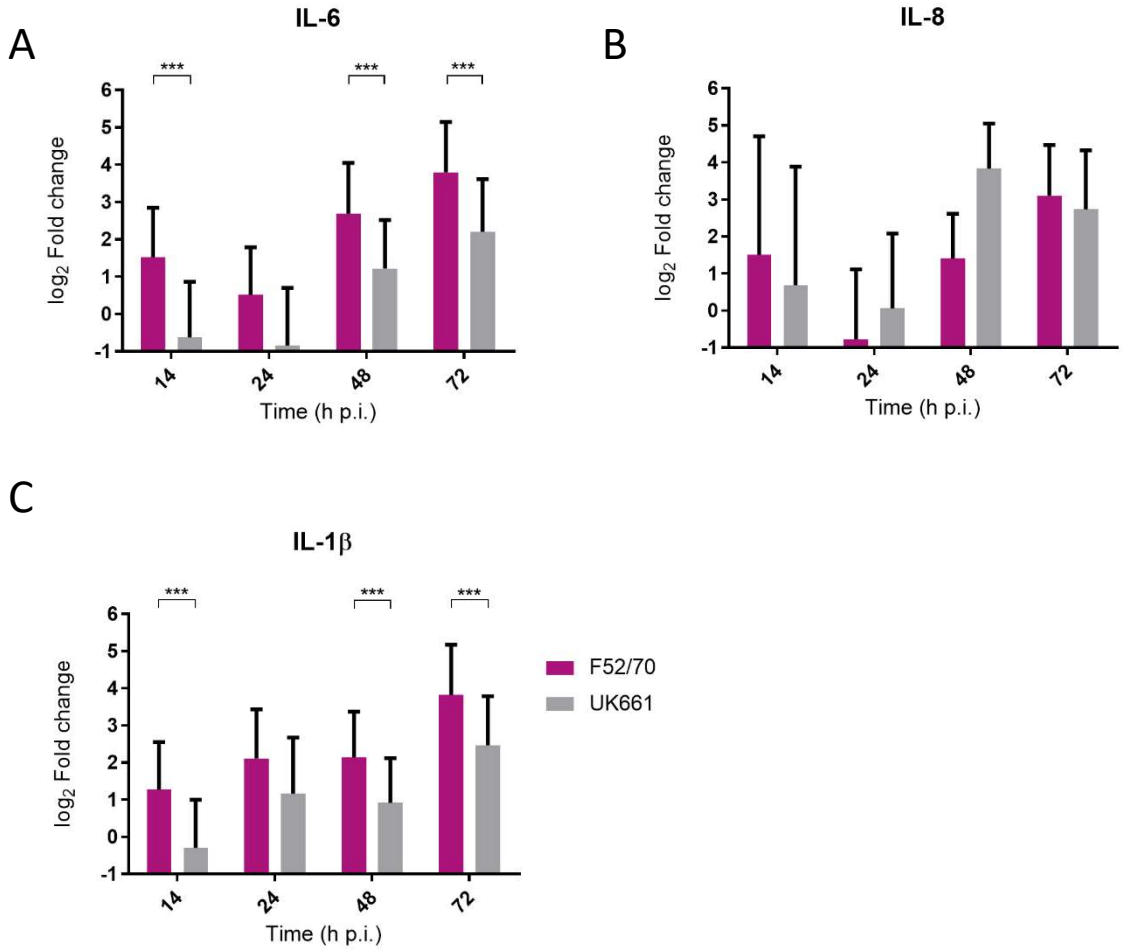

Figure 12 qRT-PCR analysis of pro-inflammatory cytokines in F52/70- and UK661-infected DT40 cells.

Extracted RNA from F52/70- (pink), UK661-infected (grey) cells collected at 14, 24, 48 and 72 h.p.i were reverse transcribed and amplified by qPCR using specific primer sets for IL-6 (A), IL-8 (B) and IL-1β (C). The Ct values of infected samples were then normalised to the housekeeping gene, RPLP0, and mock-infected samples using the $2^{-\Delta\Delta CT}$ method. Data are representative of at least three replicate experiments and passed a Shapiro-Wilk normality test before analysis using a one-way ANOVA and Tukey's multiple comparison test (***P<0.001).

4.3.3 UK661-infection is associated with a reduced survival compared to F52/70 infection *in vivo*

In order to determine whether these observations would also be recapitulated *in vivo,* groups of 18 SPF Rhode Island Red birds at 3 weeks of age and mixed gender were inoculated intranasally with the $1.8x10^3$ $TCID_{50}$/bird of either the UK661 or F52/70 virus. Clinical scores and body weights (BW) were recorded in addition to harvesting of tissues at 24, 48 and 72 h.p.i, where BF weight was also recorded to calculate the BF: BW ratio (Figure 13A). Survival rates were determined as the number of birds that reached their scheduled cull point due to their clinical score remaining below 11, which was used as the cut-off for severe disease (see Appendix A). All mock-inoculated birds survived to their scheduled cull point and although both infected groups showed a decrease in survival, 83.3% of F52/70-infected birds survived to their scheduled cull point compared to only 50% of UK661-infected birds, demonstrating that the UK661 virus had a greater virulence than the F52/70 virus (Figure 13B). The BF: BW ratio was calculated for each bird at post-mortem as it is commonly used to indicate IBDV pathology. In F52/70-infected birds there was a modest increase in BF: BW ratio at 48 h.p.i relative to mock possibly due to oedema and inflammation (Figure 13C). UK661-infected birds showed the same small increase in ratio at 48 h.p.i but unlike in F52/70-infected birds, this was followed by a decrease in ratio in the birds reaching their humane end point at 54 h.p.i, consistent with bursal atrophy due to loss of B cells. Subsequent animal studies in the lab as part of other projects have shown that the BF: BW ratio of birds infected with the UK661 strain decreases after 72 h.p.i and is significantly lower than mock controls by 2 weeks post-inoculation. The clinical scores recorded twice daily throughout infection showed a wide spread within each infected group, with F52/70-infected birds displaying higher clinical scores on average than birds infected with UK661, though this did not reach statistical significance (Figure 13D). Despite this, more UK661-infected birds reached their humane

end points at 54 h.p.i. The survival rates reported in this study have been reported previously for vv- and cIBDV strains (Ingrao *et al* 2013; van den Berg *et al.* 2000).

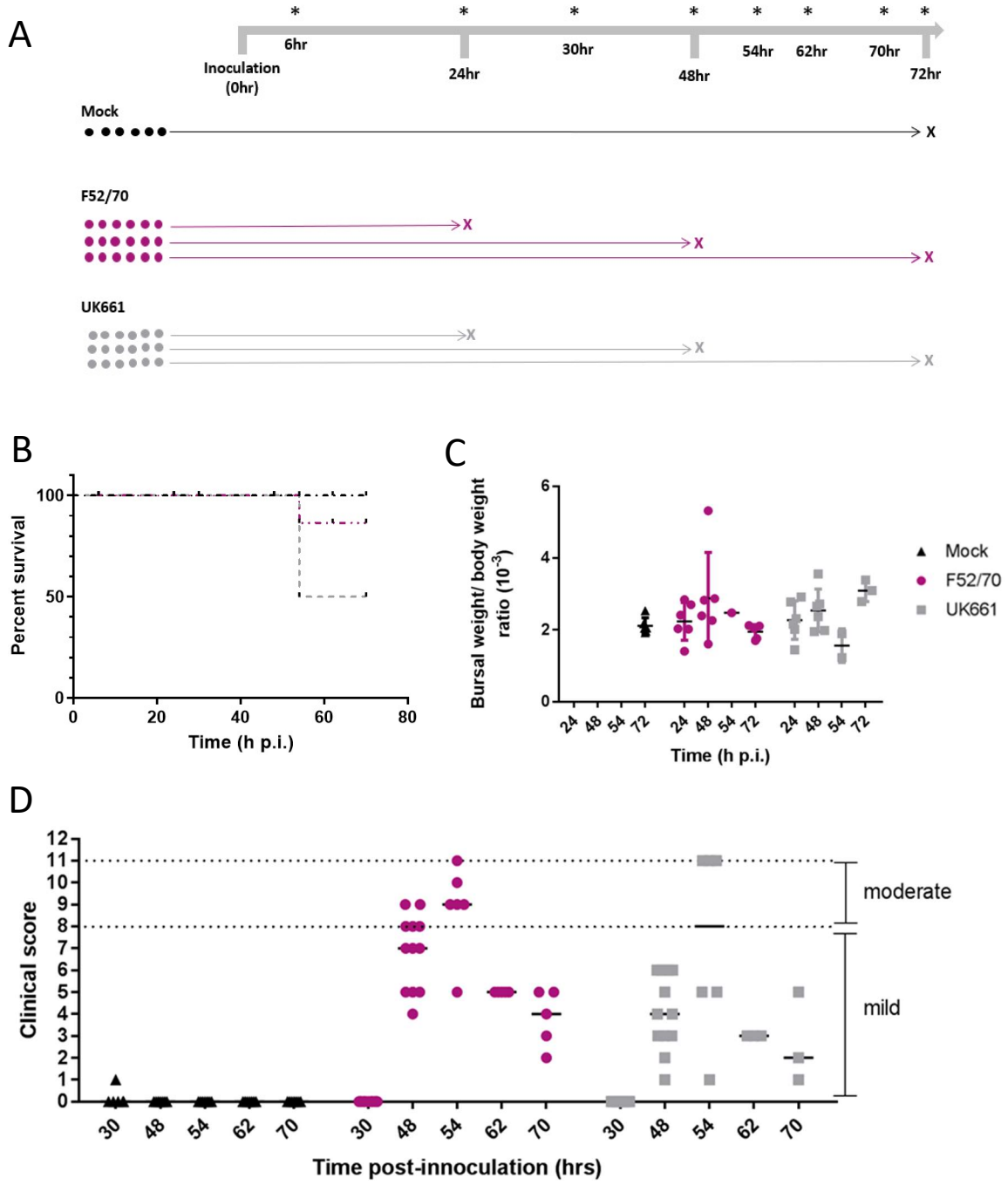

Figure 13 Survival curves, BF: BW ratios and clinical scores of chicken inoculated with F52/70 or UK661.

Schematic of the experimental design, with asterisks indicating when clinical scores were recorded (A). Survival curve of mock- (black), F52/70- (pink) or UK661-infected (grey) birds that reached their humane end point (clinical score of 11) (B). BF: BW ratios of mock-, F52/70- or UK661-infected birds at indicated time points post-inoculation (C). Birds in mock and virus infected groups were scored for clinical signs throughout the experiment with a range of between 1 and 11 (D). A clinical score of 1-7 was considered mild disease, 8-10 was considered moderate disease and birds reaching a score of 11 were humanely culled, as per clinical score sheet (Appendix A).

4.3.4 There was no significant difference in peak virus titres between UK661- and F52/70-infected birds

To identify differences in replication kinetics of UK661 and F52/70 *in vivo*, the BFs were harvested from all groups at post-mortem and either RNA was extracted for reverse transcription and qPCR, or BFs were homogenised for $TCID_{50}$ using DT40 cells. At 24 h.p.i, the amount of UK661 infectious units measured by $TCID_{50}$ was significantly lower than in F52/70-infected birds (**P<0.01), however, there was no significant difference in peak virus titres between the two viruses at subsequent time points (Figure 14A). When comparing the viral transcripts by qPCR the fold change in viral RNA was not significantly different between the two viruses at any of the time points measured (Figure 14B). The reason UK661 infection leads to a greater percentage of birds reaching their humane end-points compared to F52/70 is likely not due to differences in virus replication.

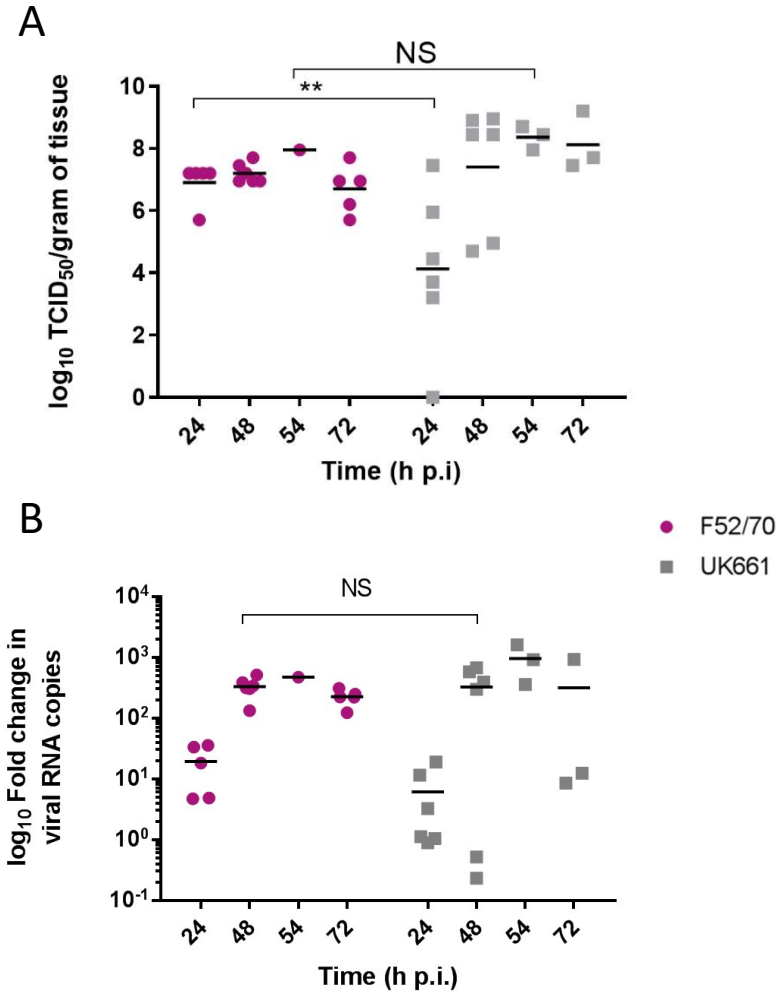

Figure 14 Viral titres of F52/70 and UK661 in BF tissue.

Birds were inoculated with $1.8x10^3$ $TCID_{50}$/bird F52/70 (pink) or UK661 (grey) and the whole BFs were harvested at 24, 48, 54 and 72 h.p.i. (A) A section of BF was homogenised in PES buffer and the virus was titrated using a $TCID_{50}$ performed on DT40 cells. Data were analysed using a one-way ANOVA and Tukey's multiple comparison test (NS, not significant; **P<0.01) (B) Remaining tissue was homogenised and RNA extracted prior to reverse transcription and the amplification of a conserved section of the VP4 gene by qPCR. VP4 gene Ct values were normalised to the RPLP0 housekeeping gene as per the $2^{-\Delta CT}$ method and subsequently passed a Shapiro-Wilk normality test before being analysed using a one-way ANOVA (NS, not significant). Data were expressed as log_{10} fold change in VP4 viral RNA copies relative to mock-infected samples as per the $2^{-\Delta\Delta CT}$ method. *In vitro* data shown are representative of at least three replicate experiments and *in vivo* data are representative of n=6 for 24hr; n=6 for 48hr; n=1 (F52/70) n=3 (UK661) for 54hr; n=5 and n=3 for 72hr for F52/70 and UK661, respectively.

4.3.5 UK661 infection induces the expression of lower levels of type I IFN and pro-inflammatory responses in BF tissue compared to F52/70 infection

The reduced survival rate seen following UK661 infection compared to F52/70 appeared to be more complex than being due to a difference in peak virus titre of the viruses *in vivo,* therefore the host response to infection was explored in more detail. The cDNA generated from BF tissue was used as the template to perform qPCR assays targeting genes involved in the type I IFN response (IFNα, IFNβ and Mx1) and pro-inflammatory cytokines (IL-6, IL-8 and IL-1β). Any fold change below -2 indicated a down-regulation in gene expression compared to mock-infected birds. IFNα expression was found to be significantly higher in F52/70- compared to UK661-infected birds at 24 h.p.i (*P<0.05) (Figure 15A). The same trend was observed in IFNβ expression with F52/70 inducing significantly higher IFNβ expression 48 h.p.i (**P<0.01) (Figure 15B). Mx1 expression was significantly higher in F52/70- compared to UK661-infected birds consistently across 24, 48 and 72 h.p.i (****P<0.0001) (Figure 15C).

For the pro-inflammatory cytokines, IL-6 showed a similar trend to IFNα and IFNβ, where expression of IL-6 was higher at 24 and 48 h.p.i, although this did not reach statistical significance between the birds of either infection group (Figure 16A). Following a different trend, IL-8 expression reached its highest for F52/70 infection at 48 h.p.i, at which point it was also significantly higher than UK661 infection (***P<0.001) (Figure 16B). IL-8 expression continued to be elevated for F52/70-infected birds for the remainder of the experiment, whereas the expression in UK661-infected birds was reduced significantly compared to F52/70-infected birds at 72 h.p.i (***P<0.001). IL-1β expression peaked at 48 h.p.i for both viruses and F52/70 induced greater expression at 24 and 48 h.p.i compared to UK661 (figure 16C), although this failed to reach statistical significance.

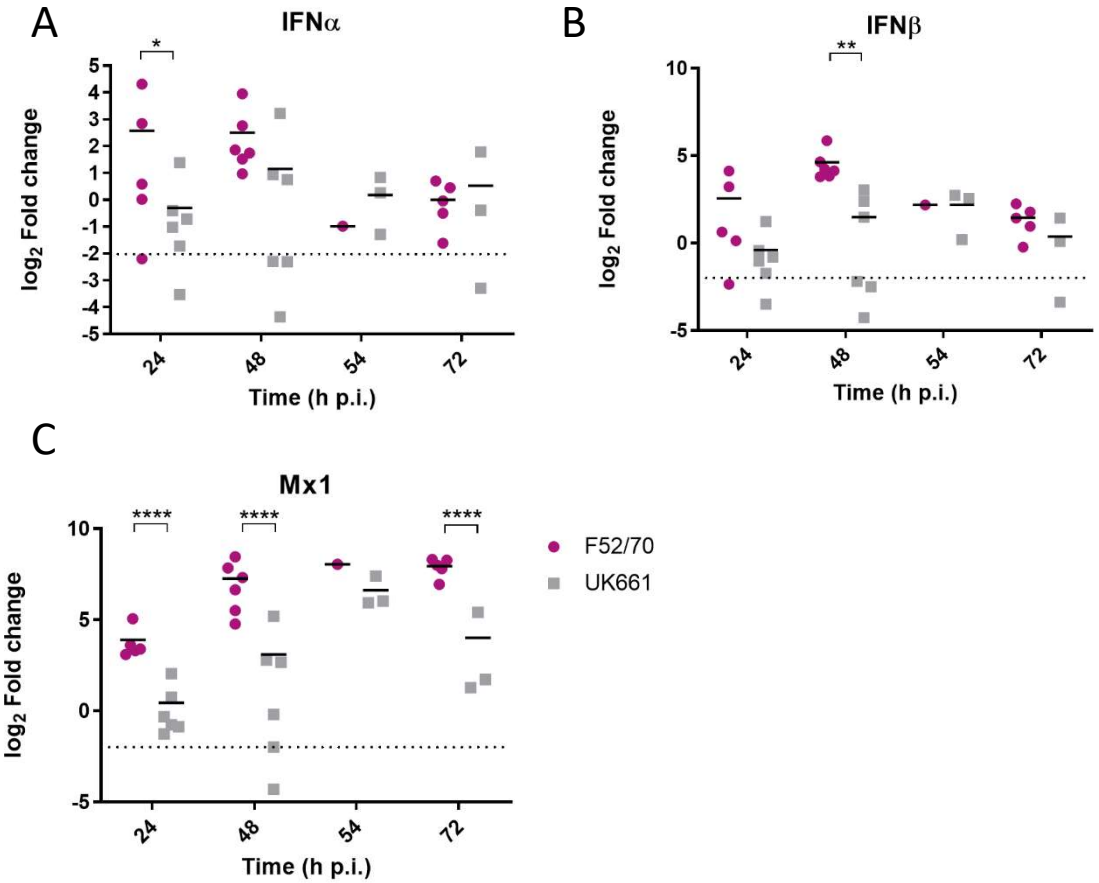

Figure 15 qRT-PCR analysis of type I IFN-related genes from F52/70- and UK661-infected BF tissue.

RNA was extracted F52/70- (pink) and UK661-infected (grey) BF tissue at 24, 48, 54 and 72 h.p.i, reverse transcribed, amplified by qPCR using specific primer sets for IFNα (A), IFNβ (B) and Mx1 (C) Ct values of infected samples were normalised to the housekeeping gene, RPLP0, and mock-infected samples using the $2^{-\Delta\Delta CT}$ method. Data are representative of n=6 for 24hr; n=6 for 48hr; n=1 (F52/70) n=3 (UK661) for 54hr; n=5 and n=3 for 72hr for F52/70 and UK661, respectively. The data passed a Shapiro-Wilk normality test before analysis using a one-way ANOVA and Tukey's multiple comparison test (*P<0.05, **P<0.01, ****P<0.0001). Dotted line indicates the divide between up- or down-regulation compared to mock.

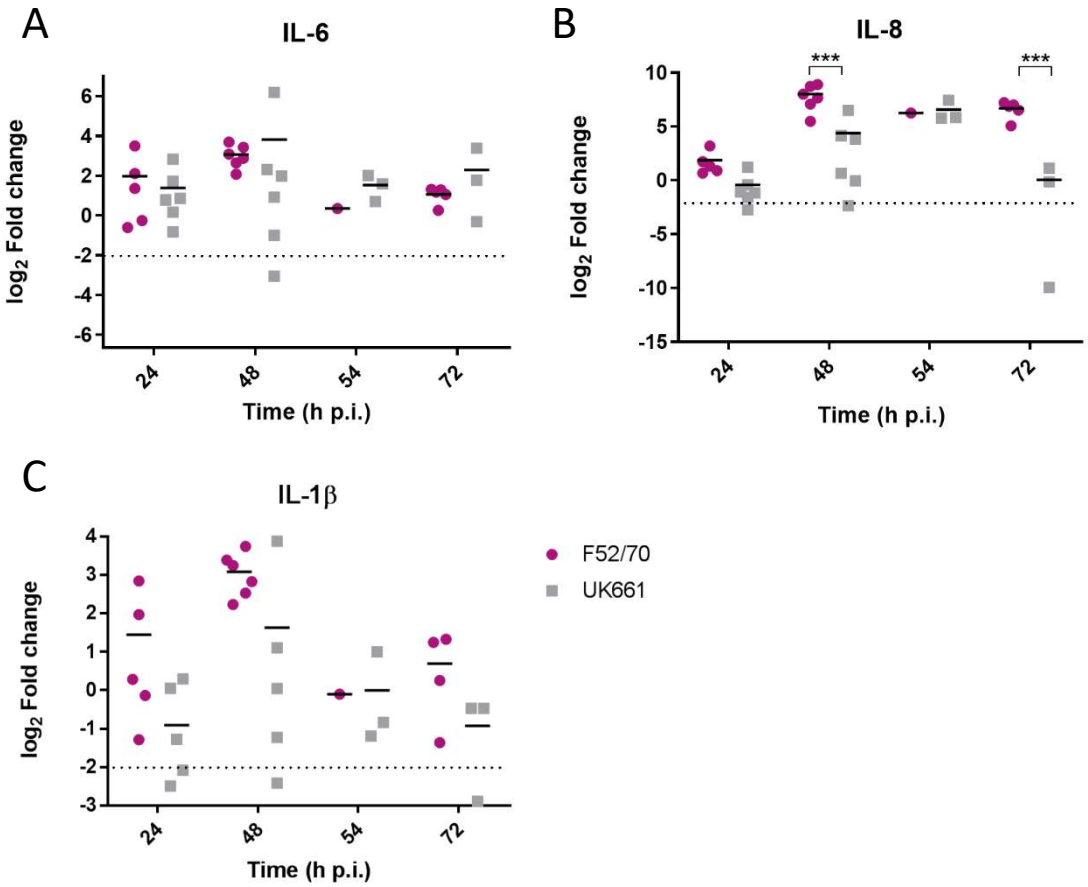

Figure 16 qRT-PCR analysis of pro-inflammatory cytokines in RNA samples from F52/70- and UK661-infected BF tissue.

RNA was extracted F52/70- (pink) and UK661-infected (grey) BF tissue at 24, 48, 54 and 72 h.p.i, reverse transcribed, amplified by qPCR using specific primer sets for IL-6 (A), IL-8 (B) and IL-1β (C) Ct values of infected samples were normalised to the housekeeping gene, RPLP0, and to mock-infected samples using the $2^{-\Delta\Delta CT}$ method. Data are representative of n=6 for 24hr; n=6 for 48hr; n=1 (F52/70) n=3 (UK661) for 54hr; n=5 and n=3 for 72hr for F52/70 and UK661, respectively. The data passed a Shapiro-Wilk normality test before analysis using a one-way ANOVA and Tukey's multiple comparison test (***P<0.001). Dotted line indicates the divide between up- or down-regulation compared to mock.

4.3.6 UK661 and F52/70 viruses were both detected in other lymphoid tissues

While the BF is the main target organ for IBDV infection, previous studies have demonstrated the presence of virus in other lymphoid tissues, for example the spleen and caecal tonsils (Zhang *et al.* 2002). Consequently, the spleen and caecal tonsils were harvested at the same time points as the BF from infected and mock groups of birds. RNA was extracted from tissues and reverse transcribed before virus titre was measured by qPCR. In the spleen, one UK661-infected bird had a high virus titre at 24 h.p.i, however, other than this bird there was little evidence of an established infection in the spleen at the time points studied (Figure 17A). On the contrary, both viruses replicated to higher titres in the caecal tonsils (Figure 17B). The UK661 virus replicated to higher titres on average than the F52/70 virus, and the UK661 titre continued to increase between 54 and 72 h.p.i, whereas the F52/70 titre reduced over the same time points. These data suggest the spleen was not targeted by either virus during this *in vivo* study, however, an increase of UK661 replication in the caecal tonsils suggests UK661 also targets this tissue during infection.

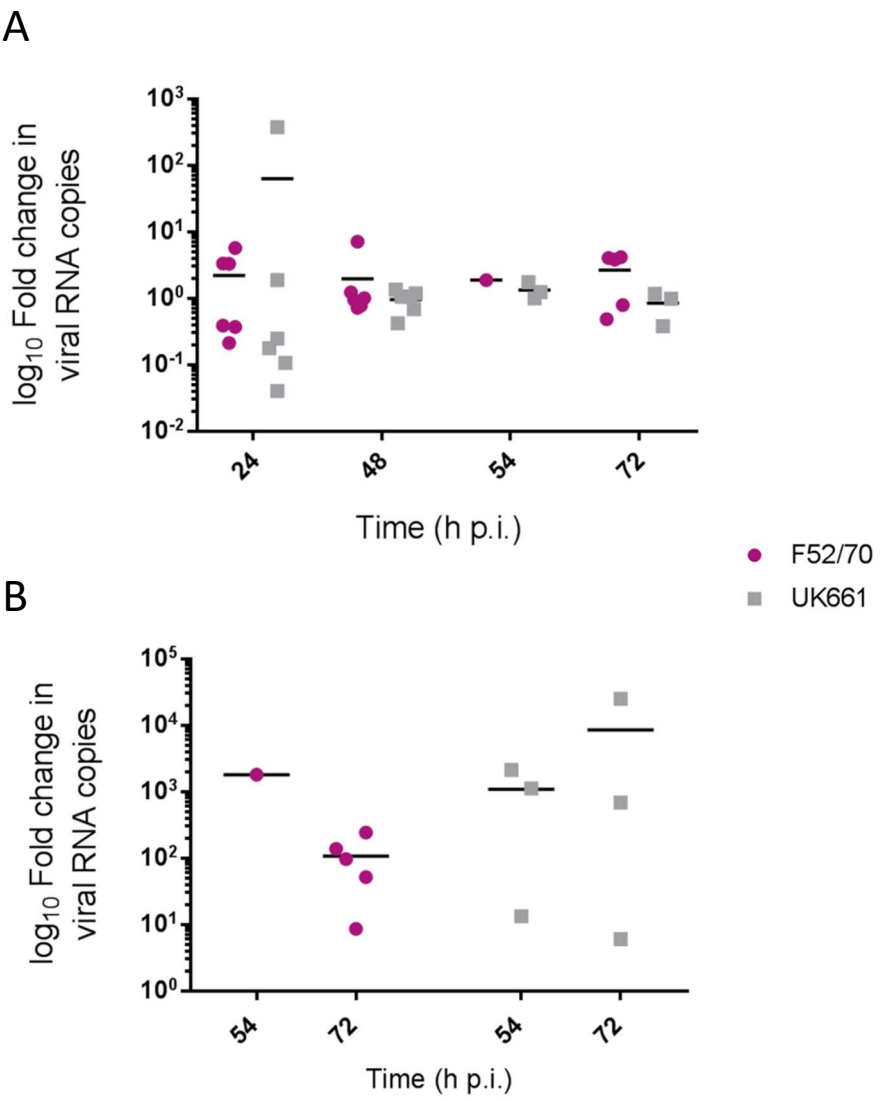

Figure 17 Viral titres of F52/70 and UK661 in spleen and caecal tonsil tissue.

Birds were inoculated with $1.8x10^3$ $TCID_{50}$/bird F52/70 (pink) or UK661 (grey) intranasally and the spleen (A) and caecal tonsil (B) tissue was harvested at 24, 48, 54 and 72 h.p.i. Tissues were homogenised and RNA extracted prior to reverse transcription and the amplification of a conserved section of the VP4 gene by qPCR. VP4 gene Ct values were normalised to the TBP housekeeping gene as per the $2^{-\Delta CT}$ method and subsequently passed a Shapiro-Wilk normality test before being analysed using a one-way ANOVA. Data were expressed as log_{10}-fold change in VP4 RNA relative to mock-infected samples as per the $2^{-\Delta\Delta CT}$ method. Data are representative of n=6 for 24hr; n=6 for 48hr; n=1 (F52/70) n=3 (UK661) for 54hr; n=5 and n=3 for 72hr for F52/70 and UK661, respectively, and bars indicate the mean. Data presented were not found to be significant.

4.3.7 A type I IFN response was detected in the spleen although there was no significant difference between the viral strains

Despite the limited replication of virus in the spleen, IBDV is known to cause a systemic infection throughout the bird and we were therefore interested to determine the expression of antiviral and pro-inflammatory cytokines in the spleen. To this end, the cDNA generated from tissues was used to quantify type I IFN, ISGs, and pro-inflammatory cytokines present expressed in the spleen by qPCR. In each group, there were a range of gene expression for the type I IFN genes and ISGs measured and this response was variable from one bird to another. For IFNα and IFNβ, birds infected with F52/70 had elevated expression of type I IFN compared to UK661 at 24, 48 and 72 h.p.i, although due to the spread of the data this trend did not reach statistical significance (Figure 18A+B). Mx1 expression was also higher in birds inoculated with F52/70 compared to UK661 24 and 48 h.p.i (Figure 18C). At 54 h.p.i, expression of all three genes was higher in UK661-infected birds, however, statistical tests cannot be performed as only one F52/70-infected bird reached its humane end point at this time point.

The pro-inflammatory cytokines, IL-6, IL-8 and IL-1β, had modest increases in expression in infected compared to mock-infected birds. At 48 and 72 h.p.i, birds infected with the F52/70 virus had elevated levels of each cytokine compared to birds inoculated with the UK661 virus, although this did not reach statistical significance. The modest changes in gene expression, spread of the data and lack of statistical significance likely result from the lack of virus replication detected in the spleen.

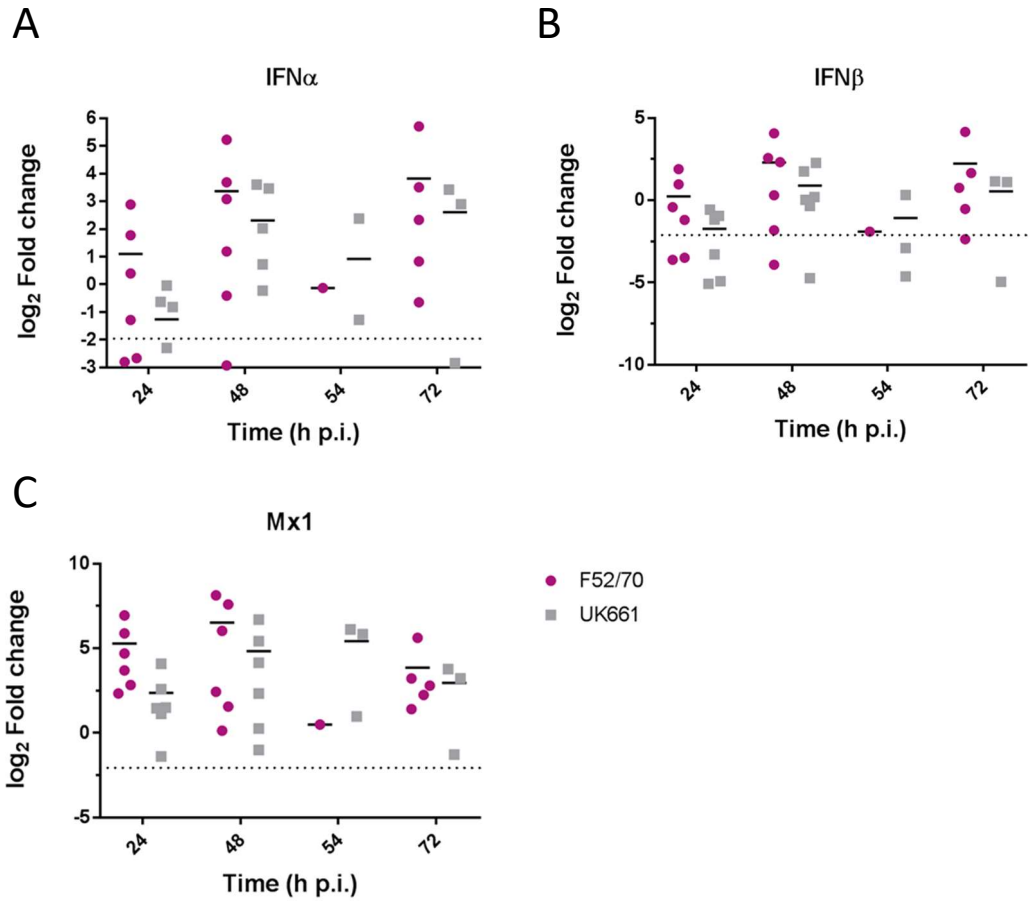

Figure 18 qRT-PCR analysis of type I IFN-related genes in F52/70- and UK661-infected spleen tissue.

RNA was extracted from F52/70- (pink), UK661- (grey) and mock-inoculated samples collected at 24, 48, 54 and 72 h.p.i, reverse transcribed, amplified by qPCR using specific primer sets for IFNα (A), IFNβ (B) and Mx1 (C). Ct values from infected samples were then normalised to the housekeeping gene, RPLP0, and to mock-infected samples using the $2^{-\Delta\Delta CT}$ method. Data are representative of n=6 for 24hr; n=6 for 48hr; n=1 (F52/70) n=3 (UK661) for 54hr; n=5 and n=3 for 72hr for F52/70 and UK661, respectively. The data passed a Shapiro-Wilk normality test before analysis using a one-way ANOVA. Data presented were not found to be significant. Dotted line indicates the divide between up- or down-regulation compared to mock.

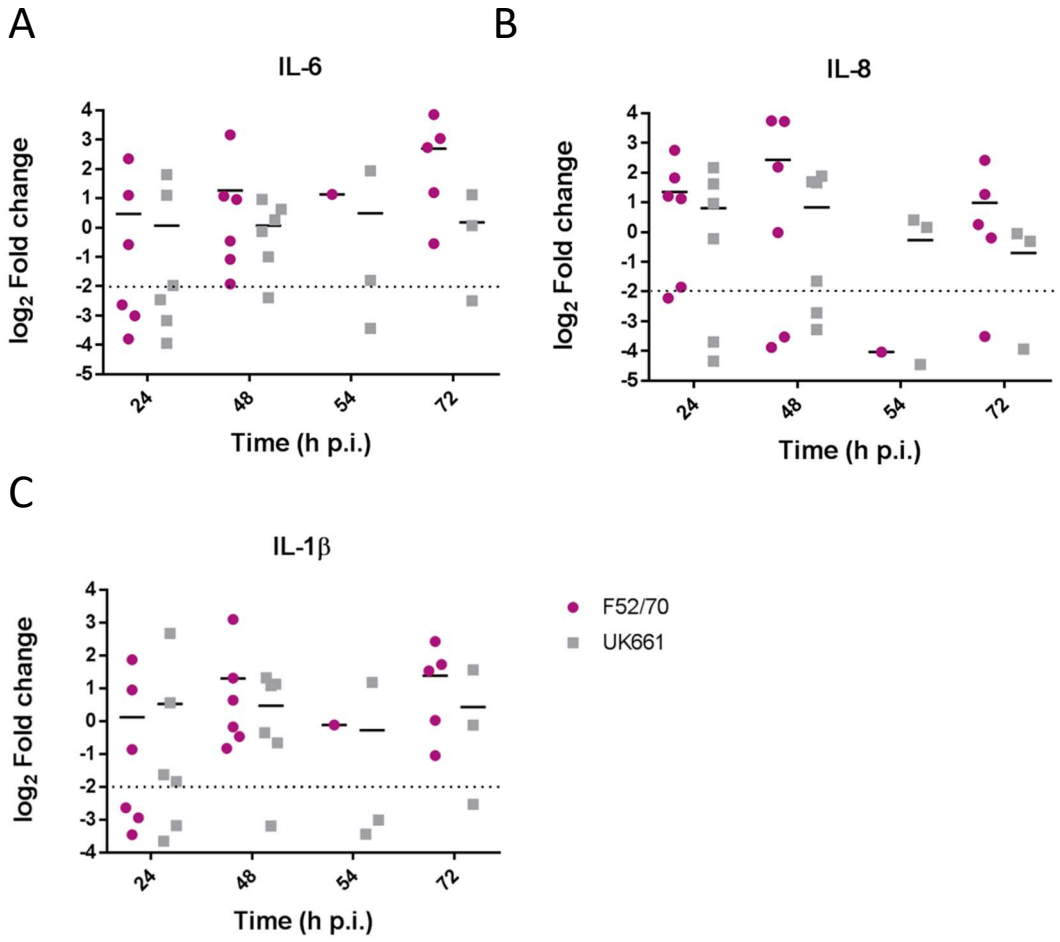

Figure 19 qRT-PCR analysis of pro-inflammatory cytokines in F52/70- and UK661-infected spleen tissue.

RNA was extracted from F52/70- (pink), UK661- (grey) and mock-inoculated samples collected at 24, 48, 54 and 72 h.p.i, reverse transcribed, amplified by qPCR using specific primer sets for IL-6 (A), IL-8 (B) and IL-1β (C). Ct values from infected samples were then normalised to the housekeeping gene, RPLP0, and to mock-infected samples using the $2^{-\Delta\Delta CT}$ method. Data are representative of n=6 for 24hr; n=6 for 48hr; n=1 (F52/70) n=3 (UK661) for 54hr; n=5 and n=3 for 72hr for F52/70 and UK661, respectively. The data passed a Shapiro-Wilk normality test before analysis using a one-way ANOVA. Data presented were not found to be significant. Dotted line indicates the divide between up- or down-regulation compared to mock.

4.3.8 High clinical score correlated with DNA damage and cytoskeleton remodelling in birds inoculated with either virus, while low clinical score was associated with an adaptive immune response

Based on the clinical score data (section 4.3.4), it was clear that at 48 and 72 h.p.i, birds infected with UK661 either had a high clinical score (≥8) or a low clinical score (≤5), despite no significant difference in viral replication in the BF. In order to determine the differences in immune responses between these two groups of birds, RNA-seq was performed on RNA extracted from the BF tissue of one UK661-infected bird that had a low score at 48 h.p.i, one UK661-infected bird that had a high score at 54 h.p.i and one F52/70-infected bird that had a high clinical score at 54 h.p.i as well as four mock birds. Having normalised gene expression to the mock-inoculated birds, pathway analysis was performed on the genes common between a UK661- and a F52/70-inocluated bird with a clinical score of 11 at 54 h.p.i compared to a UK661-inoculated bird with a clinical score of 3 at 48 h.p.i. In this analysis, the top 10 pathways identified included the down-regulation of numerous genes involved in the cell cycle and replication (HP1a, ORC5L, HisH1, MIS12, MAD2A), DNA damage (MSH2, PMS2), chromatid cohesion (ESCO1 and HisH1) and the ubiquitin-proteasomal pathway (HSP70 and SIAH2) (Table 7). Genes up-regulated were predominantly involved in cytoskeleton remodelling (GrinchGEF, RhoV, CDC42, Cortactin, PDGR-R, PDGR-RB). Analysis indicating the pathways exclusively in the UK661-inoculated bird with a clinical score of 3 at 48 h.p.i compared to the two infected birds with clinical scores of 11 at 54 h.p.i was also conducted (Table 8). This analysis highlighted differentially regulated pathways including down-regulation of genes involved in regulation of the cell cycle (SMAD3, Cyclin D1, Cyclin D2) and glucocorticoid receptor signalling (NCOA2, SMAD3) while the genes involved in the metabolic pathways in T cells were also differentially expressed (↓GLSK, ↓GLSL, ↑SLC38A1). These analyses suggest that the low clinical score observed in some birds inoculated with either virus is

due to their ability to mount an adaptive immune response, while birds with high clinical scores exhibited signs of DNA damage and cytoskeleton remodelling with the absence of an adaptive immune response.

Table 7 Pathway analysis of genes assoicated with high clinical score.

Top 10 statistically significant MetaCore pathway maps associated with the up- (red) or down-regulation (blue) of genes common between two birds infected with either UK661 or F52/70 that reached their humane end points with a clinical score of 11 at 54 h.p.i, compared to a bird infected with UK661 with a clinical score of 3 at 48 h.p.i.

Pathway	*p*-value	Molecules
Cell cycle_ Start of DNA replication in early S phase	2.186E-3	**HP1a**, **ORC5L**, **HisH1**
Cell Cycle_ The metaphase Checkpoint	3.075E-3	**HP1a**, **MIS12**, **MAD2A**
G-protein signalling_ RhoB regulation pathway	7.322E-3	**mDIA2**, **DRF**, **CDC42**
Cytoskeleton remodelling_ Regulation of actin cytoskeleton nucleation and polymerisation by Rho GTPases	6.166E-3	**GrinchGEF**, **mDIA2**
DNA damage_ Mismatch repair	1.027E-2	**MSH2**, **PMS2**
Cytoskeleton remodelling_ Regulation of actin cytoskeleton organisation by the kinase effectors of Rho GTPases	1.169E-2	**RhoV**, **CDC42**, **Cortactin**
Cell cycle_ Sister chromatid cohesion	1.366E-2	**ESCO1**, **HisH1**
Neuroprotective action of lithium	1.461E-2	**FRIZZLED**, **TAU**, **HSP70**
Proteolysis_ Role of Parkin in the Ubiquitin-Proteasomal Pathway	1.615E-2	**HSP70**, **SIAH2**
Cytoskeleton remodelling_ Role of PDGFs in cell migration	1.615E-2	**PDGF-R**, **PDGF-RB**

Table 8 Pathway analysis of genes associated with low clinical score.

Top 10 statistically significant MetaCore pathway maps associated with the up- (red) or down-regulation (blue) of genes exclusive to a bird infected with UK661 with a clinical score of 3 at 48 h.p.i, compared to two birds infected with either UK661 or F52/70 that reached their humane end points with a clinical score of 11 at 54 h.p.i.

Pathway	*p*-value	Molecules
Cell cyle_ Regulation of G1/S transition (part 1)	1.061E-3	**SMAD3**, **CyclinD**, **CyclinD2**
Cell cyle_ Nucleocytoplasmic transport of CDK/Cyclins	2.441E-3	**CyclinD**, **IMPORTINa**
Immune response_ Distinct metabolic pathways in naïve and effector CD8+ T cells	7.2125E-3	**GLSK**, **GLSL**, **SLC38A1**
Cell adhesion_ Endothelial cell contacts by non-junctional mechanisms	7.155E-3	**a-CATENIN**, **Vitronectin**
Transcription_ Mechanism of activation of the transcription of Retinoid-target genes	7.155E-3	**NCOA2**, **NCOA3**
Development_ Glucocorticoid receptor signalling	7.750E-3	**NCOA2**, **SMAD3**
Cell cycle_ Regulation of G1/S transition (part 2)	8.368E-3	**CyclinD**, **CyclinD2**
Immune response_ The effect of INDO on T cell metabolism	1.216E-2	**SLC38A1**, **GLSK**, **GLSL**
Normal and pathological TFG-beta-mediated regulation of cell proliferation	1.328E-2	**SMAD3**, **PDGF-B**
Apoptosis and survival_ Cytoplasmic/ mitochondrial transport of proapoptotic proteins Bid, Bmf and Bim	1.406E-2	**FLASH**, **HGK (MAP4K4)**

4.4 Conclusions

- The vvIBDV strain was able to replicate to higher titres than the cIBDV strain in DT40 cells.
- Despite the higher virus replication, DT40 cells infected with the vvIBDV UK661 strain showed a reduction in innate immune pathways compared to the cIBDV strain.
- Birds inoculated with the vvIBDV strain had a lower percentage survival than birds infected with the cIBDV strain, however, there was no significant difference in the peak viral titres of either vv- or cIBDV-infected birds.
- Despite replicating to the same peak titre, there was reduced expression of type I IFN and pro-inflammatory responses in birds inoculated with the vvIBDV strain compared to cIBDV strain.
- Both viruses were detected in other lymphoid tissues (caecal tonsils and spleen) and a type I IFN response was detected in the spleen, however, no significant difference was observed in host gene expression between the virus strains in these tissues.

4.5 Discussion

The principal objective of this chapter was to explore the key differences in host-IBDV interactions between c- and vvIBDV strains, focussing on the innate immune response both *in vitro* and *in vivo*. By comparing the differential gene expression following infection with these IBDV strains in DT40 cells and lymphoid tissues extracted at post-mortem, this study provides new information on how c- and vvIBDV strains interact differently with the innate immune response and lead to different disease outcomes. By identifying these key differences, the molecular determinants for IBDV virulence can be better understood.

To investigate the gene expression in B cells following infection with the cIBDV F52/70 strain or vvIBDV UK661 strain, the growth kinetics of these viruses were studied initially in DT40 cells as they have previously been shown to support infection of c- and vvIBDV strains (Terasaki *et al.* 2007). In a multi-

step growth curve performed with time points between 14 and 72 h.p.i, the UK661 strain replicated to a significantly higher titre than the F52/70 strain at three of the four time points. This difference in virus titre could be due to a combination of more efficient binding of the VP2 protein from the UK661 virus to the target receptor, more efficient replication mediated by the RdRp, or a suppression of the innate immune response that would reduce detection and clearance of the virus. To evaluate the innate immune responses to these two viruses, the expression of a panel of IFN-related genes and pro-inflammatory cytokines was measured. Expression of IFNα, IFNβ and Mx1 was significantly lower in UK661- compared to F52/70-infected cells at 14, 48 and 72 h.p.i. A reduced type I IFN response in UK661-infected cells implies the virus may manipulate host genes to suppress the type I IFN production and signalling pathways, allowing replication of the virus to a higher virus titre. The same trend was observed in IL-6 and IL-1β expression following infection with the UK661 virus, where expression of these genes was consistently lower across the course of infection than the F52/70 virus. IL-8 expression was also measured and while there was no statistically significant difference in its expression between the viruses the UK661 strain induced higher expression of IL-8 than F52/70 at 48 h.p.i, but the F52/70 virus induced higher levels of IL-8 expression than the UK661 virus by 72 h.p.i. Similarly, a study by Quan *et al.* (2017) found IL-8 expression to be up-regulated following infection of 3-4 week old chickens with a DT40-derived vvIBDV Lx strain, however, IL-6 and IL-1β were also found to be significantly up-regulated in this study. This disparity suggests the pro-inflammatory response in DT40 cells may be targeted for suppression by some, but not all, vvIBDV strains. Taken together, these data demonstrate that the type I IFN and some pro-inflammatory genes were expressed to a lower extent in DT40 cells infected with UK661 compared to the F52/70 virus.

In order to verify our *in vitro* data, gene expression of lymphoid tissues such as the BF and spleen during *in vivo* infection with F52/70 or UK661 was investigated in greater detail in this chapter. By studying these viruses *in vivo,* other key parameters such as percentage survival, clinical signs and virus dissemination could also be assessed, thus extending the *in vitro* study at the beginning of this chapter. As expected from the definitions of 'classical' and 'very virulent' IBDV strains discussed

earlier in this thesis (section 1.6), F52/70-infected birds had a higher percentage survival at 83.3%, compared to 50% of UK661-infected birds surviving to their scheduled cull point. These survival rates compare to the mortality rates reported in the literature (Rosenberger and Cloud, 1986; Chettle *et al.* 1989; van den Berg *et al.* 1991; Nunoya *et al.* 1992). The BF: BW ratios recorded in this study were variable, and while an increase is suggestive of increased oedema, and a decrease is suggestive of more severe BF damage (Rautenshlein *et al.* 2003), no statistically significant differences in the ratio were found in this study. For example, at 72 h.p.i the BF: BW ratio from UK661-inoculated birds was higher than birds inoculated with the F52/70 virus, but then there was a reduced ratio in UK661-infected birds that reached their humane end points at 54 h.p.i. How useful the BF:BW ratio is in this experiment is questionable as the timeframe of 3 days may not have been sufficient to see a difference. Clinical scores were comparable between the two strains of virus, with no significant differences identified other than between the number of birds reaching their humane end points for each infected group. Nevertheless, on average the clinical scores in birds inoculated with the F52/70 virus was higher than in birds inoculated with the UK661-virus, with more F5270-inoculated birds reaching clinical scores associated with moderate disease than UK661-inoculated birds. While this may seem counter-intuitive, the elevated type I IFN responses seen in F52/70-inoculated birds could be causing higher clinical scores, but in the long run is protective, leading to a greater percentage survival. Birds with higher clinical scores had an increase in the DNA damage and cellular remodelling pathways in the GO analysis, indicating they may struggle to elicit a successful adaptive immune response due to DNA damage in the infected B cells. It remains unknown why some birds are able to mount a protective immune response whereas others fail to accomplish this, although the sex of the birds was not found to be a contributing factor to gene expression profiles or survival.

Comparing the viral titres of these two viruses throughout infection revealed two main observations. Firstly, there was no significant difference in the peak virus titres between these two viruses measured either by viral copy number of the VP4 protein or live virus. Secondly, the amount of the UK661 virus present in the BF at 24 h.p.i was lower than in the BF of birds inoculated with the F52/70 virus. These

data suggest that the differences previously observed in percentage survival and clinical scores are unlikely to be directly connected to peak BF titre, although it could be due to differences in the kinetics of viral replication. Replication of IBDV strains of different virulence has previously been compared by Rautenschlein *et al.* (2003), where low-pathogenic intermediate IBDV strains were detected in fewer BF cells than the virulent IBDV strain. Previous work by Eldaghayes *et al.* (2006) also studied the replication of the UK661 and F52/70 viruses *in vivo* and found the F52/70 virus replicated to higher titres than the UK661 virus throughout the experiment. However, this data is from two separate *in vivo* studies, conducted on different occasions, and with different starting inoculum titres.

As such, the reason why the UK661 virus titre was considerably lower than for the F52/70 virus, may be due to a lower starting inoculum and hence the need for this present study.

The expression of a panel of type I IFN-related and pro-inflammatory genes was measured to explore the innate immune response to the UK661 and F52/70 viruses *in vivo*. IFNβ, Mx1, IL-8 and IL-1β expression was consistently lower in UK661-infected birds at 24, 48 and 72 h.p.i. This was also the case for IFNα expression at 24 and 48 h.p.i, although this difference inverted at 72 h.p.i with the UK661 virus inducing higher levels of expression. There was little difference in IL-6 expression in the BF of birds infected with either virus. These data are in agreement with our *in vitro* observations that the type I IFN response and pro-inflammatory cytokines had lower expression levels during infection with UK661 compared to the F52/70 virus *in vitro* and *in vivo*, which could potentially cause a reduced survival rate in birds infected with UK661 compared to the F52/70 virus. Type I IFN production is the first line of defence during viral infection, so consequently many viruses have evolved approaches to suppress or inhibit this response to avoid viral clearance, following the downstream up-regulation of numerous ISGs. Mx1 is a key antiviral GTPase enzyme stimulated by IFN during infection (Staeheli, 1990) with many viruses down-regulating this protein during infection, including influenza (Verhelst *et al.* 2012), NDV (Schilling *et al.* 2018) and IBDV (Eldaghayes *et al.* 2006; Smith *et al.* 2015). IL-6, IL-8 and IL-1β, identified as both ISGs and pro-inflammatory cytokines, are predominantly produced by

macrophages (IL-6 and IL-1β) and other cell types (IL-8) in response to infection and have been shown to activate and recruit T cells to the infected tissue (Zhang *et al.* 2019). A study by Kim *et al.* (1998) demonstrated that splenic macrophages were able to enhance type I IFN, IL-6 and IL-8 expression after infection with an intermediate vaccine IBDV strain. It is therefore unclear which cells in the BF are producing these cytokines following IBDV infection, as it could be either the B cell population or macrophage population, or a combination of the two. It would be of interest in future studies to include immunohistochemistry data to accompany the gene expression data, as well as sorting primary bursal cells following *in vivo* IBDV infection into B cell and macrophage pools, to quantify gene expression in the different pools to identify the probable sources of these cytokines. The study by Eldaghayes *et al.* (2006) also found IL-6, IL-1β, IFNα and IFNβ were down-regulated in vvIBDV compared to cIBDV infection *in vivo*, however, as previously stated, the starting virus inoculum was of different titres and the data for each virus was collected from separate experiments limiting the value on these conclusions. When comparing the type I IFN and pro-inflammatory responses, they found both of these defence mechanisms to be down-regulated to a greater extent in UK661-inoculated birds, compared to those inoculated with the F52/70 virus. However, it is difficult to draw conclusions as the viruses replicated to different titres, which may influence the levels of cytokine expression. Moreover, although IFNα and β were down-regulated during UK661 compared to F52/70 infection, the viruses were studied separately in *in vivo* experiments performed on separate occasions, further limiting the conclusions that can be drawn. As a result of the limitations of this study, the conclusions stated require further exploration.

While the BF is most commonly reported as the predominant site of viral replication *in vivo,* other lymphoid tissues such as the spleen and caecal tonsils have also been shown to succumb to infection with some IBDV strains. Here both the UK661 and F52/70 viruses were detected in the spleen and caecal tonsils, with higher titres, comparable to that of the BF, detected in the caecal tonsils for both

viruses, whereas viral replication in the spleen was limited. The virus titres were comparable for both viruses in the spleen, while in the caecal tonsils the UK661 virus replicated to higher titres than the F52/70 virus at 72 h.p.i, possibly linking the UK661 virus to a greater dissemination in the extra-bursal tissues of infected birds although further experiments and shedding data would be beneficial to support this conclusion. As the UK661 virus replicated to higher titres in the caecal tonsils than the F52/70 virus, this may also have an associated impact on the gut mucosal immunity, which could in turn affect the gut microbiome composition (Wang *et al.* 2009a). Previous work by Li *et al.* (2018a) has demonstrated infiltration of T cells and macrophages into the caecum during infection with vvIBDV, in addition to the ability of the virus to modulate the composition of the gut microbiota and cause the differential colonisation of bacterial species (Li *et al.* 2018a; Li *et al.* 2018b). This change in bacterial composition could cause an increased susceptibility in these birds to other pathogens gaining entry through the gut mucosa.

The expression levels of type I IFN-related and pro-inflammatory genes were lower in the spleen compared to the BF tissue, and the expression of IL-6, IL-8 and IL-1β was lower on average than IFNα, IFNβ and Mx1 expression in the spleen. These IFN-related genes were on average up-regulated to a greater extent in F52/70-infected birds, compared to birds infected with the UK661 virus, although this did not reach statistical significance. As low levels of virus replication were detected in the spleen for both viruses, which could explain the low expression of type I IFN and pro-inflammatory cytokines in the organ. It remains unknown why the replication was lower in the spleen. It would be beneficial in future infection studies to conduct immunohistochemistry on this organ to determine if IBDV-infected cells are present, and it would also be beneficial to quantify viral infection by $TCID_{50}$ as well as qPCR to validate these data. The majority of UK661-infected birds that reached their humane end points at 54 h.p.i had higher levels of expression of Mx1 and IL-8 than the F52/70-infected bird that was also culled. Conversely, this F52/70-infected bird had higher levels of IL-6, IL-1β, IFNα and IFNβ than two of the UK661-infected birds at this time point. The reason for these differences in gene

expression is unknown and further investigation is needed to shed light on the key differences in innate immune responses between these birds.

We observed a wide distribution of clinical scores, despite the Rhode Island Red flock being inbred. Clinical scoring was performed by at least two individuals to reduce bias and subjectivity, yet a wide spread of data points were recorded by both observers. While these birds are an inbred line, the wide distribution of clinical scores suggests host variation may still play a role in the efficiency of their innate and adaptive immune responses. IBDV resistance has previously been demonstrated between different inbred lines, however, variation within an inbred line leading to differences in disease outcome has not been as extensively studied (Smith *et al.* 2015).

To investigate the diversity within each infected group of birds in terms of disease outcome, next generation sequencing was performed on the RNA from BF tissue samples from these birds of interest. From this analysis, pathways involved with cell cycle and replication (↓HP1a, ↓ORC5L, ↓HisH1, ↓MIS12, ↓MAD2A), DNA damage (↓MSH2, ↓PMS2), chromatid cohesion (↓ESCO1 and ↓HisH1), ubiquitin-proteasomal pathway (↓HSP70 and ↓SIAH2) and cytoskeleton remodelling (↑GrinchGEF, ↑RhoV, ↑CDC42, ↑Cortactin, ↑PDGR-R, ↑PDGR-RB) were commonly up- or down-regulated in both the UK661- and F52/70 infected birds at 54 h.p.i with a high clinical score of 11 compared to a UK661-inoculated bird at 48 h.p.i with a low clinical score of 3. Conversely, the pathways associated exclusively with the lower clinical score of 3 were: regulation of the cell cycle (↓SMAD3, ↓Cyclin D1, ↓Cyclin D2); glucocorticoid receptor signalling (↓NCOA2, ↓SMAD3); and differential regulation of the metabolic pathways in T cells (↓GLSK, ↓GLSL, ↑SLC38A1).

Some of the differentially regulated genes were highlighted in multiple pathways: HP1a, CDC42, HisH1, HSP70, SMAD3, Cyclin D1, Cyclin D2 and NCOA2. Heterochromatin Protein 1a (HP1a) is a component of heterochromatin which has been shown to be stabilised by unphosphorylated STAT found in the nucleus, resulting in the protection of genome stability and preventing DNA damage in the cell (Quintás-Cardama and Verstovsek, 2013; Tsurumi *et al.* 2017). HSP70 is a heat shock protein

responsible for sensing oxidative damage and repairs unfolded or misfolded proteins (Xu *et al.* 2018). Cell division cycle protein 42 (CDC42) regulates actin rearrangement and the differentiation of immune cells, as well as aiding the migration and phagocytosis of macrophages (Dong *et al.* 2019). A study by Dong *et al.* (2019) identified its ability to regulate the inflammatory response by suppressing pro-inflammatory and anti-inflammatory cytokines (IL-10, TNF-α and IFN-γ) facilitating the recovery of the innate immune and inflammatory responses in mice with inflammatory bowel disease. The down-regulation of HP1a and HSP70 and up-regulation of CDC42 in birds with a high clinical score, may indicate the virus has caused extensive cellular damage, preventing the infected cell from repairing itself (↓HP1a and ↓HSP70) while the host may be up-regulating CDC42 to support phagocytosis by macrophages attracted to the BF.

Some genes exclusive to the UK661-inoculated bird at 48 h.p.i with a low clinical score of 3 were SMAD3 (↓), Cyclins D1 and D2 (↓) and NCOA2 (↓). SMAD3, or Mothers against decapentaplegic homologue 3, is part of the transforming growth factor-beta (TGF-β) pathway. A study by Pokharel *et al.* (2016) demonstrated TGF-β-SMAD2/3 signalling was required for IFNβ production during respiratory syncytial virus (RSV) infection and inhibition of signalling reduced IFNβ production in macrophages. Along with SMAD3, NCOA2, also known as glucocorticoid receptor interacting protein-1 (GRIP-1), was also associated with a low clinical score. GRIP-1 plays a role in assisting nuclear receptors in the up-regulation of DNA expression and is recruited by GILZ to the glucocorticoid response element (GRE) region activating or repressing gene transcription (Avenant *et al.* 2010). Cyclin D1 and D2 are crucial to the completion of the G1 phase of the cell cycle and entry into the S phase (Blomen and Boonstra, 2007). The down-regulation of SMAD3, Cyclin D1 and D2 in birds with a lower clinical score, may be the result of a wider shut-off of cellular protein production by the virus in an attempt to reduce the expression of antiviral genes. However, there is insufficient evidence at this time to draw this conclusion.

Taken together, type I IFN and pro-inflammatory responses following UK661 infection were lower than during F52/70 infection *in vitro* and *in* vivo, despite no significant differences in peak virus titres *in vivo*, and UK661 replicating to an elevated titre *in vitro*. Both viruses were detected in the spleen and caecal tonsils, following *in vivo* infection, in addition to the BF, with the UK661 virus replicating to higher virus titres in the caecal tonsils, whereas no differences in replication were found between the viruses in the spleen, although replication in this organ was limited. We speculate that UK661 suppresses antiviral immune responses to a greater extent than other strains of IBDV, consistent with our conclusions from Chapter 3. This may, in part, explain its enhanced virulence. In addition, next generation sequencing and pathway analysis revealed that the infiltration and activation of other innate immune cells that may be vital for the outcome of infection, which could be complemented by immunohistochemistry data in the future. As both pro-inflammatory cytokine expression and type I IFN induction can be mediated via an NF-κB-dependent pathway, and both are expressed to a lesser extent by UK661 and to a greater extent than F52/70, it is therefore possible that the UK661 IBDV strain is able to antagonise the NF-κB activation to a greater extent than the F52/70 strain, although this needs to be experimentally tested.

5. Interactions between IBDV VP4 proteins and the host immune response

5.1 Introduction

In the previous chapter, lower levels of type I IFN and pro-inflammatory responses were expressed during infection with the vvIBDV UK661 compared to the cIBDV strain F52/70, both *in vitro* in DT40 cells and *in vivo* in 3 week old chickens. As no difference was found between peak virus titres *in vivo*, we hypothesise that key interactions between the UK661 virus and the host immune response played a key part in the increased virulence and more severe disease outcome associated with chickens inoculated with this virus. Following this conclusion, this chapter aims to evaluate the molecular mechanism involved in these host-virus interactions.

As is common among other viruses, IBDV has multiple approaches to evading the cell intrinsic and innate immune responses of the cell in order to facilitate cell entry, viral replication and ultimately, release of viral progeny for transmission of the virus. The limited number of these proteins in IBDV means they are necessarily multifunctional, combining their key roles in the viral replication cycle with inhibition and manipulation of the cellular innate immune pathways.

The VP3 and VP4 proteins have both been demonstrated to play a role in the inhibition of type I IFN production and/or signalling. IBDV VP3 is an important structural protein and functions as the second most abundant capsid protein after the VP2 protein (Luque *et al.* 2009b). VP3 coats the dsRNA genome shielding it from detection by MDA5 (Tacken *et al.* 2002; Ye *et al.* 2014; Ferrero *et al.* 2015). This protective role of VP3 aids the replication process and suppresses the activation of antiviral responses downstream of MDA5, including the type I IFN pathways (Ye *et al.* 2014). One study by Busnadiego *et al.* (2012) reported the anti-apoptotic properties of VP3 and demonstrated how VP3

can inhibit the VP2-induced activation of PKR. Upon activation of PKR, the eukaryotic initiation factor 2a (eIF2a) is phosphorylated and downstream signalling concludes in apoptosis early during IBDV infection. The VP4 protein has been shown to interact with the host protein GILZ which negatively regulates NF-κB signalling by binding to the p65 subunit (Li *et al.* 2013b; Di Marco *et al.* 2007). Another study from the same laboratory, demonstrated the binding of VP4 to GILZ prevents ubiquitylation and blocks degradation of GILZ. As an accumulation of GILZ leads to the inhibition of NF-κB signalling, there is also a downstream suppression of IFNβ expression (He *et al.* 2018). VP4 has also been shown to be targeted by the cellular protein CypA to inhibit viral replication (Wang *et al.* 2015b). CypA is known to play a role in supporting the RIG-I-mediated antiviral response by controlling the ubiquitylation of RIG-I and MAVS (Liu *et al.* 2017a). This study found RIG-I-independent signalling, via MDA5, was also promoted by CypA during encephalomyocarditis virus (ECMV) infection in mammals, which suggests the CypA-VP4 interaction could also be important for the disease outcome of IBDV infection.

Viral antagonism of host innate immunity has been investigated for another member of the *Birnaviridae* family. Lauksund *et al.* (2015) showed IPNV proteins VP2, VP3, VP4 and VP5 were able to suppress type I IFN signalling. Of these proteins, IPNV VP4 was able to completely abolish type I IFN signalling, and while the JAK-STAT pathway is believed to be targeted by VP4, the mechanism remains unknown (Skjesol *et al.* 2009; Lauksund *et al.* 2015). Interactions between the VP4 protein and type I IFN response appear to be crucial to the most studied viruses in the *Birnaviridae* family, although the strategies employed by VP4 to manipulate the innate immune response require further investigation.

Few studies have explored the role of IBDV VP4 in the suppression of the innate immune response, and only VP4 proteins from vvIBDV strains have been investigated to date (Li *et al.* 2013b; Wang *et al.* 2015b; He *et al.* 2018). From the evidence presented which highlighted the importance of VP4 interactions with the innate immune pathways, comparing the VP4 proteins from IBDV strains of differing virulence, may reveal how they influence infection progression and disease outcome.

5.2 Chapter Aims

The research aim for this chapter was to explore the interactions between VP4 proteins from different IBDV strains and the host innate immune response. The objectives covered by this main aim were to compare the VP4 proteins from UK661 and F52/70 and their interactions with the type I IFN response, both in the context of the protein and as part of a chimeric virus, for studies *in vitro* and *in vivo.* The hypothesis for this chapter is that the UK661 VP4 protein contributes to the reduced expressed of the type I IFN responses, previously described in the context of whole virus in chapters 3 and 4.

5.3 Results

5.3.1 There are 9 amino acid differences in the sequence of IBDV VP4 from different strains

To determine the diversity of VP4 sequences across groups of vvIBDV, cIBDV and caIBDV strains available on the NCBI database, sequences were aligned using Clustal Omega (Sievers *et al.* 2011) identifying aa differences between the strains. The alignment shows there are 5 sites where vvIBDV strains have a mutation compared to c- and caIBDV strains (I31, Y170, N175, S205, D241) (Figure 20, yellow). There are 3 additional mutations specific to UK661 and Lx which are different from the other vvIBDV as well as all c- and caIBDV strains (Figure 20, green). In addition, one mutation is found in the F52/70 strain at position 132 that has changed K -> R (Figure 20, pink). This mutation brings the overall number of aa differences between the F52/70 and UK661 strains to 9.

The structure of the IBDV VP4 protein is yet to be determined, however, the VP4 of the Aquabirnavirus 'Yellowtail Ascites Virus (YAV) is available (Chung and Paetzel, 2013). To identify the positioning and grouping of the aa differences between UK661 and F52/70 VP4 sequences as folded proteins, the aa sequences were modelled based on the YAV VP4 (template 4izk.2.A) using the PyMOL Molecular Graphics System (Version 2.0, Schrödinger, LLC.) (Figure 21). The YAV VP4 aa sequence shares 24.75% homology with IBDV but misses the last 25 aa from the IBDV sequence so the 241 site is missing from the structures. Based on this model, the aa differences between the two VP4 proteins are distributed throughout the structure, and lead to changes in the secondary structure of the molecule (Figure 21, box).

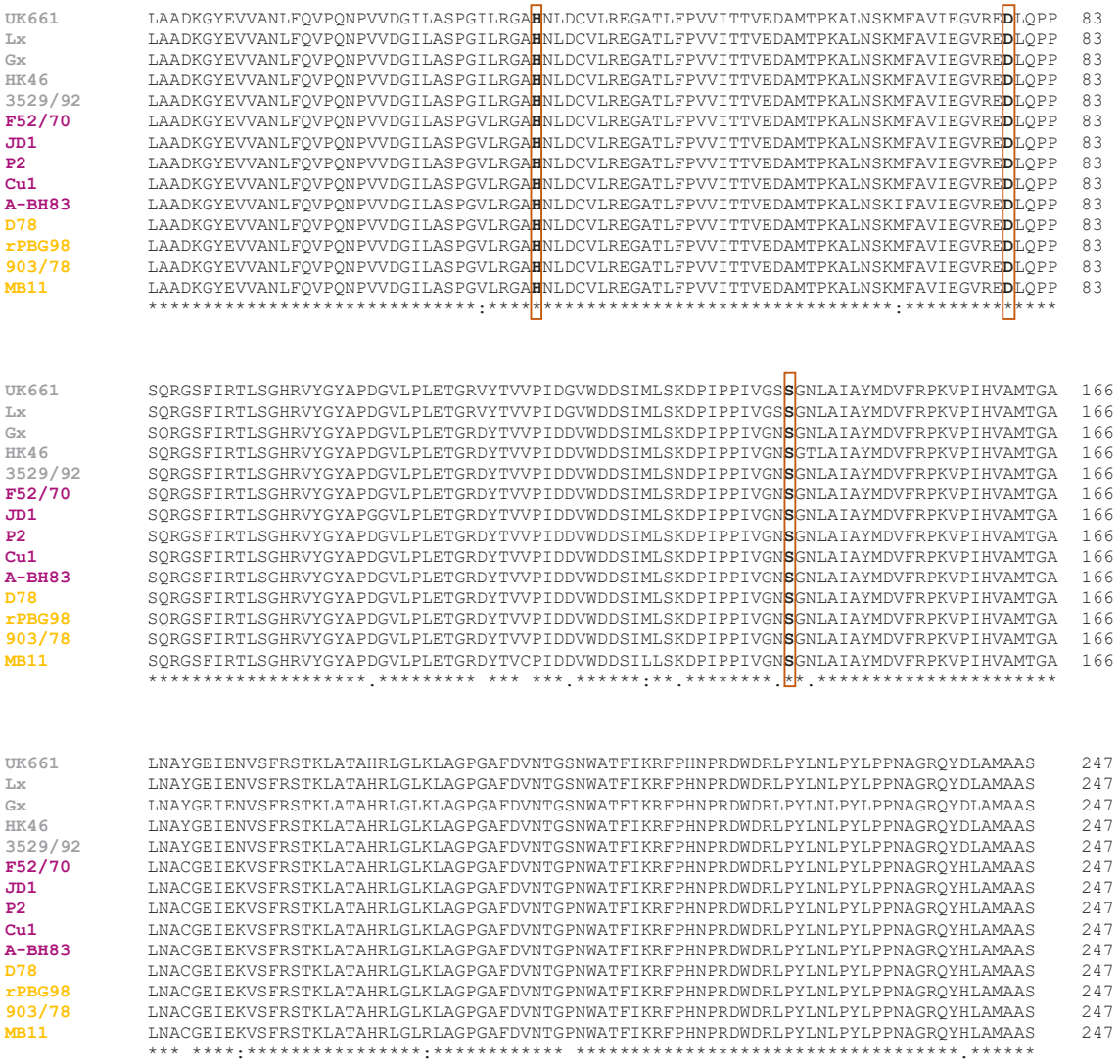

Figure 20 Amino acid sequence alignment of vvIBDV (*grey), cIBDV (*pink) and caIBDV / vaccine (orange) IBDV strains.

Amino acids highlighted in yellow are exclusive to vvIBDV strains and those in pink are specific to F52/70 compared to all other strains. Green indicates these aa are found in some but not all vvIBDV strains, while blue indicates other aa differences in the VP4 sequences aligned. The brown boxes identify the catalytic triad responsible for the protease function of VP4.

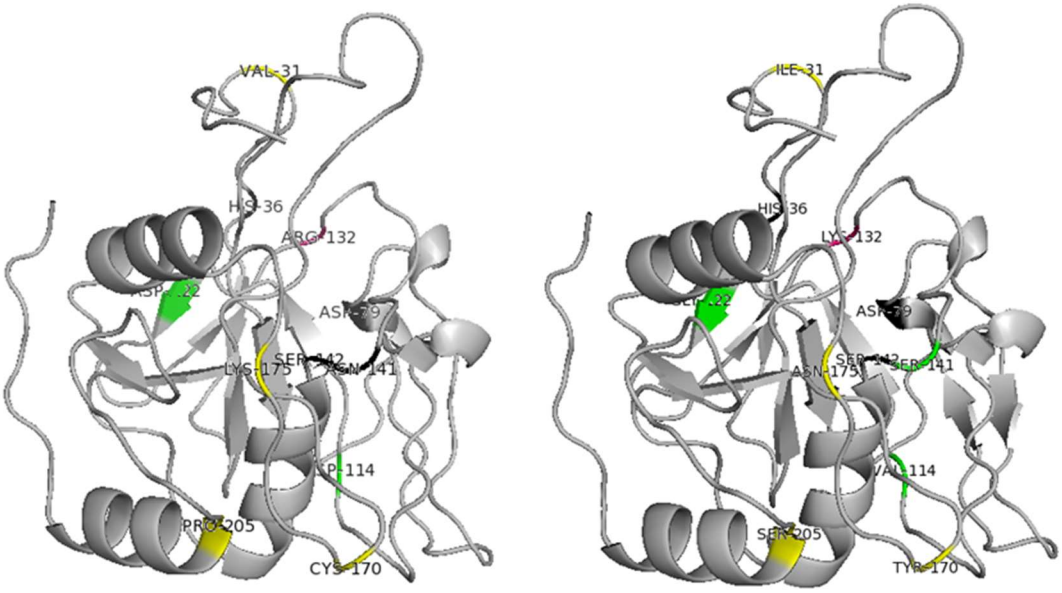

Figure 21 Predicted F52/70 and UK661 VP4 structures.

F52/70 (A) and UK661 (B) VP4 structures modelled using PyMOL based on the Yellowtail Ascites Virus VP4 (template 4izk.2.A). Mutations between F52/70 and UK661 are labelled in the same colours as indicated in Figure 20 and **black** sites indicate the location of the catalytic triad responsible for protease function.

5.3.2 The UK661 VP4 protein down-regulates IFNβ production to a greater extent than the F52/70 VP4 protein

Having identified 9 aa differences between UK661 and F52/70 VP4, the ability of the two proteins to modulate IFNβ production was measured using a chIFNβ luciferase reporter assay. Briefly, DF-1 cells were transfected with the chIFNβ luciferase reporter, a renilla plasmid as a control for protein expression, and expression plasmids containing either the UK661 or the F52/70 VP4 proteins that were tagged with eGFP at the N-terminus Previously, it has been shown that the eGFP-tagged IBDV VP4 protein from the Lx strain is functional and is a type I IFN antagonist (Li *et al.* 2013b). Cells were then transfected with poly I:C to stimulate IFNβ production which in turn correlates to luciferase expression. Very little background of IFNβ was observed in all untreated groups with little difference between those transfected with the VP4 expression plasmids and the eGFP vector control (Figure 22). Upon stimulation with poly I:C, in cells transfected with a control plasmid containing eGFP alone, there was a significant increase in IFNβ production. Cells transfected with eGFP-UK661 VP4 did not show this increase in IFNβ production compared to the eGFP-only control ($P<0.05$), or cells transfected with the eGFP-F52/70 VP4 which appeared to significantly increase IFNβ production compared to both eGFP-UK661 VP4 and the eGFP-only control (**$P<0.01$ and *$P<0.05$, respectively). These data suggest that the UK661 VP4 can reduce IFNβ production to a greater extent than the F52/70 VP4 protein.

In addition to the IFNβ induction, the ability of the VP4 proteins to manipulate IFN signalling was measured using a chMx1 luciferase reporter assay. Briefly, DF-1 cells were transfected with the chMx1 luciferase reporter, a renilla plasmid and either eGFP-UK661 or eGFP-F52/70 VP4 expression plasmids, or an eGFP-only control plasmid. Cells were then transfected with chicken IFNα to stimulate Mx1 production which in turn correlated to luciferase expression. Untreated cells had a modest increase in Mx1 production during

the experiment (Figure 23). Cells transfected with the eGFP-F52/70 VP4 plasmid produced significantly less Mx1 compared to cells transfected with the eGFP-UK661 VP4, suggesting the F52/70 VP4 protein is able to reduce IFNβ signalling to a greater extent than the UK661 VP4 protein.

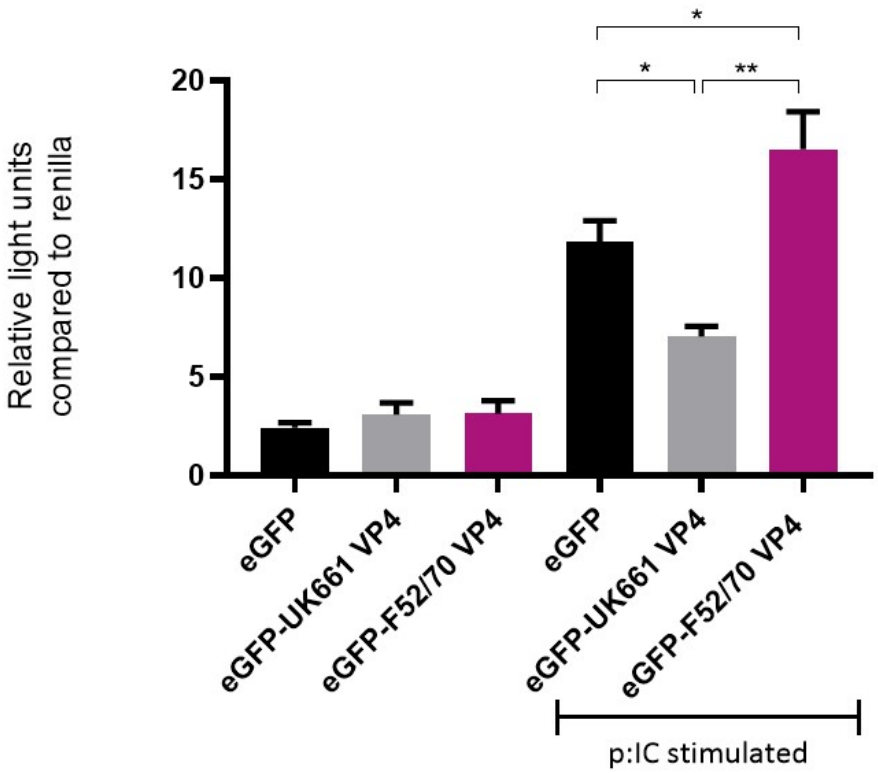

Figure 22 The ability of eGFP-tagged VP4 expression plasmids to inhibit IFNβ production.

DF-1 cells were transfected with the chicken IFNβ promoter firefly luciferase reporter, a constitutively active Renilla expression plasmid and the eGFP-tagged VP4 expression plasmids. Twenty-four hours post-transfection (h.p.t), cells were re-transfected with poly I:C. At 6 h.p.t, cells were lysed and luciferase activity quantified. Luciferase activity was normalised to Renilla expression. Data presented are the means of three independent experiments and passed a Shapiro-Wilk normality test before analysis using a one-way ANOVA and Tukey's multiple comparison test (*P<0.05).

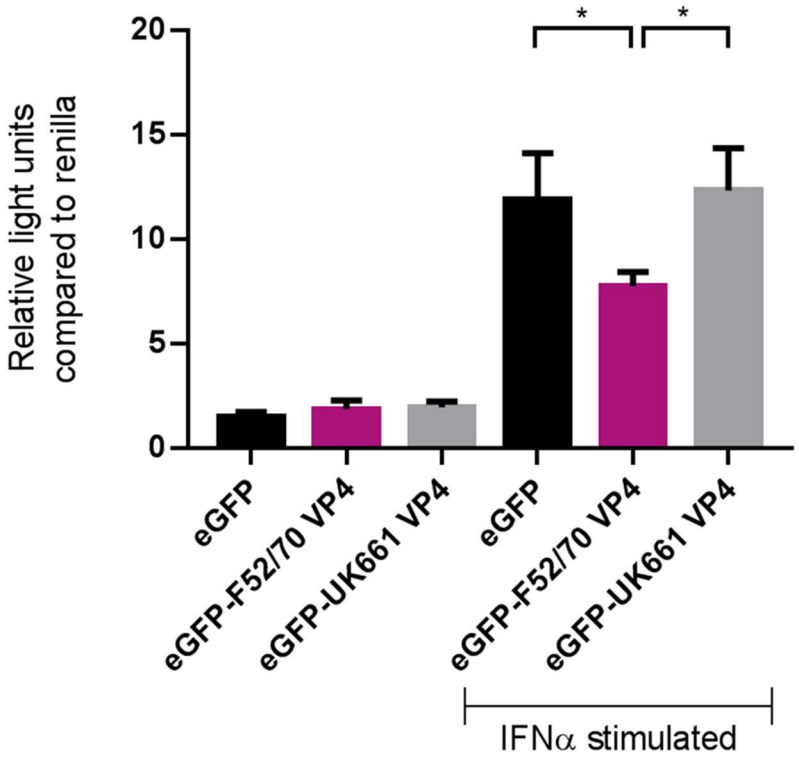

Figure 23 The ability of eGFP-tagged VP4 expression plasmids to inhibit Mx1 production.

DF-1 cells were transfected with a chicken Mx1 promoter firefly luciferase reporter, constitutively active Renilla expression plasmid and the eGFP-tagged VP4 expression plasmids. Twenty-four h.p.t, cells were re-transfected with chicken IFNα. At 6 h.p.t, cells were lysed and the luciferase activity quantified. Luciferase activity was normalised to Renilla expression. Data presented are the means of three independent experiments and passed a Shapiro-Wilk normality test before analysis using a Kruskal-Wallis and Dunn's multiple comparison test (*P<0.05).

5.3.3 IBDV VP4-mediated inhibition of IFNβ production is not dependent on its function as a protease

As the previous results suggest the VP4 proteins may have the ability to antagonise different parts of the IFN production or signalling pathways, the next step was to determine whether this was dependent or independent of VP4's function as a protease. To address this research question, protease knock-out (pKO) mutant VP4 expression plasmids were generated by mutating the histidine at position 36 to a proline (H36P). This mutation (CAC/CAT-> CCG) is in the catalytic triad was previously found to be essential for protease activity (Rodríguez-Lecompte and Kibenge, 2002). These pKO mutant VP4 expression plasmids were then transfected into DF-1 cells as described in section 5.3.2. The vector control produced a good induction of IFNβ, whereas eGFP-UK661 VP4, which was used as a positive control for IFNβ inhibition, induced a significantly lower IFNβ production than the vector control as previously observed in other experiments (Figure 24). The eGFP-UK661 VP4 pKO mutant also significantly reduced IFNβ production compared to the vector control. There was no significant difference in IFNβ production in cells transfected with F52/70 VP4 pKO compared to the vector control. These data indicate that the ability of UK661 VP4 to reduce IFNβ production is independent of its role as a protease.

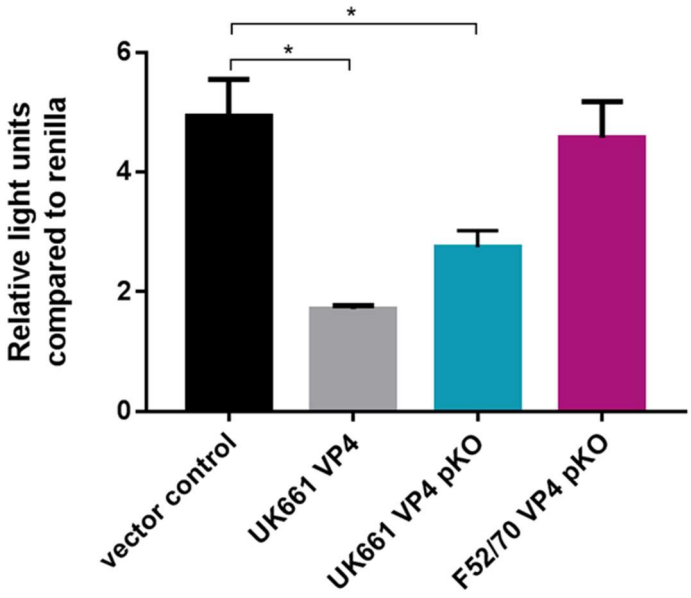

Figure 24 The ability of eGFP-tagged VP4 protease knock-out (KO) expression plasmids to inhibit IFNβ production

DF-1 cells were transfected with the chicken IFNβ promoter firefly luciferase reporter, constitutively active Renilla expression plasmid and eGFP-tagged VP4 expression plasmids from the UK661 virus, and pKO mutant VP4 proteins from the UK661 and F52/70 viruses. Twenty-four h.p.t, cells were transfected with poly I:C. At 6 h.p.t, cells were lysed and luciferase activity quantified. Luciferase activity was normalised to Renilla expression. Data presented are the means of three independent experiments and passed a Shapiro-Wilk normality test before analysis using a Kruskal-Wallis and Dunn's multiple comparison test (*P<0.05).

5.3.4 Both 5’ and 3’ regions of the VP4 sequence are required for its inhibition of the IFNβ production pathway

To investigate the region of the VP4 proteins responsible for the reduction in IFNβ production, 5’ 3’ end switch mutants were generated whereby one mutant had 5’-1-460bp UK661 VP4 and 461-729bp-3’ F52/70 VP4 (5’ UK_3’F52), and the other mutant had the opposite pair of sequences (5’F52_3’UK). The protein structures of these mutants were compared to the wt UK661 and F52/70 VP4 structures using Phyre2 (Kelley *et al.* 2015) to predict any folding abnormalities. DF-1 cells were transfected with these mutants as described above in section 5.3.2, including the wt UK661 VP4 as a control for reduced IFNβ production. The vector control induced IFNβ production and that was reduced in the presence of wt UK661 VP4, as expected (Figure 25). Both the 5’3’ switch mutants induced significantly higher IFNβ production than wt UK661 VP4 (**P<0.01), although 5’F52_3’UK induced significantly higher levels of IFNβ than 5’UK_3’F52 (*P<0.05). Therefore 5’UK_3’F52 is able to reduce IFNβ production compared to 5’F52_3’UK, but not to the same extent as wt UK661 VP4. This data suggests the 5’1-460bp of UK661 VP4 sequence may be partially responsible for the reduction in IFNβ observed, although this is dampened when the 461-729bp-3’ of F52/70 VP4 is included giving reason to believe multiple mutations throughout the VP4 sequence contribute to this function. The aa positions 31, 114, 122, 132, 141 may be important in UK661 VP4-mediated inhibition of type I IFN induction.

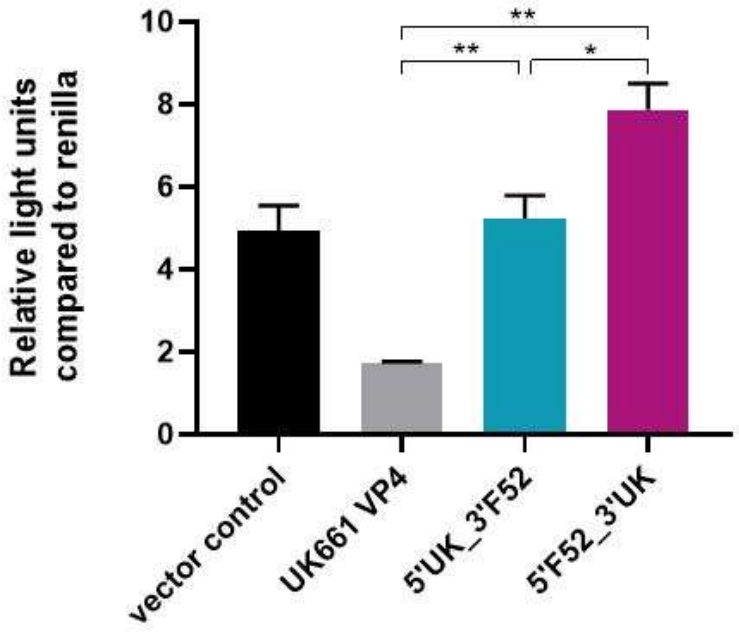

Figure 25 The ability of eGFP-tagged VP4 5'3' end switch expression plasmids to inhibit IFNβ production.

DF-1 cells were transfected with chicken IFNβ promoter firefly luciferase reporter, constitutively active Renilla expression plasmid and either the eGFP-tagged VP4 5'3'end switch expression plasmids (blue or pink) or wt eGFP-tagged UK661 VP4 expression plasmid (grey) as a positive control for inhibition. Twenty-four h.p.t, cells were transfected with poly I:C. At 6 h.p.t, cells were lysed and luciferase activity quantified. Luciferase activity was normalised to Renilla expression. Data presented are the means of three independent experiments and passed a Shapiro-Wilk normality test before analysis using a one-way ANOVA and Tukey's multiple comparison test (*P<0.05, **P<0.01).

5.3.5 Chimeric viruses with UK661 or F52/70 VP4 replicated *in vitro* causing differential expression of innate immune genes

Having found that the UK661 VP4 protein inhibited the induction of type I IFN to a greater extent than the F52/70 VP4 protein by luciferase reporter assays, we were interested in studying the VP4 proteins in the context of a whole virus. To this end, chimeric VP4 viruses were generated using a reverse genetics system developed in the lab for the caIBDV strain PBG98. The VP4 genes from the UK661 and F52/70 viruses were cloned independently into the PBG98 backbone, replacing the PBG98 VP4 sequence. The chimeric viruses were then rescued, and virus stocks grown in DF-1 cells, before titration. To compare the replication kinetics of the chimeric VP4 viruses to the parental PBG98 virus, DF-1 cells were infected at an MOI of 1 and RNA was extracted, reverse transcribed and viral RNA quantified at several time points up to 72 h.p.i. All three viruses replicated to peak virus titres of between 10^4 and 10^5 fold change in genome copies (Figure 26), and there was no significant difference at any of the time points.

IFNβ expression in cells infected with the PBG+UK661 VP4 virus was less at 6 h.p.i compared to the other two viruses confirming our findings with transfected proteins. However, this difference was no longer present at 12 h.p.i and both chimeric VP4 viruses induced higher IFNβ expression at 24 h.p.i compared to the PBG98 virus (Figure 27A). Cells infected with the PBG98 virus expressed more Mx1 than cells infected with the chimeric VP4 viruses at 6 and 12 h.p.i. However, by 24 h.p.i levels of Mx1 expression was higher in PBG+F52/70 VP4-infected cells than in cells infected with either PBG98 or PBG+UK661 VP4 viruses (Figure 27B). For both chimeric VP4 viruses MDA5 was significantly upregulated at 6 h.p.i compared to PBG98 (Figure 27C). MDA5 expression spiked for a second time at 24 h.p.i for both chimeric VP4 viruses, having previously dropped for all viruses at 12 h.p.i. IFIT5 expression peaked at 6 h.p.i with both chimeric VP4 viruses inducing more IFIT5 than PBG98 (Figure 27D). Following a similar trend to

MDA5, IFIT5 expression spiked again at 24 h.p.i having dropped at 12 hours. There was little difference in RSAD2 expression throughout the experiment, but PBG+F52/70 VP4 induced more RSAD2 than the other two viruses at 48 and 72 h.p.i (Figure 27E). STAT1 expression peaked at 6 h.p.i where both chimeric VP4 viruses induced significantly higher STAT1 expression compared to PBG98 (Figure 27F). There was little difference in STAT1 expression at the later time points.

To investigate interactions with the chimeric VP4 viruses and type I IFN pathways before 6 h.p.i, DF-1 cells were infected with the chimeric VP4 viruses and PBG98 at an MOI of 5 to ensure a high percentage of cells were infected. RNA was then extracted, reverse transcribed and viral RNA measured by qPCR. The replication kinetics showed no significant difference between the viruses at any of the time points, although PBG+UK661 VP4 replicated to a higher virus titre than the other viruses at 6 h.p.i (*$P<0.05$) (Figure 28). The same cDNA was also used to measure expression of genes in the IFN pathways as described earlier in this section. At 2 h.p.i the viruses induced the same gene expression trend across all of the genes measured, whereby the PBG+F52/70 VP4 virus induced much lower levels of each gene compared to the other two viruses (Figure 29). At 6 h.p.i, the PBG+UK661 VP4 virus induced more IFNα and β expression than the other two viruses, although this didn't reach statistical significance. Mx1 expression was lower at 6 h.p.i with the PBG+F52/70 VP4 virus, compared to the other two viruses, having spiked at 4 h.p.i.

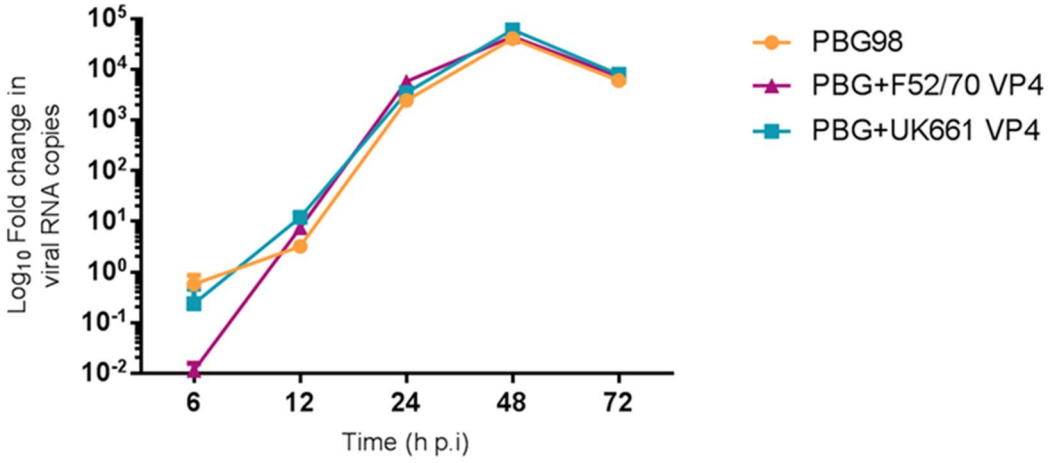

Figure 26 Replication of the PBG98, PBG+UK661 VP4 and PBG+F52/70 VP4 viruses in DF-1 cells.

Cells were infected with PBG98 (orange), PBG+F52/70 VP4 (pink) or PBG+UK661 VP4 (blue) at an MOI of 1. RNA was extracted from cells at the indicated time points, reverse transcribed, and a conserved region of the VP4 gene was amplified by qPCR. The VP4 gene Ct values were normalised to the RPLP0 housekeeping gene as per the $2^{-\Delta CT}$ method and a one-way ANOVA was performed where no significant difference was found at any time point between the three viruses. Data were expressed as $\log_{10}$-fold change in VP4 RNA relative to mock-infected samples as per the $2^{-\Delta\Delta CT}$ method. Data shown are representative of at least three replicate experiments, and error bars indicate the standard deviation of the mean.

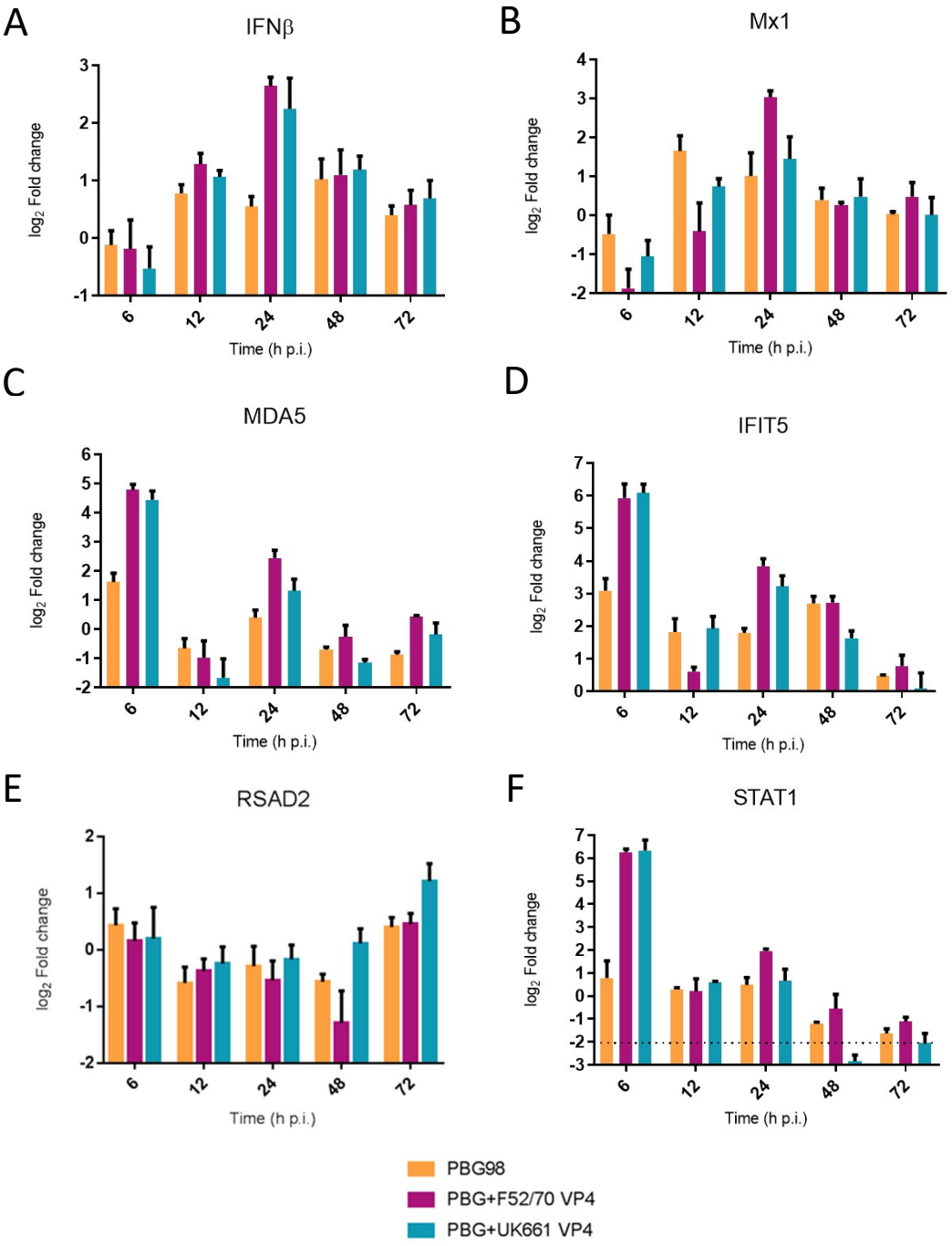

Figure 27 qRT-PCR analysis of type I IFN-related genes in PBG98-, PBG+F52/70 VP4 and PBG+UK661 VP4-infected DF-1 cells late during infection.

RNA was extracted from DF-1 cells infected with PBG98 (orange), PBG+F52/70 VP4 (pink) or PBG+UK661 VP4 (blue) with an MOI of 1 at 6, 12, 24, 48 and 72 h.p.i. RNA was reverse transcribed and amplified by qPCR with a panel of IFN-related genes; IFNβ (A), Mx1 (B) MDA5 (C), IFIT5 (D) RSAD2 (E) and STAT1 (F), before normalisation of infected samples to mock-infected samples and the housekeeping gene RPLP0 using the $2^{-\Delta\Delta CT}$ method. Data are representative of at least three replicate experiments and passed a Shapiro-Wilk normality test before analysis using a one-way ANOVA (not significant).

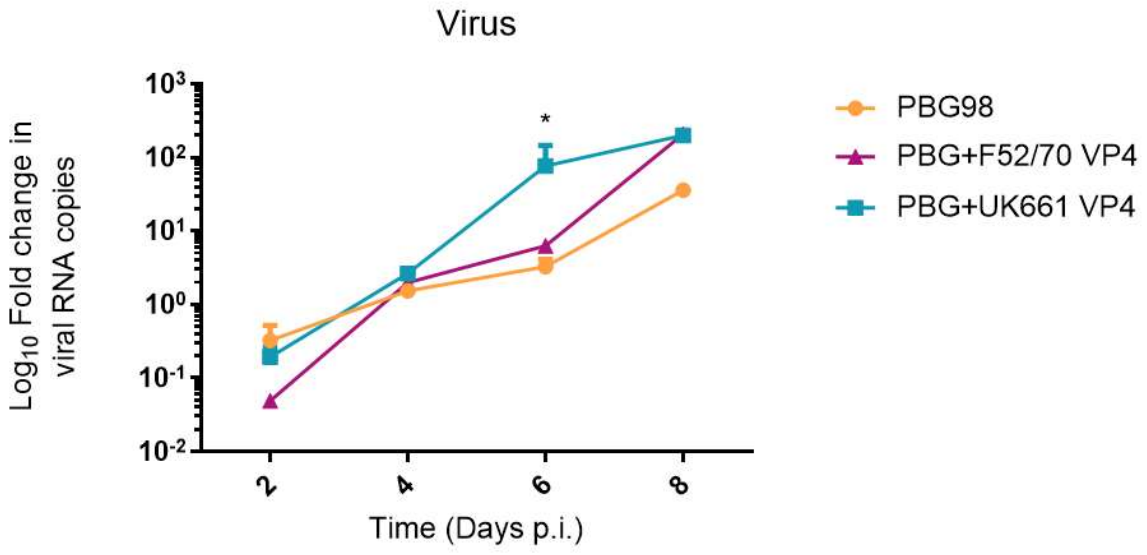

Figure 28 Replication of PBG98, PBG+F52/70 VP4 and PBG+UK661 VP4 in DF-1 cells

Cells were infected with PBG98 (orange), PBG+F52/70 VP4 (pink) or PBG+UK661 VP4 (blue) at an MOI of 5, before RNA extraction from cells at the indicated time points. RNA was reverse transcribed and a conserved section of the VP4 gene was amplified by qPCR. VP4 gene Ct values were normalised to the RPLP0 housekeeping gene as per the $2^{-\Delta CT}$ method and a one-way ANOVA and Tukey's multiple comparison test ($P<0.05$). Data were expressed as $\log_{10}$-fold change in VP4 RNA relative to mock-infected samples as per the $2^{-\Delta\Delta CT}$ method. Data shown are representative of at least three replicate experiments, and error bars indicate the standard deviation of the mean.

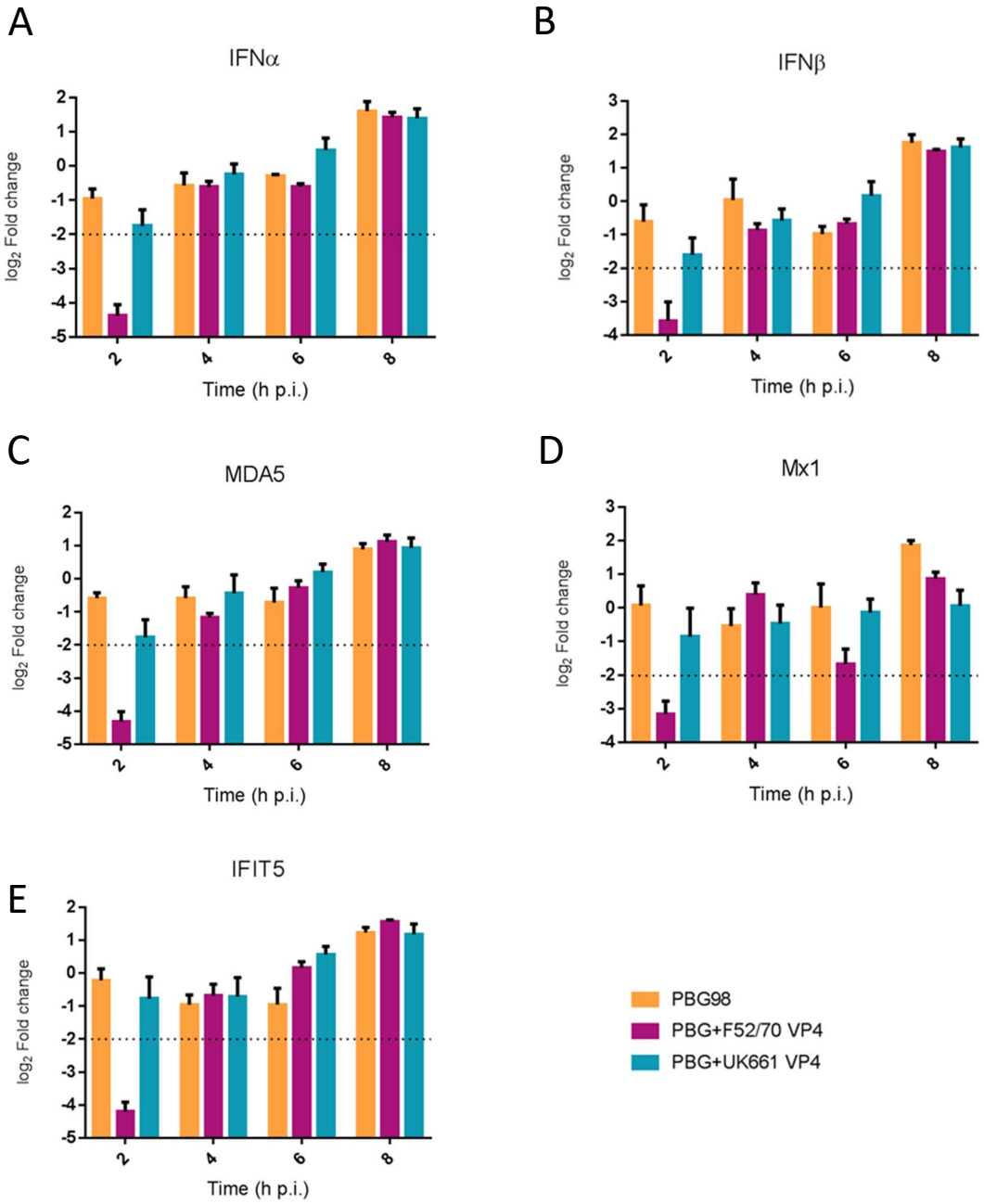

Figure 29 qRT-PCR analysis of type I IFN-related genes in PBG98-, PBG+F52/70 VP4- and PBG+UK661 VP4-infected DF-1 cells early during infection.

RNA was extracted from DF-1 cells infected with PBG98 (orange), PBG+F52/70 VP4 (pink) or PBG+UK661 VP4 (blue) with an MOI of 5 at 2, 4, 6 and 8 h.p.i with a panel of IFN-related genes; IFNα (A), IFNβ (B), MDA5 (C), Mx1 (D) IFIT5 (E). Extracted RNA from infected and mock samples were reverse transcribed and amplified by qPCR using specific primer sets for target genes, before normalisation of infected samples to mock-infected samples and the housekeeping gene RPLP0 using the $2^{-\Delta\Delta CT}$ method. Data are representative of at least three replicate experiments and passed a Shapiro-Wilk normality test before analysis using a one-way ANOVA test where no significant difference was found at any time point between the three viruses.

5.3.6 Birds inoculated with either chimeric VP4 virus showed 100% survival and low clinical scores

The chimeric VP4 viruses generated for experiments in section 5.3.5 were used to study the effect of UK661 and F52/70 VP4 during infection *in vivo.* Three week old SPF Rhode Island Red birds were inoculated with the same titre of either PBG+UK661 VP4 or PBG+F52/70 VP4 viruses, in addition to control groups that were inoculated with the PBG98 virus or the wt UK661 virus (Figure 30A). Clinical scores were recorded twice daily, BWs were recorded once daily throughout the study, and tissues were harvested at 2, 4 and 14 d.p.i where the BF weights were also recorded. As expected, 50% of the birds infected with the UK661 virus reached their humane end points (a clinical score of 11) which is comparable to the previous *in vivo* study in chapter 4 (Figure 30B). In contrast, all birds infected with PBG98, chimeric VP4 viruses or mock-infected survived to their scheduled cull points. Birds infected with the UK661 virus had a significantly lower BF: BW ratio at day 14 compared to all the other groups (Figure 30C). The clinical score of birds infected with the UK661 virus peaked between 72 and 78 h.p.i with 3 birds reaching a score of 8-11, associated with moderate disease (Figure 30D). Comparatively, birds infected with the PBG98 or PBG+UK661 VP4 viruses reached a maximum clinical score of 1 at either 96 or 30 h.p.i, respectively. Of the birds infected with the PBG+F52/70 VP4, one bird reached a maximum clinical score of 8 at 78 h.p.i while another of 3 at 96 h.p.i.

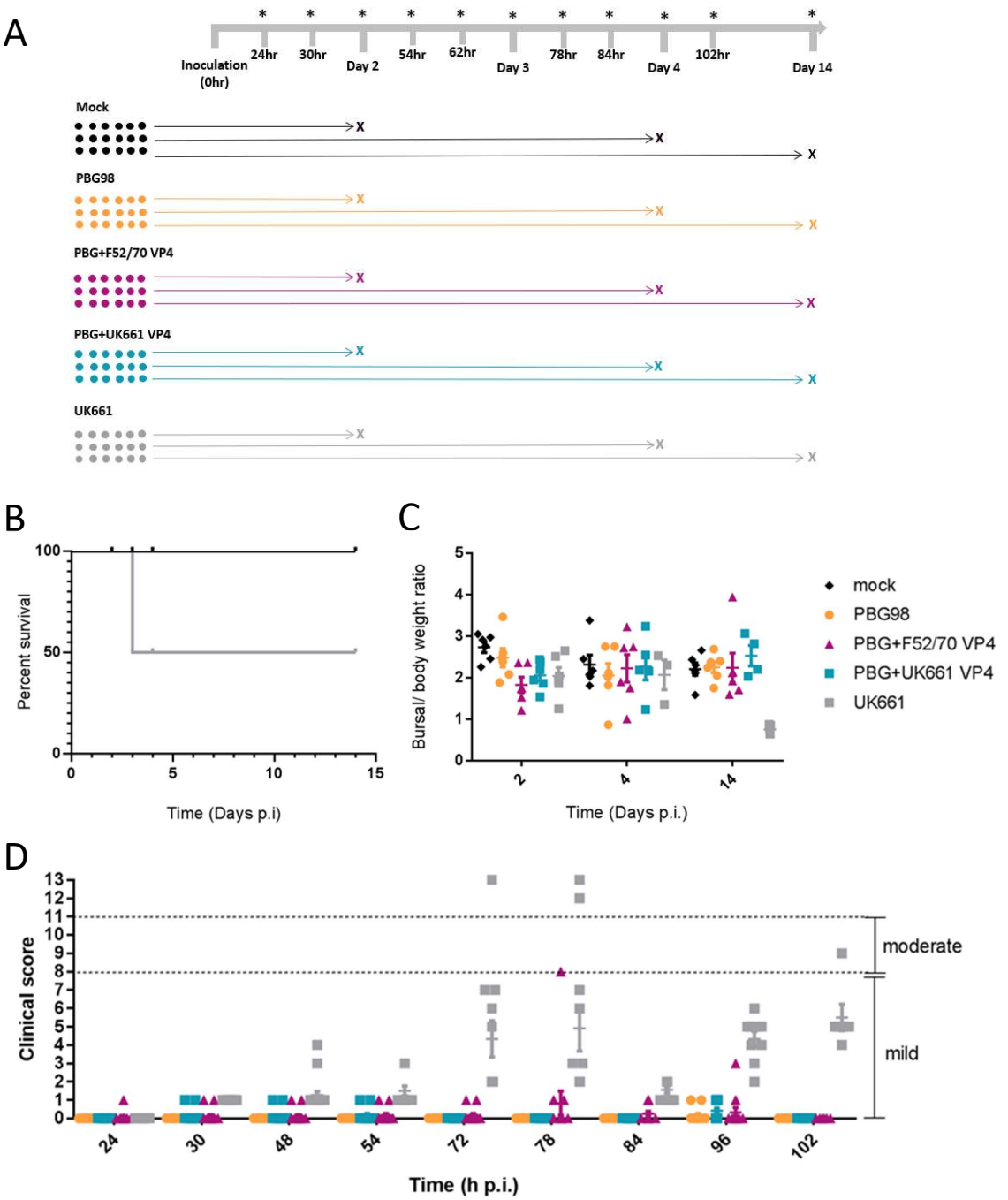

Figure 30 Survival curves, BF: BW ratios and clinical scores of chickens inoculated with PBG98, PBG+F52/70 VP4, PBG+UK661 VP4 or UK661

Schematic of the experimental design, with asterisks indicating when clinical scores were recorded (A). Survival curve of mock- (black), PBG98- (orange), PBG+F52/70 VP4- (pink), PBG+UK661 VP4- (blue) or UK661-infected (grey) birds that reached their humane end point (clinical score of 11) (B). BF: BW ratios of mock- (black), PBG98- (orange), PBG+F52/70 VP4- (pink), PBG+UK661 VP4- (blue) or UK661-infected (grey) birds at indicated time points post-inoculation (C). Birds in mock and virus groups were scored for clinical signs throughout the experiment with a range of between 1 and 11 (D). A clinical score of 1-7 was considered mild disease, 8-11 was considered moderate disease and birds reaching a score of 11 were humanely culled (Appendix A).

5.3.7 Chimeric VP4 viruses replicated poorly *in vivo*

To determine the replication kinetics of the chimeric VP4 viruses *in vivo,* the BF was harvested from each bird at post-mortem and RNA was extracted for reverse transcription and qPCR. At day 2 post-inoculation, there was no significant difference in viral RNA between any of the infection groups (Figure 31). From day 3 post-inoculation, high virus titres of over 10^5 fold change in viral genome copy number was detected in birds infected with UK661, peaking at day 4 post-inoculation (****P<0.0001). PBG98 peaked in replication at day 4 post-inoculation at 10^3 fold change, while PBG+F52/70 VP4 peaked at day 2 at 10^2 and PBG+UK661 VP4 at day 14 at 10^2.

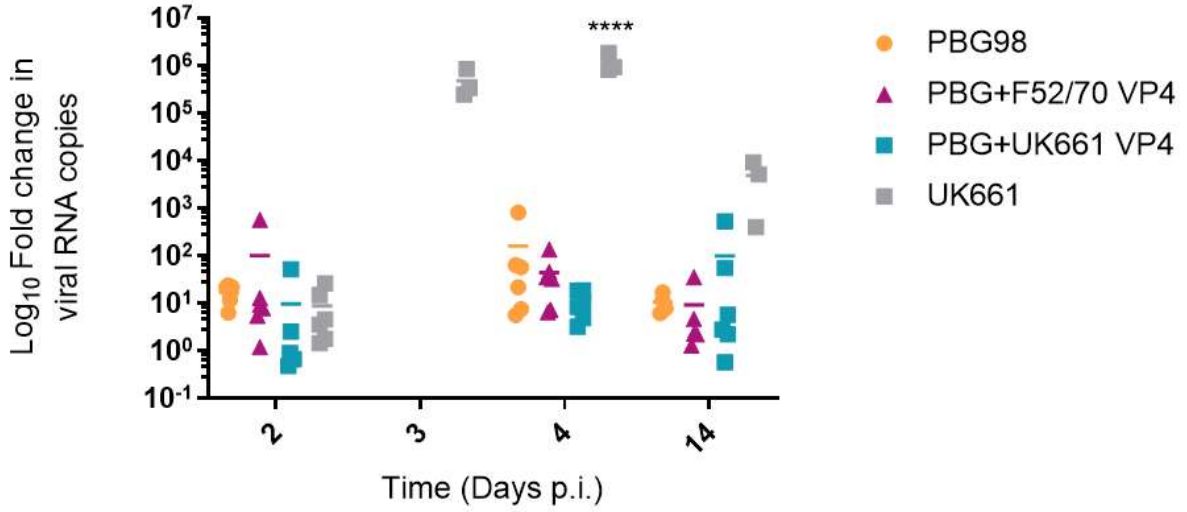

Figure 31 Viral titres of PBG98, PBG+F52/70 VP4, PBG+UK661 VP4 and UK661 in BF tissue.

Birds were inoculated with $1.8x10^3$ $TCID_{50}$/bird of PBG98 (orange), PBG+F52/70 VP4 (pink), PBG+UK661 VP4 (blue) or UK661 (grey) and whole BFs were harvested at 2, 3, 4 and 14 d.p.i. BF tissue was homogenised, and RNA extracted prior to reverse transcription and the amplification of a conserved section of the VP4 gene by qPCR. VP4 gene Ct values were normalised to the TBP housekeeping gene as per the $2^{-\Delta CT}$ method and subsequently passed a Shapiro-Wilk normality test before being analysed using a two-way ANOVA and Tukey's multiple comparisons test where UK661 replication was significantly higher at day 4 post-inoculation compared to the other viruses (****P<0.0001). Data were expressed as log_{10}-fold change in VP4 viral RNA relative to mock-infected samples as per the $2^{-\Delta\Delta CT}$ method. Data are representative of n=6 for 24hr; n=6 for 48hr; n=1 (F52/70) n=3 (UK661) for 54hr; n=5 and n=3 for 72hr for F52/70 and UK661, respectively, and bars indicate the mean.

5.3.8 Expression of type I IFN-related genes were comparable between chimeric VP4 viruses and the parental backbone virus

A panel of key type I IFN and pro-inflammatory genes were measured by qPCR to elucidate differences in gene expression between viruses following infection *in vivo*. Consistent with previous data presented in this chapter, at day 2 post-inoculation, IFNα was significantly lower in PBG+UK661 VP4- and PBG+F52/70 VP4-infected birds compared to UK661-infected birds (****P<0.0001) (Figure 32A). This trend was the same at day 4 post-inoculation although this was not statistically significant. Birds infected with the wt UK661 virus expressed significantly more IFNβ than birds infected with the other three viruses at both day 2 and 4 post-inoculation (****P<0.0001) (Figure 32B). PBG98 and the chimeric VP4 viruses were similar in the levels of IFNβ expression they induced at day 2 post-inoculation, but at day 4 the PBG+UK661 VP4 virus induced a lower level of expression than the PBG98 virus as did five out of six PBG+F52/70 VP4-infected birds. Mx1 expression was similar for PBG98 and the chimeric VP4 viruses at days 2 and 4 post-inoculation (*P<0.05) (Figure 32C). For UK661-infected birds, Mx1 expression was lower on average than the other three viruses at day 2 post-inoculation, although this changed at day 4 post-inoculation where UK661-infected birds had significantly higher Mx1 expression than the other three infection groups. IFIT5 expression in the birds infected with either of the chimeric VP4 viruses was lower than PBG98 and UK661 at day 2 post-inoculation, although this didn't reach statistical significance (Figure 32D). At the same time point there was no significant difference in IFIT5 expression between PBG98- and UK661-infected birds, however, at day 4 post-inoculation expression was significantly higher in UK661-infected birds (***P<0.001).

There was no significant difference in IL-8 expression between any of the virus groups compared to mock at day 2 post-inoculation (Figure 33A). At day 4 post-inoculation, however, UK661 infection induced a large increase in IL-8 expression compared to the

other three viruses (****P<0.0001). The chimeric VP4 viruses and PBG98 induced less IL-1β expression than UK661 at day 2 post-inoculation, however, this was statistically significant at day 4 post-inoculation (****P<0.0001) (Figure 33B).

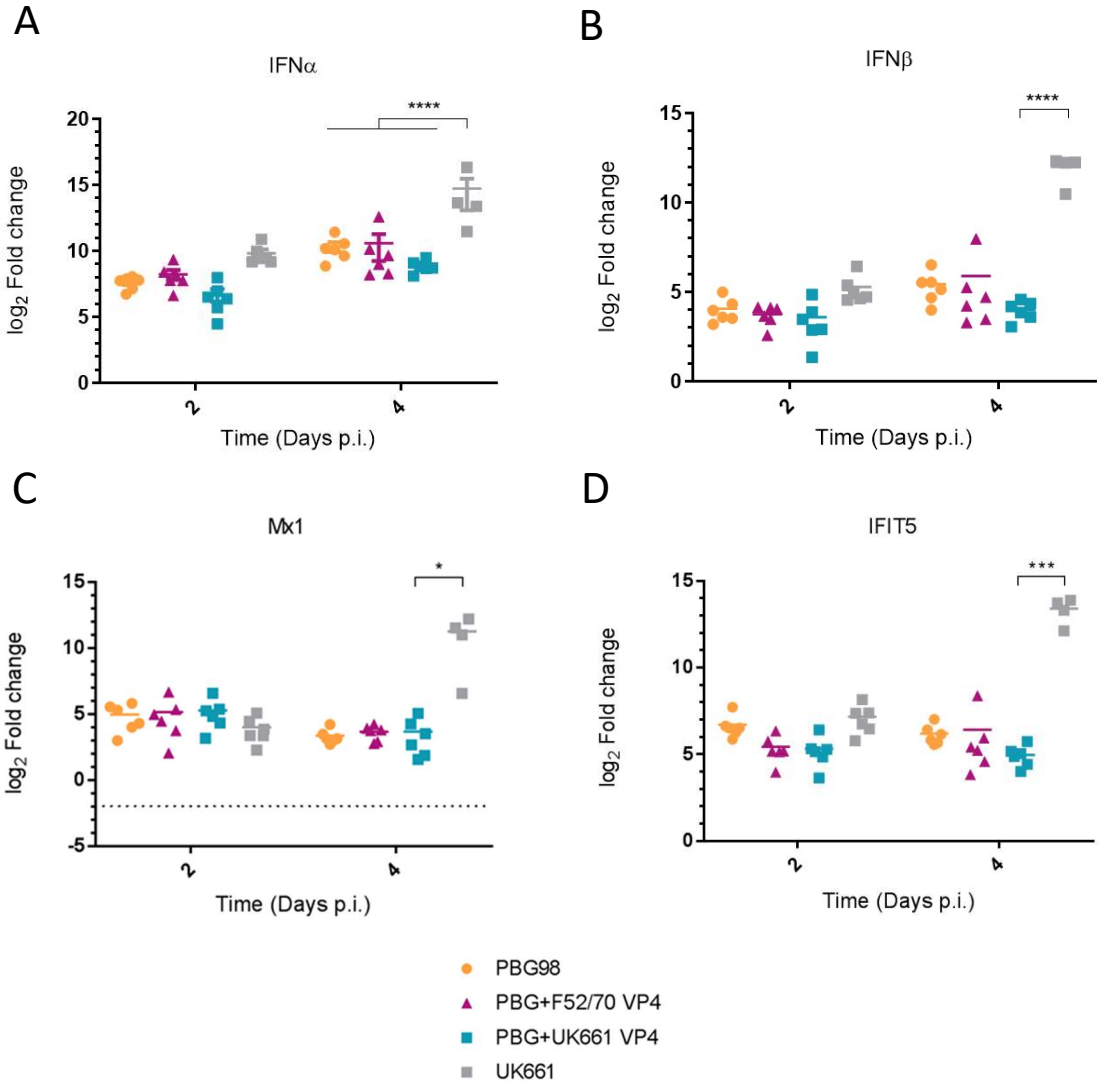

Figure 32 qRT-PCR analysis of type I IFN-related genes in PBG98-, PBG+F52/70 VP4-, PBG+UK661 VP4- and UK661-infected BF tissue.

RNA was extracted from PBG98- (orange), PBG+F52/70 VP4- (pink), PBG+UK661 VP4- (blue) and UK661-infected (grey) BF tissue collected at 2 and 4 d.p.i. Extracted RNA from infected and mock samples were reverse transcribed and amplified by qPCR using specific primer sets for IFNα (A), IFNβ (B), Mx1 (C) IFIT5 (D), before normalisation of infected samples to mock-infected samples and the housekeeping gene RPLP0 using the $2^{-\Delta\Delta CT}$ method. Data are representative of n=6 for 24hr; n=6 for 48hr; n=1 (F52/70) n=3 (UK661) for 54hr; n=5 and n=3 for 72hr for F52/70 and UK661, respectively. The data passed a Shapiro-Wilk normality test before analysis using a one-way ANOVA and Tukey's multiple comparison test (*P<0.05, ***P<0.001, ****P<0.0001).

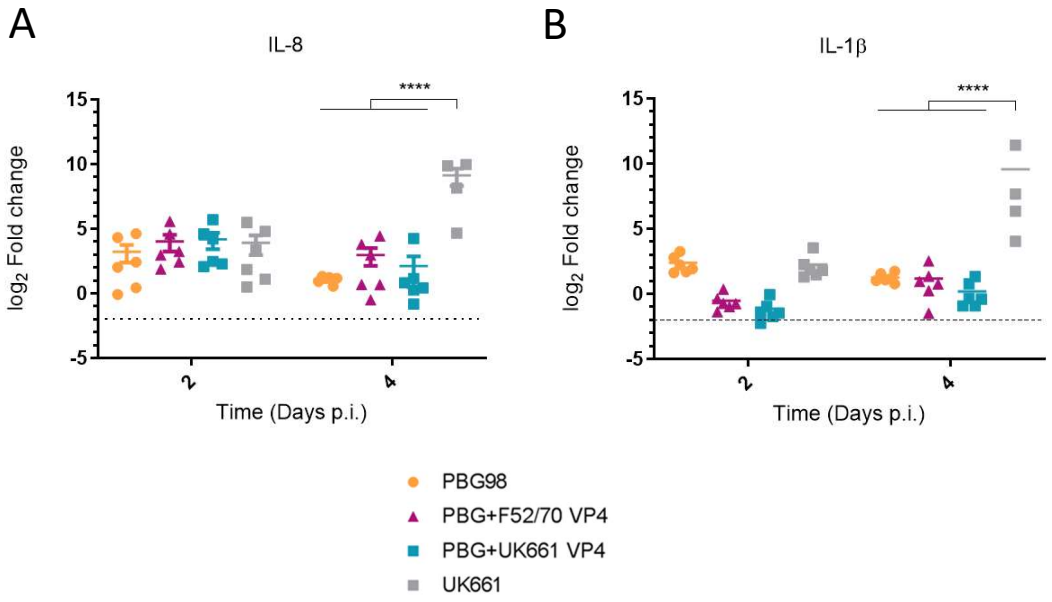

Figure 33 qRT-PCR analysis of pro-inflammatory cytokines in PBG98-, PBG+F52/70 VP4-, PBG+UK661 VP4- and UK661-infected BF tissue.

RNA was extracted from PBG98- (orange), PBG+F52/70 VP4- (pink), PBG+UK661 VP4- (blue) and UK661-infected (grey) BF tissue collected at 2 and 4 d.p.i. Extracted RNA from infected and mock samples were reverse transcribed and amplified by qPCR using specific primer sets for IFNα (A), IFNβ (B), Mx1 (C) IFIT5 (D), before normalisation of infected samples to mock-infected samples and the housekeeping gene RPLP0 using the $2^{-\Delta\Delta CT}$ method. Data are representative of n=6 for 24hr; n=6 for 48hr; n=1 (F52/70) n=3 (UK661) for 54hr; n=5 and n=3 for 72hr for F52/70 and UK661, respectively. The data passed a Shapiro-Wilk normality test before analysis using a one-way ANOVA and Tukey's multiple comparison test (****P<0.0001).

5.4 Conclusions

- The UK661 VP4 protein down-regulates IFNβ production to a greater extent than the VP4 protein from the F52/70 virus by luciferase assay. However, this difference is reversed for IFN signalling with the F52/70 VP4 protein suppressing Mx1 production.
- The VP4-mediated inhibition of IFNβ production is independent of its function as a protease.
- There are 9 aa differences between the UK661 and F52/70 VP4 proteins, and both the 5' and 3' regions of VP4 protein were required for its ability to inhibit IFNβ production.
- Chimeric VP4 viruses, generated from the PBG98 reverse genetics system, replicated in DF-1 cells and genes involved in IFN production and signalling were differentially expressed between the viruses.
- *In vivo,* these chimeric VP4 viruses were unable to replicate to high titres in the BF and innate immune responses were comparable between viruses.

5.5 Discussion

In this chapter, the ability of different VP4 proteins from c- and vvIBDV strains to antagonise the type I IFN responses was explored in detail. By investigating these proteins independently of other IBDV proteins and additionally in the context of whole chimeric viruses, strain-dependent differences in viral evasion of innate immunity were studied. The aims for this chapter focussed on investigating the ability of each VP4 protein to suppress the type I IFN response and identify possible mechanisms for these interactions.

The birnavirus VP4 protein has previously been identified as an IFN antagonist for both IPNV and IBDV (Li *et al.* 2013b; Lauksund *et al.* 2015; He *et al.* (2018). While the mechanism for IPNV VP4-mediated IFN antagonism is still unclear, recent work by He *et al.* (2018) has demonstrated an interaction between IBDV VP4 and the host protein GILZ. The binding of VP4 to GILZ prevents its degradation,

and as GILZ accumulates in the cytoplasm, its binding to NF-κB prevents the translocation of p65 to the nucleus and the downstream signalling of pro-inflammatory genes. The VP4 protein has also been shown to form tubule-like structures during infection which ultimately deform the host cytoskeleton and, potentially, results in cell lysis (Zheng *et al.* 2015b). This demonstrates there are several complex interactions between VP4 and the host cell during IBDV infection, although differences between VP4 proteins from different IBDV strains has not been investigated at the time of writing this thesis.

To explore strain differences in the role of VP4 in IFN antagonism, multiple VP4 sequences were aligned from ca-, c- and vvIBDV strains commonly used in IBDV research. From this analysis, 9 aa differences were identified between UK661 and F52/70, although these differences were not consistently present in all members of the pathotype. For example, 3 of these aa differences between UK661 and the cIBDVs were not present in all vvIBDV strains. The first study to identify the IBDV VP4 as an IFN antagonist (Li *et al.* 2013b), used the vvIBDV Lx strain in their experiments. This has the same VP4 aa sequence as the UK661 strain. A limitation of this study was only investigating one vvIBDV strain and one cIBDV strain, and more work is necessary to establish whether all vvIBDV strains suppress type I IFN production more than strains of lower virulence.

By measuring the IFNβ production upon stimulation with poly I:C, work presented here showed that cells transfected with the UK661 VP4 had suppressed IFNβ induction compared to cells transfected with the F52/70 VP4 protein. Furthermore, the F52/70 VP4-transfected cells induced a greater level of IFNβ expression than the vector control suggesting the type I IFN production pathway is stimulated by the presence of F52/70 VP4. This data supports the findings by Li *et al.* (2013b) and builds on those foundations to add the importance of strain-specific differences in the interactions between IBDV VP4 and the type I IFN response. In the previous chapter, the suppression of type I IFN responses and pro-inflammatory cytokines by the UK661 virus was demonstrated compared to the cIBDV strain F52/70 *in vitro* and *in vivo,* consistent with other studies that also conclude this key host-virus interaction may be essential to disease outcome of infected birds (Eldaghayes *et al.* 2006; Quan *et al.* 2017). The data

from these experiments demonstrates that this phenotype is, in part, due to the differences in the VP4 protein between these strains.

Despite this suppression by the UK661 VP4 of IFNβ production, the opposite appears to be the case for IFN signalling according to the results presented here. Using the same approach, Mx1 expression was measured following IFNα stimulation in cells transfected with either the UK661 or F52/70 VP4 proteins. Conversely to the trend with IFNβ production, the F52/70 VP4 protein was able to suppress Mx1 expression compared to the UK661 VP4- and mock-transfected cells. These data make the case for several different interactions taking place between the VP4 proteins of these viruses and the type I IFN response. One explanation is that the VP4 proteins of these two viruses act at different times, either earlier during the type I IFN response in the case of the UK661 VP4 to inhibit IFN production, or later, during IFN signalling, to reduce the impact following ISG up-regulation. Another explanation is that vvIBDV strains may target the IFN production branch of the pathway through interaction with GILZ, and perhaps other host proteins, to reduce both production of type I IFN and pro-inflammatory cytokines. Most viruses encode viral proteins able to target and manipulate IFN production and/or signalling in order to promote viral replication and transmission. Several flaviviruses, including Zika virus (ZiV) Dengue virus (DeV) and West Nile Fever virus (WNV), target IFN signalling to evade the immune response (Umareddy *et al.* 2008; Huang *et al.* 2016; Setoh *et al.* 2017). A study by Umareddy *et al.* (2008) identified strain-specific differences between the interactions of DeV and IFN signalling, whereby some strains were able to suppress STAT1 and STAT2 activation, preventing the downstream expression of ISGs in response to infection. More recently, DeV has been shown to suppress MAVS-mediated ISG expression to prevent the early induction of ISGs independent of JAK-STAT signalling (Huang *et al.* 2016). The NS5 of both DENV and ZIKV has been shown to cause the degradation of STAT2, suggesting this is a conserved trait of flavivirus NS5 proteins (Grant *et al.* 2016). The NS3 protein of more virulent WNVs were also found to inhibit IFN signalling (Setoh *et al.* 2017).

In this work, the ability of the IBDV VP4 protein to suppress IFNβ production was found to be independent of its function as a protease. Knocking-out the protease function by mutating a key residue for catalytic activity (H36) had little impact on the F52/70 VP4 protein, although cells transfected with UK661 VP4 pKO produced significantly less IFNβ than F52/70 VP4 pKO. While the protease function is not integral to this role in suppressing type I IFN, the UK661 VP4 pKO induced more IFNβ than the UK661 VP4 with a functioning catalytic site, suggesting there may be another site nearby or protein folding may be important. A previous study by Zheng *et al.* (2015b) revealed that the VP4 catalytic site is inactivated after VP4 assembly early during infection, in order to prevent premature cell lysis due to toxicity. This finding supports the protease knock-out work presented here demonstrating the protease function is independent of its role in type I IFN suppression.

The proteases of other viruses have been shown to act as IFN antagonists, including Hepatitis E virus (HEV) (Kim and Myoung, 2018), Herpes Simplex virus-1 (HSV-1) (Zhang *et al.* 2016) and many coronaviruses such as porcine epidemic diarrhoea virus (PEDV) and Middle East respiratory syndrome virus (MERS) (Yang *et al.* 2014; Wang *et al.* 2015a). The HEV protease PCP strongly down-regulates MDA5 to inhibit downstream IFN production (Kim and Myoung, 2018), while the Herpes Simplex Virus-1 protease, VP24, was shown to interact with TBK1 and IRF3 to impair IRF3 activation to prevent IFN production. The MERS papain-like protease, PLpro, was also shown to target IRF3, blocking phosphorylation and translocation of IRF3 to the nucleus (Yang *et al.* 2014), whereas the PEDV 3C-like protease, nsp5, targets NF-κB essential modulator (NEMO) by cleaving the protein and preventing downstream signalling via NF-κB (Wang *et al.* 2015a). Along with other viral proteases, the interaction between the IPNV VP4 and RIG-I/MDA5 signalling pathway has been investigated (Lauksund *et al.* 2015). This study concluded that while neither IRF1 nor IRF3 were targeted by VP4 for degradation, an interaction with another signalling member of this pathway is expected.

Having established the protease function of VP4 is not responsible for its role in IFNβ suppression, mutants of the UK661 and F52/70 VP4 proteins were synthesised to clarify whether the important residues for the IFN suppression phenotype were located in the first 5 different or last 4 different aa changes between the two viral strains. Neither of the 5'UK_3'F52 or 5'F52_3'UK mutants were able to suppress IFNβ production to the same extent as UK661 VP4, however, cells transfected with the 5'UK_3'F52 mutant had lower levels of IFNβ than the 5'F52_3'UK mutant suggesting the first 5 aa changes (31, 114, 122, 132, 141) may be more important for this phenotype than the last 4 aa (170, 175, 205, 241). Limited conclusions can be drawn from this experiment as the VP4 structures depicted in this chapter were modelled based on the YAV VP4 protein using PyMOL, as the crystal structure for IBDV VP4 remains unsolved. Although these structures did highlight some more variable regions between the UK661 and F52/70 VP4 proteins, the poor similarity between YAV and IBDV VP4 sequences means additional studies are required to verify that the mutants used in these experiments are correctly folded. Future studies aimed at determining the residues responsible for the difference in IFNβ suppression could also be investigated by conducting site-directed mutagenesis.

Following the differences in type I IFN responses observed with the VP4 proteins independently of the other viral proteins, chimeric VP4 viruses were generated using the cell-culture adapted PBG98 virus as the backbone for the chimeras. These chimeric VP4 viruses were used to study the VP4 protein in the context of a complete infectious virus. The presence of other virus proteins, transcripts and viral RNA could either up-regulate the type I IFN response due to sensing, or as some other proteins are known IFN antagonists, their presence could contribute to the suppression of type I IFN by alternative mechanisms. It was also reasoned that studying the chimeric VP4 viruses, with either the F52/70 or UK661 VP4 swapped for the wild type VP4 in the PBG98 backbone, was fundamental for determining the value of the VP4 protein in vaccine development. For example, an over-attenuated strain could potentially be made "hotter" by incorporating the VP4 protein from UK661.

Experiments to study these chimeric VP4 viruses centred on infecting DF-1 cells with either of the chimeric VP4 viruses or the PBG98 strain in both single-step (MOI of 5) and multi-step (MOI of 1) growth curves. No significant difference in the replication of these viruses over multiple rounds of replication was observed, although the PBG+F52/70 VP4 virus titre was lower than the other viruses at 6 h.p.i. However, in the single-step replication cycle measured up to 8 h.p.i, the PBG+UK661 VP4 virus reached a higher peak titre at 6 h.p.i (*P<0.05), whereas replication of PBG+F52/70 VP4 peaked later at 8 h.p.i. This may suggest the PBG+UK661 VP4 virus was less impaired by the innate immune response than the other viruses. Alternatively, previous work by Wang *et al.* (2015b) identified the role of CypA in inhibiting viral replication through binding with the VP4 protein, therefore CypA may be able to interact more effectively with the PBG98 and PBG+F52/70 VP4 viruses than the PBG+UK661 VP4 virus to impair replication. There are likely to be other host proteins involved in the inhibition of viral replication early during infection, although this area requires further research.

The low levels of chimeric VP4 virus replication followed by significantly lower expression levels of type I IFN-related genes and pro-inflammatory cytokines, suggests the PBG98 virus was too cell culture-adapted for *in vivo* studies. The chimeric VP4 viruses may have failed to reach the BF either because macrophages and dendritic cells were able to clear the virus before infection was established in the BF or viral replication in the BF was controlled and cleared by resident phagocytic cells. Previous work by Liu and Vakharia (2004) investigated the role of segments A and B in tissue tropism using reassortant chimeric viruses and found the cell-culture adapted D78 virus replicated poorly *in vivo*. Additionally, a reassortant virus with a caIBDV segment A and vvIBDV segment B replicated more effectively in the BF than the parental caIBDV. In the context of the *in vivo* study described in this chapter, this may implicate segment B of the PBG98 virus in hindering efficient replication.

For future studies, a reverse genetics system based on a field strain of the virus with a tropism for B cells, would be invaluable for investigating the role of the VP4 proteins from different IBDV strains. This has long been a problem for IBDV research as establishing reverse genetics systems has primarily

used cell culture-adapted strains to enable the chimeric viruses to be rescued in fibroblast cell lines. While some previous studies have used intra-BF injection to rescue chimeric viruses with field strain backbones (Zierenberg *et al.* 2004), this is not a cost or time effective approach and is also a welfare issue. The *ex vivo* bursal cell culture system detailed in chapter 3 could potentially be used to rescue field strains and chimeric viruses with the backbone from field strains, which would allow the chimeric VP4 viruses to be generated with UK661+ F52/70 VP4 and F52/70+ UK661 VP4. Using chimeric VP4 viruses with field strain backbones would enable thorough investigation of the mechanisms used by VP4 proteins from different strains to suppress the innate immune response. Moreover, it may be useful in the development of a rationally designed live vaccine, where a recombinant field strain antigenically matched to circulating strains is engineered to contain the VP4 protein from an attenuated strain of IBDV.

Taken together, these data demonstrate that the vvIBDV strain UK661 is able to suppress type I IFN production to a greater extent than the cIBDV F52/70 strain and this is, in part, due to differences in the VP4 protein. While studies using the VP4 proteins in isolation yielded more significant results, the effect was dampened in the context of the whole virus *in vitro* and *in vivo,* suggesting that other factors contribute to the phenotype.

6. Discussion

6.1 Contributions to IBDV research

IBDV has a severe impact on the growing poultry industry worldwide, resulting in economic losses due morbidity and mortality caused by infection. Further to these costs, IBDV-associated immunosuppression in surviving birds extends the impact of these economic losses due to secondary infections and vaccine failure against other pathogens (Subler *et al.* 2006; Spackman *et al.* 2018). Consequently, IBDV control is a priority for the poultry industry, using vaccination programs and surveillance of emerging and reassortant strains to monitor this threat. There are a wide range of vaccines currently in use which provide adequate control of the cIBDV and some vIBDV strains, however, the emergence of new vIBDV and vvIBDV strains continue to test the efficacy of these vaccines (Müller *et al.* 2003). Reassortment events in the field are also highlighting the importance of surveillance. Fundamental research identifying the IBDV-host interactions responsible for virulence is vital for the development of new vaccines for more virulent strains that can minimise the IBDV burden in the field, without contributing to the problem.

The work presented in this thesis draws attention to the differences in host-virus interactions between IBDV strains of differing virulence. The expression levels of the type I IFN response was lower during infection with the vvIBDV strain, UK661, in primary bursal cells, DT40 cells and *in vivo* compared to either the caIBDV, D78, or cIBDV, F52/70, strains. The pro-inflammatory response was also down-regulated following infection with this virus compared to F52/70 in DT40 cells and *in vivo*. This suppression of the innate immune responses following UK661 infection also coincided with higher levels of UK661 replication in DT40 cells, and higher incidences of mortality *in vivo* compared to F52/70. Furthermore, the lower expression of the type I IFN and pro-inflammatory responses during infection with UK661 may contribute to the more severe disease outcome associated with this virus, although further work on the mechanisms of these interactions are required to support this

interpretation. Differences in the innate immune response have previously been reported between IBDV strains (Eldaghayes *et al.* 2006; Li *et al.* 2010; Rauf *et al* 2011; Yu *et al.* 2015), including one study that compared UK661 and F52/70 strains (Eldaghayes *et al.* 2006). However, unlike the latter study, in this thesis, these viruses have been studied alongside each other in the same experiment and with the same MOI or infectious dose/ bird.

Having identified the lower expression of the innate immune response following infection with the UK661 virus, the next step was to confirm which IBDV protein was responsible. As vvIBDV VP4 was previously described to act as an IFN antagonist (Li *et al.* 2013b), the research direction focussed on determining whether this is a strain-specific phenomenon linked to virulence. The UK661 VP4 was shown to down-regulate IFNβ production, demonstrating that our observation that UK661 suppresses type I IFN responses and pro-inflammatory cytokine expression to a greater extent than other strains was, in part, mediated by the VP4 protein. Interestingly, the F52/70 VP4 was found to suppress Mx1 expression following stimulation. This suggests both VP4 proteins manipulate the type I IFN response to benefit viral replication and transmission. However, we speculate that by reducing IFN production rather than signalling, the UK661 VP4 interaction has a more beneficial outcome for the UK661 virus compared to the F52/70 virus by acting earlier during infection. UK661 VP4-mediated suppression of IFNβ production was found to be independent of its role as a protease, and the work in this thesis suggest that multiple aa are involved in this interaction. As previous work showed vvIBDV VP4 binds to the host protein GILZ resulting in the dysregulation of NF-κB signalling and downstream apoptosis, we hypothesise that the VP4-GILZ interaction is strain-dependent and a signature of vvIBDV VP4 proteins. For example, the F52/70 VP4 may not interact with GILZ, or the interaction may be weaker or more transient in nature, thus not preventing the induction of type I IFN. The F52/70 VP4 protein instead interact with the JAK-STAT pathway to prevent ISG expression. However, this should be explored in the future.

When the chimeric VP4 viruses were investigated, the antagonism of the type I IFN response observed with the UK661 VP4 protein alone was reduced. This suggests the VP4 protein is not the sole determinant for this phenotype, consistent with previous work identifying both IBDV segments as containing virulence factors (Le Nouën *et al.* 2012).

6.2 Limitations

The optimisation of the *ex vivo* bursal cell culture system allowed the study of field strains of IBDV in B cells without the contamination with other viruses such as ALV in DT40 cells. The gene expression levels in these bursal cells was determined to be that of infected B cells in the bursal cell population, however, the bursal cells were not sorted following extraction from the BF. While B cells were found to be up to 98-99% of the bursal cell population in another study in our lab (data not included in this thesis), there are also macrophages and other immune cells present which may interact with the virus and affect gene expression. Sorting the $Bu1^+$ population would ensure the gene expression was representative of B cells. Another reason to sort the bursal cells prior to infection, would be to exclude the dead cells using a dye for live/dead staining. As many cells undergo apoptosis during the extraction process, these cells will contribute to the gene expression signature of this cell population. Moreover, it was necessary to use chCD40L to stimulate proliferation of the bursal cell population, which would also have altered the expression of cellular genes. However, gene expression following IBDV infection was compared to mock-infected cells that similarly stimulated with chCD40L, to account for this.

The immune response to c- and vvIBDV strains was investigated *in vitro* and *in vivo* in order to explore the gene expression profiles of cells infected with these viruses. For studies *in vitro,* DT40 cells were used to compare gene expression between these strains. Primary cells would be the preferred choice for this work, to avoid the undetermined effects of ALV on gene expression in B cells, however, during this study, the BF tissues from which the primary bursal cell cultures are derived were contaminated

and unable to be used. Harvesting the BF requires dexterity to avoid contamination from the gut contents and for several months primary cultures were unable to be used so we resorted to DT40 cells.

When comparing these two viruses *in vivo*, a spread in the data was observed for several genes measured despite the birds originating from an inbred line. Increasing the dose of the inoculum may reduce the variation in gene expression due to a more stimulated immune response. When some of the UK661-infected birds reached their humane end point at 54 h.p.i due to welfare, it would have been beneficial to randomly select a matched number of F52/70-inoculated birds to also be culled at the same time point to ensure the number of birds culled at 54 h.p.i inoculated with each virus was the same, and enable statistical analyses to be carried out. In addition, adding mock-inoculated birds at all time points, rather than just at 72 h.p.i, would have allowed more in-depth investigation into gene expression between infected birds by RNA-seq analysis, as it would have provided time-matched controls for normalisation.

The lower expression levels of the type I IFN and pro-inflammatory responses demonstrated *in vitro* and *in vivo,* led to further studies of the VP4 protein uncovering its role in the suppression of the type I IFN production (UK661) or signalling (F52/70). The eGFP-tagged VP4 expression plasmids generated for these experiments were transfected into DF-1 cells, the eGFP signal used to gauge transfection efficiency, and the IFNβ or Mx1 expression was measured by luciferase assay. As DF-1 cells have suppressed SOCS1 expression and therefore express ISGs to a lesser extent than CEF cells (Giotis *et al.* 2017) it may be advantageous to conduct these assays in a cell line with a more competent IFN signalling pathway to confirm these findings. Moreover, if this assay were to be repeated with a smaller tag than eGFP, such as a FLAG or HIS tag it would reduce the probability of the tag interfering with the localisation of the VP4 protein in the cell. The VP4 protein is 247 aa in length which is a similar size to eGFP which has a length of 239. For the generation of the protease knock-out VP4 proteins, the H36P mutation was introduced as it has been shown to prevent this function (Rodríguez-Lecompte

and Kibenge, 2002). As this has previously been shown in the literature, a cleavage assay was not performed, however, this would be useful to confirm the successful knock-out of this function. In addition, it is possible that the eGFP-tagged VP4 proteins with functioning protease activity may cleave itself from eGFP as the cleavage sites were included in the VP4 protein sequence. Conversely, the VP4 proteins with knocked-out protease function would not be able to cleave off the eGFP molecule. This may have impaired the IFN antagonistic role of VP4 resulting in the increased IFNβ expression in UK661 VP4 pKO compared to wt UK661 VP4. VP4 mutants with the first 5 aa from UK661 and the last 4 from F52/70 and vice versa were compared for their ability to suppress IFNβ production. The first 5 aa of the UK661 VP4 appeared to be more important than the last 4 aa, however, generating single aa mutants by site-directed mutagenesis would have been beneficial to narrow down the sites responsible for IFN antagonism by UK661 VP4. When comparing the chimeric VP4 viruses *in vivo* the PBG98 backbone the UK661 and F52/70 VP4 proteins were cloned into was too cell-adapted resulting in low replication in the BF at days 2 and 4 post-inoculation. Harvesting a wider range of tissues, including the beak (the inoculate site) and gut may have demonstrated the chimeras struggled to reach the BF. Replication in the tissues would have suggested the virus's tropism for fibroblast cells prevented the establishment of a productive infection in the BF and other lymphoid tissues.

6.3 Further areas of study

This thesis has explored the differences in the innate immune response to different IBDV strains and identified a role for VP4 in this interaction. To build on the foundations outlined here and further investigate the host-virus interactions responsible for the different disease outcomes reported following IBDV infection, it would be beneficial to characterise the mechanisms by which the UK661 or F52/70 VP4 proteins interact with the type I IFN pathways to either suppress IFN production or signalling. There are several approaches to define these mechanisms. The first would be to transfect cells with overexpression plasmids for the constituents of the type I IFN production and signalling

pathways, assessing the suppression of these genes by each VP4 protein using a luciferase reporter and measuring mRNA expression using by luciferase assay and qPCR and protein expression by western blot. This could also be further explored using mass spectrometry to identify cellular proteins that differentially bind the F52/70 and UK661 VP4 proteins, which would be confirmed by co-immunoprecipitation assays.

In addition, the ability to rescue field strains of IBDV would benefit this work. The *ex vivo* bursal cell culture system optimised in chapter 3 could be used to rescue these strains as well as chimeric VP4 viruses by electroporating the segment A and B plasmids into the B cells following sorting from other bursal cells. Generation of chimeric viruses with a UK661 backbone and F52/70 VP4 and vice versa could be used to demonstrate a loss or gain in ability to suppress IFN production, respectively. This rescue system would contribute significantly to the field and be invaluable in enabling other research questions to use chimeric viruses generated from a variety of different B cell-tropic IBDV strains. The *ex vivo* B cell culture system could also be used to determine whether IgM is the target receptor for IBDV, by sorting the IgM^+ B cells by fluorescence-activated cell sorting (FACS) and infecting these *in vitro*.

Following on from the *in vivo* work presented in chapter 4, the BF tissue samples from this study frozen in OCT compound could be processed for cryosectioning and immunohistochemistry to allow comparison of the BF architecture following infection with UK661 or F52/70, while also staining for immune cells, such as B cells ($Bu1^+$), macrophages ($KUL01^+$) and T cells ($CD3^+$). This would show the infiltration of different cells over the course of infection, with each virus resulting in the differences in pro-inflammatory cytokines detected in this tissue. This immunological insight could be compared to next generation sequencing data, to provide a snapshot of infection at each time point in terms of gene expression, the presence/absence of immune cells and level of damage in the BF and other sites of IBDV replication.

6.4 Summary and concluding remarks

It is apparent there are key differences between the approaches taken by IBDV strains of differing virulence in evading the innate immune response. In *ex vivo* cultured bursal cells, it was clear wide range of ISGs as well as IFN were expressed to lower levels during infection with UK661 compared to mock- and caIBDV-infected cells. Further investigation in DT40 cells, confirmed this phenotype of UK661 compared to a cIBDV strain F52/70, moreover, a suppression of pro-inflammatory cytokines was demonstrated in UK661-infected cells. This interaction between UK661 and the host immune response was confirmed *in vivo*, where type I IFN, a range of ISGs and pro-inflammatory genes were down-regulated in UK661-inoculated birds compared to those inoculated with the F52/70 virus. This suppressed immune response would be expected to delay the commonly described 'cytokine storm', which may indicate why the average clinical scores were lower and mortality rate higher in UK661-inoculated birds. The replication kinetics of the two viruses are unlikely to be responsible for this UK661-mediated suppression of the immune response as there was no significant difference in the peak virus titres. Both viruses were, however, detected in the caecal tonsils and, to a lesser extent, the spleen. The higher UK661 titres detected in the caecal tonsils may also indicate further dissemination of the virus, which may contribute to the increased mortality rate. The VP4 proteins from both viruses suppressed the type I IFN pathway *in vitro*, with UK661 VP4 targeting production and F52/70 VP4 suppressing signalling or ISG production. This strain-specific difference in VP4 antagonism of the type I IFN response was independent of its role as a protease and the aa residues responsible are expected to be located throughout the VP4 aa sequence. In the context of a whole virus, the effect on type I IFN was less prominent than with VP4 proteins alone, suggesting the cell-adapted backbone of the chimeric viruses was likely too adapted for study *in vivo*.

Together, this work supports the hypothesis that the vvIBDV strain, UK661, can differentially modulate the innate immune response compared to the cIBDV strain, F52/70. By suppressing the induction of

type I IFN to a greater extent than F52/70, infection with UK661 results in the suppression of antiviral genes which may, in part, explain its enhanced virulence.

7. References

1. Adler HE, DaMassa AJ (1979) Toxicity of endotoxin to chicks. *Avian Diseases,* 23 (1): 174-8.
2. Alexander DJ, Chettle NJ (1998) Heat inactivation of serotype I infectious bursal disease virus. *Avian Pathology,* 27 (1): 97-9.
3. Ansari AR, Li NY, Sun ZJ, Huang HB, Zhao X, Cui L, Hu YF, Zhong JM, Karrow NA, Liu HZ (2017) Lipopolysaccharide induces acute bursal atrophy in broiler chicks by activating TLR4-MAPK-NF-κB/AP-1 signalling. *Oncotarget,* 8 (65): 108375-91.
4. Ariel E, Olesen N (2002) Finfish in aquaculture and their disease- A retrospective view on the European community. *Bulletin of the European Association of Fish Pathologists,* 22: 72-84.
5. Avenant C, Kotitschke A, Hapgood JP (2010) Glucocorticoid Receptor Phosphorylation Modulates Transcription Efficacy through GRIP-1 Recruitment. *Biochemistry,* 49 (5): 972-85.
6. Baba TW, Giroir BP, Humphries EH (1985) Cell lines derived from avian lymphomas exhibit two distinct phenotypes. *Virology,* 144 (1): 139-51.
7. Barber MR, Aldridge JR, Webster RG, Magor KE (2010) Association of RIG-I with innate immunity of ducks to influenza. *PNAS,* 107 (13): 5913-8.
8. Bayliss CD, Peters RW, Cook JK, Reece RL, Howes K, Binns MM, Boursnell ME (1991) A recombinant fowlpox virus that expresses the VP2 antigen of infectious bursal disease virus induces protection against mortality caused by the virus. *Archives of Virology,* 120 (3-4): 193-205.
9. Bayliss CD, Spies U, Shaw K, Peters RW, Papageorgiou A, Müller H, and Boursnell MEG (1990) A comparison of the sequences of segment A of four infectious bursal disease virus strains and identification of a variable region in VP2. *Journal of General Virology,* 71 (6): 1303-12.

10. Becht H, Müller H, Müller HK (1988) Comparative studies on structural and antigenic properties of two serotypes of infectious bursal disease virus. *Journal of General Virology,* 69 (3): 631-40.

11. Ben Abdeljelil N, Khabouchi N, Kassar S, Miled K, Boubaker S, Ghram A, Mardassi H (2014) Simultaneous alteration of residues 279 and 284 of the VP2 major capsid protein of a very virulent Infectious Bursal Disease Virus (vvIBDV) strain did not lead to attenuation in chickens. *Virology Journal,* 11: 199.

12. Benfield CT, Lyall JW, Tiley LS (2010) The cytoplasmic location of chicken mx is not the determining factor for its lack of antiviral activity. *PLoS One,* 5 (8): e12151.

13. Benjamini Y, Hochberg Y (1995) Controlling the false discovery rate: a practical and powerful approach to multiple testing. *Journal of the Royal Statistical Society B,* 57:289-300.

14. Benton WJ, Cover MS, Rosenberger JK, Lake RS (1967) Physicochemical properties of the infectious bursal agent (IBA). *Avian Diseases*, 11 (3): 430-8.

15. Bernasconi D, Schultz U, Staeheli P (1995) The interferon-induced Mx protein of chickens lacks antiviral activity. *Journal of Interferon Cytokine Research,* 15 (1): 47-53.

16. Birghan C, Mundt E, Gorbalenya AE (2000) A non-canonical lon proteinase lacking the ATPase domain employs the ser-Lys catalytic dyad to exercise broad control over the life cycle of a double-stranded RNA virus. *The EMBO journal,* 19 (1): 114-23.

17. Block H, Meyer Block K, Rebeski DE, Scharr H, de Wit S, Rohn K, Rautenschlein S (2007) A field study on the significance of vaccination against infectious bursal disease virus (IBDV) at the optimal time point in broiler flocks with maternally derived IBDV antibodies. *Avian Pathology,* 36 (5): 401409.

18. Blomen VA, Boonstra J (2007) Cell fate determination during G1 phase progression. *Cellular and Molecular Life Sciences*, 64 (23): 3084-104.

19. Boot HJ, ter Huurne AA, Hoekman AJ, Peeters BP, Gielkens AL (2000) Rescue of a very virulent and mosaic infectious bursal disease virus from cloned cDNA: VP2 is not the sole determinant of the very virulent phenotype. *Journal of Virology,* 74 (15): 6701-11.

20. Böttcher B, Kiselev MA, Stel'Mashchuk VY, Perevozchikova NA, Borisov AV, Crowther RA (1997) Three-dimensional structure of infectious bursal disease virus determined by electron microscopy. *Journal of Virology,* 71 (1): 325-30.

21. Boyd AC, Peroval MY, Hammond JA, Prickett MD, Young JR, Smith AL (2012) TLR15 is unique to avian and reptilian lineages and recognizes a yeast-derived agonist. *Journal of Immunology,* 189 (10): 4930-8.

22. Brandt M, Yao K, Liu M, Heckert RA, Vakharia VN (2001) Molecular determinants of virulence, cell tropism, and pathogenic phenotype of infectious bursal disease virus. *Journal of Virology,* 75 (24): 11974-82.

23. Brown MD, Skinner MA (1996) Coding sequences of both genome segments of a European 'very virulent' infectious bursal disease virus. *Virus Research,* 40 (1): 1-15.

24. Brownlie R, Allan B (2011) Avian toll-like receptors. *Cell and Tissue Research,* 343 (1): 121-30.

25. Brownlie R, Zhu J, Allan B, Mutwiri GK, Babiuk LA, Potter A, Griebel P (2009) Chicken TLR21 acts as a functional homologue to mammalian TLR9 in the recognition of CpG oligonucleotides. *Molecular Immunology,* 46 (15): 3163-70.

26. Busnadiego I, Maestre AM, Rodríguez D, Rodríguez JF (2012) The infectious bursal disease virus RNA-binding VP3 polypeptide inhibits PKR-mediated apoptosis. *PLoS One,* 7 (10): e46768.

27. Buttigieg K, Laidlaw SM, Ross C, Davies M, Goodbourn S, Skinner MA (2013) Genetic screen of a library of chimeric poxviruses identifies an ankyrin repeat protein involved in resistance to the avian type I interferon response. *Journal of Virology,* 87 (9): 5028-40.

28. Carballeda JM, Zoth SC, Gómez E, Lucero MS, Gravisaco MJ, Berinstein A (2014) Immune response elicited by the oral administration of an intermediate strain of IBDV in chickens. *Brazilian Journal of Microbiology,* 45 (4): 1521-5.

29. Chattopadhyay S, marques JT, Yamashita M, Peters KL, Smith K, Desai A, Williams BR, Sen GC (2010) Viral apoptosis is induced by IRF-3-mediated activation of Bax. *EMBO Journal,* 29 (10): 1762-73.

30. Chen G, He X, Yang L, Wei P (2018) Antigenicity characterization of four representative natural reassortment IBDVs isolated from commercial three-yellow chickens from Southern China reveals different subtypes co-prevalent in the field. *Veterinary Microbiology,* 219: 183-9.

31. Cheng Y, Sun Y, Wang H, Yan Y, Ding C, Sun J (2015) Chicken STING mediates activation of the IFN gene independently of the RIG-I gene. *Journal of Immunology,* 195 (8): 3922-36.

32. Cheng Y, Zhu W, Ding C, Niu Q, Wang H, Yan Y, Sun J (2019) IRF7 Is Involved in Both STING and MAVS Mediating IFN-β Signaling in IRF-3 Lacking chickens. *Journal of Immunology,* ji1900293.

33. Chettle N, Stuart JC, Wyeth PJ (1989) Outbreak of virulent Infectious Bursal Disease in East Anglia. *Veterinary Record,* 125 (10) 271-2.

34. Chevalier C, Galloux M, Pous J, Henry C, Denis J, da Costa B, Navaza J, Lepault J, Delmas B (2005) Structural peptides of a nonenveloped virus are involved in assembly and membrane translocation. *Journal of Virology,* 79 (19): 12253-63.

35. Chi J, You L, Li P, Teng M, Zhang G, Luo J, Wang A (2018) Surface IgM λ light chain is involved in the binding and infection of infectious bursal disease virus (IBDV) to DT40 cells. *Virus Genes,* 54 (2): 236-45.

36. Chung IY, Paetzl M (2013) Crystal structures of yellowtail ascites virus VP4 protease: trapping an internal cleavage site trans acyl-enzyme complex in a native Ser/Lys dyad active site. *Journal of Biological Chemistry,* 288 (18): 13068-81.

37. Cormican P, Lloyd AT, Downing T, Connell SJ, Bradley D, O'Farrelly C (2009) The avian Toll-Like receptor pathway- Subtle differences amidst general conformity. *Developmental and Comparative Immunology,* 33 (9): 967-73.

38. Cosgrove AS (1962) An apparently new disease of chickens. Avian Nephrosis. *Avian Disease,* 6 (1): 385-9.

39. Coulibaly F, Chevalier C, Gutsche I, Pous J, Navaza J, Bressanelli S, Delmas B, Rey FA (2005) The birnavirus crystal structure reveals structural relationships among icosahedral viruses. *Cell,* 120 (6): 761-72.

40. Cubas-Gaona LL, Diaz-Beneitez E, Ciscar M, Rodríguez JF, Rodríguez D (2018) Exacerbated Apoptosis of cells Infected with Infectious Bursal Disease Virus upon Exposure to Interferon Alpha. *Journal of Virology,* 92 (11): e00364-18.

41. Darteil R, Bublot M, Laplace E, Bouquet JF, Audonnet JC, Riviere M (1995) Herpesvirus of turkey recombinant viruses expressing infectious bursal disease virus (IBDV) VP2 immunogen induce protection against an IBDV virulent challenge in chickens. *Virology*, 211 (2): 481-90.

42. Decker T, Kovarik P, Meinke A (1997) GAS Elements: A Few Nucleotides with a Major Impact on Cytokine-Induced Gene Expression. *Journal of Interferon and Cytokine Research,* 17 (3): 121-34.

43. Delmas D, Attoui H, Ghosh S, Malik YS, Mundt E, Vakharia VN, ICTV Report Consortium (2019) ICTV Virus Taxonomy Profile: *Birnaviridae. Journal of General Virology,* 100 (1): 5-6

44. Deng L, Zeng Q, Wang M, Cheng A, Jia R, Chen S, Zhu D, Liu M, Yang Q, Wu Y, Zhao X, Zhang S, Liu Y, Yu Y, Zhang L, Chen X (2018) Suppression of NF-κB Activity: A Viral Immune Evasion Mechanism. *Viruses,* 10 (8): E409.

45. Di Marco B, Massetti M, Bruscoli S, Macchiarulo A, Di Virgilio R, Velardi E, Donato V, Migliorati G, Riccardi C (2007) Glucocorticoid-induced leucine zipper (GILZ)/ NF-kappaB interaction: role of GILZ homo-dimerization and C-terminal domain. *Nucleic Acids Research,* 35 (2): 517-28.

46. Dong LM, Chen XW, He XX, Jiang XP, Wu F (2019) Cell division cycle protein 42 regulates the inflammatory response in mice bearing inflammatory bowel disease. *Nanomedicine and Biotechnology,* 47 (1): 1833-8.

47. Dongaonkar VD, Rao KN (1979) Serological prevalence of infectious bursal disease in Madhya Pradesh and Maharashtra. *The Indian Veterinary Journal,* 56 (10): 811-5.

48. Dulwich KL, Giotis ES, Gray A, Nair V, Skinner MA, Broadbent AJ (2017) Differential gene expression in chicken primary B cells infected *ex vivo* with attenuated and very virulent strains of infectious bursal disease virus (IBDV). *Journal of General Virology,* 98 (12): 2918-30.

49. Eldaghayes I, Rothwell L, Williams A, Withers D, Balu S, Davison F, Kaiser P (2006) Infectious bursal disease virus: strains that differ in virulence differentially modulate the innate immune response to infection in the chicken bursa. *Viral Immunology,* 19 (1): 83-91.

50. Escaffre O, Le Nouën C, Amelot M, Ambroggio X, Ogden KM, Guionie O, Toquin D, Müller H, Islam MR, Eterradossi N (2013) Both genome segments contribute to the pathogenicity of very virulent infectious bursal disease virus. *Journal of Virology,* 87 (5): 2767-80.

51. Fahey KJ, Erny K, Crooks J (1989) A conformational immunogen on VP-2 of infectious bursal disease virus that induces virus-neutralizing antibodies that passively protect chickens. *Journal of General Virology,* 70 (6): 1473-81.

52. Fan B, Dun SH, Gu JQ, Guo Y, Ikuyama S (2015) Pycnogenol Attenuates the Release of Proinflammatory Cytokines and Expression of Perilipin 2 in Lipopolysaccharide-Stimulated Microglia in Part via Inhibition of NF-κB and AP-1 Activation. *PLoS One,* 10: e0137837.

53. Faragher JT (1972) Infectious bursal disease of chicken. *Veterinary Bulletin,* 42: 361-9.

54. Feng GS, Ouyang YB, Hu DP, Shi QZ, Gentz R, Ni J (1996) Grpa is a novel SH3-Sh2-Sh3 adaptor protein that couples tyrosine kinases to the Ras pathway. *Journal of Biological Chemistry,* 271 (21): 12129-32.

55. Fernández-Arias A, Martínez S, Rodríguez JF (1997) The major antigenic protein of infectious bursal disease virus, VP2, is an apoptotic inducer. *Journal of Virology,* 71 (10): 9014-8.

56. Ferrero D, Garriga D, Navarro A, Rodríguez JF, Verdaguer N (2015) Infectious bursal disease virus VP3 upregulates VP1-mediated RNA-dependent RNA replication. *Journal of Virology,* 89 (2): 11165-8.

57. Francois A, Eterradossi N, Delmas B, Payet V, Langlois P (2001) Construction of avian adenovirus CELO recombinants in cosmids. *Journal of Virology,* 75 (11): 5288-301.

58. Fujiwara N, Hidano S, Mamada H, Ogasawara K, Kitamura D, Cooper MD, Hozumi N, Chen CL, Goitsuka R (2006) A novel avian homologue of CD72, chB1r, down modulates BCR-mediated activation signals. *International Immunology,* 18 (5): 775-83.

59. Galloux M, Libersou S, Morellet N, Bouaziz S, Da Costa B, Ouldali M, Lepault J, Delmas B (2007) Infectious bursal disease virus, a nonenveloped virus, possesses a capsid-associated peptide that deforms and perforates biological membranes. *Journal of Biological Chemistry*. 282 (28): 20774-84.

60. Gao L, Li K, Qi X, Gao H, Gao Y, Qin L, Wang Y, Shen N, Kong X, Wang X (2014) Triplet amino acids located at positions 145/146/147 of the RNA polymerase of very virulent infectious bursal disease virus contribute to viral virulence. *Journal of General Virology,* 95 (4): 888-97.

61. Gao M, Guo Y, Du J, Song Z, Luo X, Wang J, Han W (2018) Evolutional conservation of molecular structure and antiviral function of a type I interferon, IFN-kappa, in poultry. *Developmental and Comparative Immunology,* 89: 44-53.

62. Gao S, Wang Z, Jiang H, Sun J, Diao Y, Tang Y, Hu J (2019) Transcriptional analysis of host responses related to immunity in chicken spleen tissues infected with reticuloendotheliosis virus strain SNV. *Infection, Genetics and Evolution,* 74: 103932.

63. Gargan S, Ahmed S, Mahony R, Bannan C, Napoletano S, O'Farrelly C, Borrow P, Bergin C, Stevenson NJ (2018) HIV-1 Promotes the Degradation of Components of the Type 1 IFN JAK/STAT Pathway and Blocks Anti-viral ISG Induction. *EBioMedicine,* 30: 203-16.

64. Garriga D, Querol-Audi J, Abaitua F, Saugar I, Pous J, Verdaguer N, Caston JR, Rodríguez JF (2006) The 2.6-angstrom structure of infectious bursal disease virus-derived T=1particles reveals new stabilizing elements of the virus capsid. *Journal of Virology,* 80 (14): 6895-905.

65. Ghosh A, Shao L, Sampath P, Zhao B, Zhu J, Behl B, Parise RA, Beumer JH, O'Sullivan RJ, DeLuca NA, Thorne SH, Rathinam VAK, Li P, Sarkar SN (2019) Oligoadenylate-Synthetase-Family protein OASL inhibits activity of the DNA sensor cGAS during DNA virus infection to limit interferon production. *Immunity,* 50 (1): 51-63.

66. Giambrone JJ (1979) Effects of early infectious bursal disease virus infection on immunity to Newcastle disease in adult chickens. *Poultry Science,* 58 (4): 794-8.

67. Giménez MC, Rodríguez JF, Colombo MI, Delgui LR (2012) Study of the internalization pathway involved in infectious bursal disease virus infection. *Biocell,* 36 (Suppl): 78.

68. Giménez MC, Zanetti FA, Terebiznik MR, Colombo MI, Delgui LR (2018) Infectious Bursal Disease Virus Hijacks Endosomal Membranes as the Scaffolding Structure for Viral Replication. *Journal of Virology,* 92 (11): e01964-17.

69. Gimeno IM, Schat KA (2018) Virus-Induced Immunosuppression in Chickens. *Avian Diseases,* 62 (3): 272-85.

70. Giotis ES, Ross CS, Robey RC, Nohturfft A, Goodbourn S, Skinner MA (2017) Constitutively elevated levels of SOCS1 suppress innate immune responses in DF-1 immortalised chicken fibroblast cells. *Scientific Reports,* 7 (1): 17485.

71. Goossens KE, Karpala AJ, Rohringer A, Ward A, Bean AGD (2015) Characterisation of chicken viperin. *Molecular Immunology,* 63 (2): 373-80.

72. Goubau D, Schlee M, Deddouche S, Pruiissers AJ, Zillinger T, Goldeck M, Schuberth C, Van der Veen AG, Fujimura T, Rehwinkel J, Iskarpatyoti JA, Barchet W, Ludwig J, Dermody TS, Hartmann G, Reis e Sousa C (2014) Antiviral immunity via RIG-I-mediated recognition of RNA bearing 5'-diphosphates. *Nature,* 514 (7522): 372-5.

73. Grant A, Ponia SS, Tripathi S, Balasubramaniam V, Miorin L, Sourisseau M, Schwarz MC, Sánchez-Seco MP, Evans MJ, Best SM, García- Sastre A (2016) Zika Virus Targets Human STAT2 to Inhibit Type I Interferon Signaling. *Cell Host Microbe,* 19 (6): 882-90.

74. Guan J, Chan M, Brooks BW, Rohonczy L (2014) Inactivation of infectious bursal disease and Newcastle disease viruses at temperatures below 0 C using chemical disinfectants. *Avian Disease,* 58 (2): 249-54.

75. Guo B, Cheng G (2007) Modulation of the interferon antiviral response by the TBK1/ IKKi adaptor protein TANK. *Journal of Biological Chemistry,* 282 (16): 11817-26.

76. Guo X, Wang L, Cui D, Ruan W, Liu F, Li H (2012) Differential expression of the Toll-like receptor pathway and related genes of chicken bursa after experimental infection with infectious bursa disease virus. *Archives of Virology,* 157 (11): 2189-99.

77. Gurung A, Kamble N, Kaufer BB, Pathan A, Behboudi S (2017) Association of Marek's Disease induced immunosuppression with activation of a novel regulatory T cells in chickens. *PLoS Pathogens,* 13 (12): e1006745.

78. Häcker H, Redecke V, Blagoev B, Kratchmarova I, Hsu LC, Wang GG, Kamps MP, Raz E, Wagner H, Häcker G, Mann M, Karin M (2006) Specificity in Toll-like receptor signalling through distinct effector functions of TRAF3 and TRAF6. *Nature,* 436 (7073): 204-7.

79. Hassan MK, Nielsen CK, Ward LA, Jackwood DJ, Saif YM (1996) Antigenicity, pathogenicity, and immunogenicity of small and large plaque infectious bursal disease virus clones. *Avian Diseases,* 40 (4): 832-6.

80. He X, Chen G, Yang L, Xuan J, Long H, Wei P (2016) Role of naturally occurring genome segment reassortment in the pathogenicity of IBDV field isolates in Three-Yellow chickens. *Avian Pathology,* 45 (2): 178-86.

81. He X, Chen Y, Kang S, Chen G, Wei P (2017) Differential Regulation of the chTLR3 by Infectious Bursal Disease Virus with Different Virulence *In Vitro* and *In Vivo*. *Viral Immunology,* 30 (7): 490-9.

82. He Z, Chen X, Fu M, Tang J, Li X, Cao H, Wang Y, Zheng SJ (2018) Infectious bursal disease virus protein VP4 suppressed type I interferon expression via inhibiting K84-linked ubiquitylation of glucocorticoid-induced leucine zipper (GILZ). *Immunobiology,* 223 (4-5): 374-82.

83. Himly M, Foster DN, Bottoli I, Iacovoni JS, Vogt PK (1998) The DF-1 chicken fibroblast cell line: transformation induced by diverse oncogenes and cell death resulting from infection by avian leukosis viruses. *Virology,* 248 (1): 295-304.

84. Hirai K, Funakoshi T, Nakai T, Shimakura S (1981) Sequential changes in the number of surface immunoglobulin-bearing B lymphocytes in infectious bursal disease virus-infected chickens. *Avian disease,* 25 (2) 484-96.

85. Huang B, Qi ZT, Xu Z, Nie P (2010) Global characterization of interferon regulatory factor (IRF) genes in vertebrates: Glimpse of the diversification in evolution. *BMC Immunology,* 11 (22).

86. Huang X, Yue Y, Li D, Zhao Y, Qiu L, Chen J, Pan Y, Xi J, Wang X, Sun Q, Li Q (2016) Antibody-dependent enhancement of dengue virus infection inhibits RLR-mediated Type-I IFN-dependent signalling through upregulation of cellular autophagy. *Scientific Reports,* 6: 22303.

87. Hui RK, Leung FC (2015) Differential expression profile of chicken embryo fibroblast DF-1 cells infected with cell-adapted infectious bursal disease virus. *PLoS One,* 10 (6): e0111771.

88. Hulo C, de Castro E, Masson P, Bougueleret L, Bairoch A, Xenarios I, Le Mercier P (2011) ViralZone: a knowledge resource to understand virus diversity. *Nucleic Acid Research,* 39 (Database issue): D576-82.

89. Hussein EA, Hair-Bejo M, Liew PS, Adamu L, Omar AR, Arshad SS, Mohammed MH, Aini I (2019) Infectious bursal disease virus tissue tropism and pathogenesis of the infection in chickens by application of in situ PCR, immunoperoxase and HE staining. *Microbial Pathogenesis,* 129: 195-205.

90. Ingrao F, Rauw F, Lambrecht B, van den Berg T (2013) Infectious Bursal Disease: a complex host-pathogen interaction. *Developmental and Comparative Immunology,* 41 (3): 429-38.

91. Intayoung P, Limtrakul P, Yodkeeree S (2016) Anti-inflammatory Activities of Crebanine by Inhibition of NF-κB and AP-1 Activation through Suppressing MAPKs and Akt Signaling in LPS-Induced RAW264.7 Macrophages. *Biological and Pharmaceutical Bulletin,* 39 (1): 54-61.

92. Intervet (2019) Gumboro: Vaccination [online] available at: http://www.gumboro.com/control/vaccination/index.asp.

93. Irigoyen N, Garriga D, Navarro A, Verdaguer N, Rodriguez JF, Castón JR (2009) Autoproteolytic activity derived from the infectious bursal disease virus capsid protein. *Journal of Biological Chemistry,* 284 (12): 8064-72.

94. Isaacs A, Lindenmann J (1957) Virus interference. I. The interferon. *Proceedings of the Royal Society of London. Series B, Biological Sciences,* 147 (927): 258-67.

95. Jackwood DH, Saif YM (1987) Antigenic diversity of Infectious bursal Disease Virus. *Avian Diseases,* 31 (4): 766-70.

96. Jackwood DJ, Schat KA, Michel LO, de Wit S (2018) A proposed nomenclature for infectious bursal disease virus isolates. *Avian Pathology,* 47 (6): 576-84.

97. Jackwood DJ, Sommer-Wagner SE, Crossley BM, Stoute ST, Woolcock PR, Charlton BR (2011) Identification and pathogenicity of a natural reassortant between a very virulent serotype 1 infectious bursal disease virus (IBDV) and a serotype 2 IBDV. *Virology,* 420 (2): 98-105.

98. Jackwood DJ, Sreedevi B, LeFever LJ, Sommer-Wagner SE (2008) Studies on naturally occurring infectious bursal disease viruses suggest that a single amino acid substitution at position 253 in VP2 increases pathogenicity. *Virology,* 377 (1): 110-6.

99. Jackwood DJ, Stoute ST, Crossley BM (2016) Pathogenicity of Genome Reassortant Infectious Bursal Disease Viruses in Chickens and Turkeys, *Avian Diseases,* 60 (4): 765-72.

100. Jahromi MZ, Bello MB, Abdolmaleki M, Yeap SK, Hair-Bejo M, Omar AR (2018) Differential activation of intraepithelial lymphocyte-natural killer cells in chickens infected with very virulent and vaccine strains of infectious bursal disease virus. *Developmental & Comparative Immunology,* 87: 116-23.

101. Jeurissen SH, Janse EM, Lehrbach PR, Haddad EE, Avakian A, Whitfill CE (1998) The working mechanism of an immune complex vaccine that protects chickens against infectious bursal disease. *Immunology,* 95 (3): 494-500.

102. Karpala AJ, Stewart C, McKay J, Lowenthal JW, Bean AG (2011) Characterization of chicken Mda5 activity: regulation of IFN-beta in the absence of RIG-I functionality. *Journal of Immunology,* 186 (9): 5397-405.

103. Kawai T, Akira S (2010) The role of pattern-recognition receptors in innate immunity: update on Toll-like receptors. *Nature Immunology,* 11 (5): 373-84.

104. Keestra AM, can Putten JP (2008) Unique properties of the chicken TLR4/MD-2 complex: selective lipopolysaccharide activation of the MyD88-dependent pathway. *Journal of Immunology,* 181 (6): 4354-62.

105. Keestra AM, de Zoete MR, Bouwman LI, Vaezirad MM, van Putten JP (2013) Unique features of chicken Toll-like receptors. *Developmental and Comparative Immunology,* 41 (3): 316-23.

106. Kelley LA, Mezulis S, Yates CM, Wass MN, Sternberg MJ (2015) The Phyre2 web portal for protein modeling, prediction and analysis. *Nature Protocols,* 10 (6): 845-58.

107. Khatri M, Palmquist JM, Cha RM, Sharma JM (2005) Infection and activation of bursal macrophages by virulent infectious bursal disease virus. *Virus Research,* 113 (1): 44-50.

108. Khatri M, Sharma JM (2007) Replication of infectious bursal disease virus in macrophages and altered tropism of progeny virus. *Veterinary Immunology and Immunopathology,* 117 (1-2): 106-15.

109. Kim E, Myoung J (2018) Hepatitis E Virus Papain-Like Cysteine Protease Inhibits Type I Interferon Induction by Down-Regulating Melanoma Differentiation-Associated Gene 5. *Journal of Microbiology and Biotechnology,* 28 (11): 1908-15.

110. Kim IJ, Karaca K, Pertile TL, Erickson SA, Sharma JM (1998) Enhanced expression of cytokine genes in spleen macrophages during acute infection with infectious bursal disease virus in chickens. *Veterinary Immunology and Immunopathology,* 61 (204): 331-41.

111. Kim TH, Zhou H (2015) Functional Analysis of Chicken IRF7 in Response to dsRNA Analog Poly(I:C) by Integrating Overexpression and Knockdown. *PLoS One,* 10 (9): e0137672.

112. Ko KH, Lee IK, Kim G, Gu MJ, Kim HY, Park BC, Park TS, Han SH, Yun CH (2018) Changes in bursal B cells in chicken during embryonic development and early life after hatching. *Scientific Reports,* 8 (1): 16905.

113. Korte J, Fröhlich T, Kohn M, Kaspers B, Arnold GJ, Härtle S (2013) 2D DIGE analysis of the bursa of Fabricius reveals characteristic proteome profiles for different stages of chicken B-cell development. *Proteomics,* 13 (1): 119-33.

114. Kothlow S, Morgenroth I, Tregaskes CA, Kaspers B, Young JR (2008) CD40 ligand supports the long-term maintenance and differentiation of chicken B cells in culture. *Developmental and Comparative Immunology,* 32 (9): 1015-26.

115. Laidlaw SM, Robey R, Davies M, Giotis ES, Ross C, Buttigieg K, Goodbourn S, Skinner MA (2013) Genetic screen of a mutant poxvirus library identifies an ankyrin repeat protein involved in blocking induction of avian type I interferon. *Journal of Virology,* 87 (9): 5041-52.

116. Lam KM (1998) Alteration of chicken heterophil and macrophage functions by the infectious bursal disease virus. *Microbial Pathogenesis*; 25 (3): 147-55.

117. Lasher HN, Davis VS (1997) History of infectious bursal disease in the U.S.A- the first two decades. *Avian Diseases,* 41 (1): 11-9.

118. Lauksund S, Greiner-Tollersrud L, Chang CJ, Robertsen B (2015) Infectious pancreatic necrosis virus proteins VP2, VP3, VP4 and VP5 antagonize IFNa1 promoter activation while VP1 induces IFNa1. *Virus Research,* 196: 112-21.

119. Laurent-Rolle M, Morrison J, Rajsbaum R, Macleod JM, Pisanelli G, Pham A, Ayllon J, Miorin L, Martinez-Romero C, tenOever BR, García- Sastre A(2014) The interferon signaling antagonist function of yellow fever virus NS5 protein is activated by type I interferon. *Cell Host Microbe,* 16 (3): 314-27.

120. Le Nouën C, Toquin D, Müller H, Raue R, Kean KM, Langlois P, Cherbonnel M, Eterradossi N (2012) Different domains of the RNA polymerase of infectious bursal disease virus contribute to virulence. *PLoS One,* 7 (1): e28064.

121. Lee CC, Ko TP, Chou CC, Yoshimura M, Doong SR, Wang MY, Wang AH (2006) Crystal structure of infectious bursal disease virus VP2 subviral particle at 2.6 Å resolution: implications in virion assembly and immunogenicity. *Journal of Structural Biology,* 155 (1): 74-86.

122. Lee CC, Wu CC, Lin TL (2014) Chicken melanoma differentiation-associated gene 5 (MDA5) recognizes infectious bursal disease virus infection and triggers MDA5-related innate immunity. *Archives of Virology,* 159 (7): 1671-86.

123. Lee HJ, Jang I, Shin SH, Lee HS, Choi KS (2017) Genome Sequence of a Novel Reassortant and Very Virulent Strain of Infectious Bursal Disease Virus. *Genome Announcements,* 5 (34): e00730-17.

124. Lee HJ, Kim JY, Kye SJ, Seul HJ, Jung SC, Choi KS (2015) Efficient self-assembly and protective efficacy of infectious bursal disease virus-like particles by a recombinant baculovirus co-expressing precursor polyprotein and VP4. *Virology Journal,* 12 (1): 177-85.

125. Lejal N, Da Costa B, Huet JC, Delmas B (2000) Role of Ser-652 and Lys-692 in the protease activity of infectious bursal disease virus VP4 and identification of its substrate cleavage sites. *Journal of General Virology,* 81 (4): 983-92.

126. Leong JC, Brown D, Dobos P, Kibenge FSB, Ludert JE, Muller H, Mundt E, Nicholson B (2000) Family *Birnaviridae. In "*Virus Taxonomy- Classification and Nomenclature of Viruses: Seventh Report of the International Committee on Taxonomy of Viruses" (MHV van Regenmortel, CM Faquet, DHL Bishop, EB Carstens, MK Estes, SM Lemon, J Maniloff, MA Mayo, DJ McGeoch, CR Pringle and RB Wickner, Eds) pp. 481-90. *Springer-Verlag,* Wien/New York.

127. Letzel T, Mundt E, Gorbalenya AE (2007) Evidence for functional significance of the permuted C motif in Co2+- stimulated RNA dependent RNA polymerase of infectious bursal disease virus. *Journal of General Virology,* 88 (10): 2824-33.

128. Ley DH, Yamamoto R, Bickford AA (1983) The Pathogenesis of Infectious Bursal Disease: Serologic, Histopathologic, and Clinical Chemical Observations. *Avian Diseases,* 27 (4) 1060-85.

129. Li G, Chen S, Duan Z, Qu L, Xu G, Yang N (2013a) Comparison of protoporphyrin IX content and related gene expression in the tissues of chicken laying brown-shelled eggs. *Poultry Science,* 92 912): 3120-4.

130. Li K, Liu Y, Zhang Y, Gao L, Liu C, Cui H, Gao Y, Zhong L, Wang X (2017) Protective efficacy of a novel recombinant Marek's disease virus vector vaccine against infectious bursal disease in chickens with or without maternal antibodies. *Veterinary Immunology and Immunopathology,* 186: 55-9.

131. Li L, Kubasová T, Rychlik I, Hoerr FJ, Rautenschlein, S (2018a) Infectious bursal disease virus infection leads to changes in the gut associated-lymphoid tissue and the microbiota composition. *PLoS One,* 13 (2): e0192066.

132. Li L, Pielsticker C, Han Z, Kubasová T, Rychlik I, Kaspers B, Rautenschlein S (2018b) Infectious bursal disease virus inoculation infection modifies Campylobacter jejuni–host interaction in broilers. *Gut Pathogens,* 10: 13.

133. Li YP, Handberg KJ, Juul-Madsen HR, Zhang MF, Jørgensen PH (2007) Transcriptional profiles of chicken embryo cell cultures following infection with infectious bursal disease virus. *Archives of Virology,* 152 (3): 463-78.

134. Li Z, Wang Y, Li X, Li X, Cao H, Zheng SJ (2013b) Critical roles of glucocorticoid-induced leucine zipper in infectious bursal disease virus (IBDV)- induced suppression of type I interferon expression and enhancement of IBDV growth in host cells via interaction with VP4. *Journal of Virology,* 87 (2): 1221-31.

135. Li Z, Wang Y, Xue Y, Li X, Cao H, Zheng SJ (2012) Critical role for voltage-dependent anion channel 2 in infectious bursal disease virus-induced apoptosis in host cells via interaction with VP5. *Journal of Virology,* 86 (3): 1328-38.

136. Liang J, Yin Y, Qin T, Yang Q (2015) Chicken bone marrow-derived dendritic cells maturation in response to infectious bursal disease virus. *Veterinary Immunology and Immunopathology,* 164 (1-2): 51-5.

137. Lim BL, Cao Y, Yu T, Mo CW (1999) Adaptation of very virulent infectious bursal disease virus to chicken embryonic fibroblasts by site-directed mutagenesis of residues 279 and 284 of viral coat protein VP2. *Journal of Virology,* 73 (4): 2854-62.

138. Lin J, Xia J, Zhang K, Yang Q (2016) Genome-wide profiling of chicken dendritic cell response to infectious bursal disease. *BMC Genomics,* 17 (1): 878-90.

139. Lin Tw, Lo CW, Lai SY, Fan RJ, Lo CJ, Chou YM, Thiruvengadam R, Wang AH, Wang MY (2007) chicken heat shock protein 90 is a component of the putative cellular receptor complex of infectious bursal disease virus. *Journal of Virology,* 81 (16): 8730-41.

140. Lin W, Zhang Z, Xu Z, Wang B, Li X, Cao H, Wang Y, Zheng SJ (2015) The association of receptor of activated protein kinase C 1 (RACK1) with infectious bursal disease virus viral protein VP5 and voltage-dependent anion channel 2 (VDAC2) inhibits apoptosis and enhances viral replication. *Journal of Biological Chemistry,* 290 (13): 8500-10.

141. Liniger M, Summerfield A, Zimmer G, McCullough KC, Ruggli N (2012) Chicken cells sense influenza A virus infection through MDA5 and CARDIF signalling involving LGP2. *Journal of Virology,* 86 (2): 705-17.

142. Liu M, Vakharia VN (2004) VP1 protein of infectious bursal disease virus modulates virulence *in vivo*. *Virology,* 330 (1): 62-73.

143. Liu M, Vakharia VN (2006) Nonstructural protein of infectious bursal disease virus inhibits apoptosis at the early stage of virus infection. *Journal of Virology,* 80 (7): 3369-77.

144. Liu W, Li J, Zheng W, Shang Y, Zhao Z, Wang S, Bi Y, Zhang S, Xu C, Duan Z, Zhang L, Wang YL, Jiang Z, Liu W, Sun L (2017a) Cyclophilin A-regulated ubiquitination is critical for RIG-mediated antiviral immune responses. *Elife,* 6: e24425.

145. Liu Y, Liang HM, Lv YQ, Tang SM, Cheng P (2019) Blockade of SDF-1/CXCR4 reduces adhesion-mediated chemoresistance of multiple myeloma cells via interacting with interleukin-6. *Journal of Cellular Physiology,* 2019: 1-13.

146. Liu Y, Olagnier D, Lin R (2017b) Host and Viral Modulation of RIG-I-Mediated Antiviral Immunity. *Frontiers in Immunology,* 7: 662.

147. Liu H, Zhang M, Han H, Yuan J, Li Z (2010) Comparison of the expression of cytokine genes in the bursal tissues of the chickens following challenge with infectious bursal disease viruses of varying virulence. *Virology Journal,* 7: 364.

148. Lombardo E, Maraver A, Castón JR, Rivera J, Fernández-Arias A, Serrano A, Carrascosa JL, Rodriguez JF (1999) VP1, the putative RNA-dependent RNA polymerase of infectious bursal disease virus, forms complexes with the capsid protein VP3, leading to efficient encapsidation into virus-like particles. *Journal of Virology,* 73 (8): 6973-83.

149. Lombardo E, Maraver A, Espinosa I, Fernández-Arias A, Rodriguez JF (2000) VP5, the non-structural polypeptide of infectious bursal disease virus accumulates within the host plasma membrane and induces cell lysis. *Virology,* 277 (2): 345-57.

150. Loo YM, Gale M Jr (2011) Immune signalling by RIG-I-like receptors. *Immunity,* 34 (5): 680-92.

151. Luo J, Zhang H, Teng M, Fan JM, You LM, Xiao ZJ, Yi ML, Zhi YB, Li XW, Zhang GP (2010) Surface IgM on DT40 cells may be a component of the putative receptor complex responsible for the binding of infectious bursal disease virus. *Avian Pathology*, 39 (5): 359-65.

152. Luque D, Rivas G, Alfonso C, Carrascosa JL, Rodríguez JF, Castón JR (2009a) Infectious bursal disease virus is an icosahedral polyploid dsRNA virus. *PNAS,* 106 (7): 2148-52.

153. Luque D, Saugar I, Rejas MT, Carrascosa JL, Rodriguez JF, Castón JR (2009b) Infectious Bursal disease virus: ribonucleoprotein complexes of a double-stranded RNA virus. *Journal of Molecular Biology,* 386 (3): 891-901.

154. Lynn DJ, Lloyd AT, O'Farrelly C (2003) In silico identification of components of the Toll-like receptor (TLR) signaling pathway in clustered chicken expressed sequence tags (ESTs). *Veterinary Immunology and Immunopathology,* 93 (3-4): 177-84.

155. Mackay F, Browning JL (2002) BAFF: a fundamental survival factor for B cells. *Nature Reviews Immunology,* 2 (7):465-75.

156. Magor KE, Miranzo Navarro D, Barber MRW, Petkau K, Fleming-Canepa X, Blyth GAD, Blaine AH (2013) Defense genes missing from the flight division. *Developmental and Comparative Immunology,* 41 (3): 377-88.

157. Mahgoub HA, Bailey M, Kaiser P (2012) An overview of infectious bursal disease. *Archives of Virology,* 157 (11): 2047-57.

158. Mandeville WF. III, Cook FK, Jackwood DJ (2000) Heat lability of five strains of infectious bursal disease virus. *Poultry Science,* 79 (6): 838-42

159. Masuda Y, Matsuda A, Tatsufumi USUI, Sugai T, Asano A, Yamano Y (2012) Biological effects of chicken type III interferon on expression of interferon-stimulated genes in chickens: comparison with type I and type II interferons. *Journal of Veterinary Medical Science,* 74 (11): 1381-6.

160. Mata CP, Mertens J, Fontana J, Luque D, Allende-Ballestero C, Reguera D, Trus BL, Steven AC, Carrascosa JL, Castón JR (2018) The RNA-Binding Protein of a Double-Stranded RNA Virus Acts like a Scaffold Protein. *Journal of Virology,* 92 (19): e00968-18.

161. McFerran JB, McNulty MS, Killop ER, Connor TJ, McCracken RM, Collins PS, Allan GM (1980) Isolation and serological studies with infectious bursal disease virus from fowl, turkeys and ducks: demonstration of a second serotype. *Avian Pathology*, 9 (3): 395-404.

162. Méndez F, Romero N, Cubas LL, Delgui LR, Rodríguez D, Rodríguez JF (2017) Non-Lytic Egression of Infectious Bursal Disease Virus (IBDV) Particles from Infected Cells. *PLos One,* 12 (1): e0170080.

163. Mertens J, Casado S, Mata CP, Hernando-Pérez M, de Pablo PJ, Carrascosa JL, Castón JR (2015) A protein with simultaneous capsid scaffolding and dsRNA-binding activities enhances the birnavirus capsid mechanical stability. *Scientific Reports,* 4 (5): 13486.

164. Meulemans G, Halen P (1982) Efficacy of some disinfectants against infectious bursal disease virus and avian reovirus. *Veterinary Record,* 111 (18): 412-3.

165. Müller H, Nitschke R (1987) The two segments of the infectious bursal disease virus genome are circularized by a 90000-Da protein. *Virology,* 159 (1): 174-7.

166. Mundt E (1999) Tissue culture infectivity of different strains of infectious bursal disease virus is determined by distinct amino acids in VP2. *Journal of General Virology,* 80 (8): 2067-76.

167. Mundt E, Beyer J, Müller H (1995) Identification of a novel viral protein in infectious bursal disease virus-infected cells. *Journal of General Virology,* 76 (2): 437-43.

168. Nunoya T, Otaki Y, Tajima M, Hiraga M, Saito T (1992) Occurrence of acute Infectious Bursal Disease with high mortality in Japan and pathogenicity of field isolates in Specific-Pathogen-Free chickens. *Avian Diseases,* 36 (3): 597-609.

169. O'Neill LA, Bowie AG (2007) The family of five: TIR-domain-containing adaptors in toll-like receptor signalling. *Nature Reviews. Immunology.* 7 (5): 353-64.

170. Oganesyan G, saha SK, Guo B, He JQ, Shahangian A, Zarnegar B, Perry A, Cheng G (2006) Critical role of TRAF3 in the toll-like receptor-dependent and-independent antiviral response. *Nature,* 439 (7073): 208-11.

171. Onunkwo O (1975) An outbreak of infectious bursal disease (IBD) of chickens in Nigeria. *Veterinary Record,* 97 (22): 433.

172. Oppling V, Müller H, Becht H (1991) Heterogeneity of the antigenic site responsible for the induction of neutralizing antibodies in infectious bursal disease virus. *Archives of Virology,* 119 (3-4): 211-23.

173. Ou C, Wang Q, Zhang Y, Kong W, Zhang S, Yu Y, Ma J, Liu X, Kong X (2017) Transcription profiles of the response of chicken bursae of Fabricius to IBDV in different timing phases. *Virology Journal,* 14 (1): 93-102.

174. Ouyang W, Wang YS, Meng K, Pan QX, Wang XL, Xia XX, Zhu YM, Bi ZW, Zhang HB, Luo K (2017) gga-miR-2127 downregulates the translation of chicken p53 and attenuates chp53-mediated innate immune response against IBDV infection. *Veterinary Microbiology,* 198: 34-42.

175. Palmquist JM, Khatri M, Cha RM, Goddeeris BM, Walcheck B, Sharma JM (2006) *In vivo* activation of chicken macrophages by infectious bursal disease virus. *Viral Immunology,* 19 (2): 305-15.

176. Paludan SR (2016) Innate antiviral defences independent of inducible IFNα/β production. *Trends in Immunology,* 37 (9): 588-96.

177. Perozo F, Villegas AP, Fernandez R, Cruz J, Pritchard N (2009) Efficacy of single dose recombinant herpesvirus of turkey infectious bursal disease virus (IBDV) vaccination against a variant IBDV strain. *Avian Diseases,* 53 (4): 624-8.

178. Piaszyk- Borychowska A, Széles L, Csermely A, Chiang HC, Wesoly J, Lee CK, Nagy L, Bluyssen HAR (2019) Signal Integration of IFN-I and IFN-II With TLR4 Involves Sequential Recruitment of STAT1-Complexes and NF-κB to Enhance Pro-inflammatory Transcription. *Frontiers in Immunology,* 4 (10): 1253.

179. Pikula A, Lisowska A, Jasik A, Śmietanka K (2018) Identification and assessment of virulence of a natural reassortant of infectious bursal disease virus. *Veterinary Research,* 49 (1): 89-99.

180. Platanias LC (2005) Mechanisms of type-I-and type-II-interferon-mediated signalling. *Nature Reviews. Immunology.* 5 (5): 375-86.

181. Pokharel SM, Shil NK, Bose S (2016) Autophagy, TGF-β, and SMAD-2/3 Signaling Regulates Interferon-β Response in Respiratory Syncytial Virus Infected Macrophages. *Frontiers in Cellular and Infection Microbiology*, 6: 174.

182. Psifidi A, Banos G, Matika O, Desta TT, Bettridge J, Hume DA, Dessie T, Christley R, Wigley P, Hanotte O, Kaiser P (2016) Genome-wide association studies of immune, disease and production traits in indigenous chicken ecotypes. *Genetics, Selection and Evolution,* 48 (1): 74-90.

183. Qi X, Gao H, Gao Y, Qin L, Wang Y, Gao L, Wang X (2009) Naturally occurring mutations at residues 253 and 284 in VP2 contribute to the cell tropism and virulence of very virulent infectious bursal disease virus. *Antiviral Research,* 84 (3): 225-33.

184. Qi X, Zhang L, Chen Y, Gao L, Wu G, Qin L, Wang Y, Ren X, Gao Y, Gao H, Wang X (2013) Mutations of residues 249 and 256 in VP2 are involved in the replication and virulence of infectious bursal disease virus. *PLoS One,* 8 (7): e70982.

185. Qi Y, Yan B, Chen S, Chen H, Wang M, Jia R, Zhu D, Liu M, Liu F, Yang Q, Sun K, Wu Y, Chen X, Jing B, Cheng A (2016) CpG oligodeoxynucleotide-specific goose TLR21 initiates an anti-viral immune response against NGVEV but not AIV strain H9N2 infection. *Immunobiology,* 221 (3): 454-61.

186. Qin Y, Xu Z, Wang Y, Li X, Cao J, Zheng SJ (2017) VP2 of Infectious Bursal Disease Virus Induces Apoptosis via Triggering Oral Cancer Overexpressed 1 (ORAOV1) Protein Degradation. *Frontiers in Microbiology,* 8: 1351.

187. Qin Y, Zheng S (2017) Infectious Bursal Disease Virus-Host Interactions: Multifunctional Viral Proteins that Perform Multiple and Differing Jobs. *International Journal of Molecular Sciences,* 18 (1): pii: E161.

188. Quan R, Zhu S, Wei L, Wang J, Yan X, Li Z, Liu J (2017) Transcriptional profiles in bursal B-lymphoid DT40 cell infected with very virulent infectious bursal disease virus. *Virology Journal,* 14 (1): 7-18.

189. Randall RE, Goodbourn S (2008) Interferons and viruses: an interplay between induction, signalling, antiviral responses and virus countermeasures. *Journal of General Virology,* 89 (1): 1-47.

190. Rasoli M, Yeap SK, Tan SW, Roohani K, Kristeen-Teo YW, Alitheen NB, Rahaman YA, Aini I, Bejo MH, Kaiser P, Omar AR (2015) Differential modulation of immune response and cytokine profiles in the bursae and spleen of chickens infected with very virulent infectious bursal disease virus. *BMC Veterinary Research,* 11 (1): 75-88.

191. Ratcliffe MJ, Antibodies, immunoglobulin genes and the bursa of Fabricius in chicken B cell development. *Developmental and Comparative Immunology,* 30 (1-2): 101-18.

192. Raue R, Islam MR, Islam MN, Islam KM, Badhy SC, Das PM, Müller H (2004) Reversion of molecularly engineered, partially attenuated, very virulent infectious bursal disease virus during infection of commercial chickens. *Avian Pathology,* 33 (2): 181-9.

193. Rauf A, Khatri M, Murgia MV, Jung K, Saif YM (2011) Differential modulation of cytokine, chemokine and Toll like receptor expression in chickens infected with classical and variant infectious bursal disease virus. *Veterinary Research,* 42 (1): 85.

194. Rautenschlein S, Kraemer C, Vanmarcke J, Montiel E (2005) Protective efficacy of intermediate and intermediate plus infectious bursal disease virus (IBDV) vaccines against very virulent IBDV in commercial broilers. *Avian Diseases,* 49 (2): 231-7.

195. Rautenschlein S, Yeh HY, Sharma JM (2002) The role of T cells in protection by an inactivated infectious bursal disease virus vaccine. *Veterinary Immunology and Immunopathology,* 89 (3-4): 159-67.

196. Rautenschlein S, Yeh HY, Sharma JM (2003) Comparative Immunopathogenesis of Mild, Intermediate, and Virulent Strains of Classic Infectious Bursal Disease Virus. *Avian Diseases,* 47 (1): 66-78.

197. Reed LJ, Muench H (1938) A simple method of estimating fifty percent endpoints. *American Journal of Epidemiology*, 27 (3): 494-7.

198. Ribatti D, Tamma R, Elieh Ali Komi D (2019) The morphological basis of development of the chick embryo immune system. *Experimental Cell Research,* 381 (2): 323-9.

199. Rodriguez JJ, Parisien JP, Horvath CM (2002) Nipah virus V protein evades alpha and gamma interferons by preventing STAT1 and STAT2 activation and nuclear accumulation. *Journal of Virology,* 76 (22): 11476-83.

200. Rodríguez-Lecompte JC, Kibenge FS (2002) Site-directed mutagenesis of Avibirnavirus VP4 gene. *Virology* 292 (2):241-6.

201. Rodríguez-Lecompte JC, Niño-Fong R, Lopez R, Frederick Markham RJ, Kibenge FS (2005) Infectious bursal disease virus (IBDV) induces apoptosis in chicken B cells. *Comparative Immunology, Microbiology and Infectious Diseases,* 28 (4): 321-37.

202. Rosenberger JK, Cloud SS (1986) Isolation and characterization of variant infectious bursal disease viruses. *Abstracts 123rd American Veterinary Medical Association (AVMA) Meeting, 20-24th July, Atlanta, Georgia,* AVMA, Schaumburg Ilinois, Abstract No. 181, 104.

203. Rosenberger JK, Gelb J (1976) Immunosuppressive effects of the infectious bursal agent and relationships to other poultry diseases. *PNAS,* 80: 283-9.

204. Ruby T, Whittaker C, Withers DR, Chelbi-Alix MK, Morin V, Oudin A, Young JR, Zoorob R (2006) Transcriptional profiling reveals a possible role for the timing of the inflammatory response in determining susceptibility to a viral infection. *Journal of Virology,* 80 (18): 9207-16.

205. Salman A, Shuaib MA, Suleiman TH, Ginawi M (1983) Infectious bursal disease in the Sudan. *Tropical Animal Health and Production,* 15 (4): 219-20.

206. Santhakumar D, Iqbal M, Nair V, Munir M (2017a) Chicken IFN Kappa: A Novel Cytokine with Antiviral Activities. *Scientific Reports,* 7 (1): 2719.

207. Santhakumar D, Rohaim MAMS, Hussein HA, Hawes P, Ferreira HL, Behboudi S, Iqbal M, Nair V, Arns CW, Munir M (2018) Chicken interferon-induced protein with tetratricopeptide repeats 5 antagonizes replication of RNA viruses. *Scientific Reports,* 8 (1): 6794.

208. Santhakumar D, Rubbenstroth D, Martinez-Sobrido L, Munir M (2017b) Avian Interferons and Their Antiviral Receptors. *Frontiers in Immunology,* 8: 49.

209. Saugar I, Luque D, Oña A, Rodriguez JF, Carrascosa JL, Trus BL, Castón JR (2005) Structural polymorphism of the major capsid protein of a double-stranded RNA virus: an amphipathic α helix as a molecular switch. *Structure,* 13 (7): 1007-17.

210. Schermuly J, Greco A, Härtle S, Osterrieder N, Kaufer BB, Kaspers B (2015) *In vitro* model for lytic replication, latency, and transformation of an oncogenic alphaherpesvirus. *PNAS,* 112 (23): 7279-84.

211. Schilling MA, Katani R, Memari S, Cavanaugh M, Buza J, Radzio-Basu J, Mpenda FN, Diest MS, Lamont SJ, Kapur V (2012) Transcriptional Innate Immune Response of the Developing Chicken Embryo to Newcastle Disease Virus Infection. *Frontiers in Genetics,* 27 (9): 61.

212. Schlee M, Hartmann G (2016) Discriminating self from non-self in nucleic acid sensing. *Nature Reviews. Immunology.* 16 (9): 566-80.

213. Seth RB, Sun L, Ea CK, Chen ZJ (2005) Identification and characterization of MAVS, a mitochondrial antiviral signaling protein that activates NF-kappaB and IRF 3. *Cell,* 122 (5): 669-82.

214. Setoh YX, Periasamy P, Peng NYG, Amarilla AA, Slonchak A, Khromykh AA (2017) Helicase Domain of West Nile Virus NS3 Protein Plays a Role in Inhibition of Type I Interferon Signalling. *Viruses,* 9 (11): E326.

215. Sharma JM, Kim IJ, Rautenschlein S, Yeh HY (2000) Infectious bursal disease virus of chicken: pathogenesis and immunosuppression. *Developmental and Comparative Immunology,* 24 (2-3): 223-35.

216. Shaw I, Davison TF (2000) Protection from IBDV-induced bursal damage by a recombinant fowlpox vaccine, fpIBD1, is dependent on the titre of challenge virus and chicken genotype. *Vaccine*, 18 (28): 3230-41.

217. Shaw ML, García-Sastre A, Palese P, Basler CF (2004) Nipah virus V and W proteins have a common STAT1-binding domain yet inhibit STAT1 activation from the cytoplasmic and nuclear compartments, respectively. *Journal of Virology,* 78 (11): 5633-41.

218. Sheppard M, Werner W, Tsatas E, McCoy R, Prowse S, Johnson M (1998) Fowl adenovirus recombinant expressing VP2 of infectious bursal disease virus induces protective immunity against bursal disease. *Archives of Virology,* 143 (5): 915-30.

219. Sievers F, Wilm A, Dineen D, Gibson TJ, Karplus K, Li W, Lopez R, McWilliam H, Remmert M, Söding J, Thompson JD, Higgins DG (2011) Fast, scalable generation of high-quality protein multiple sequence alignments using Clustal Omega. *Molecular Systems Biology,* 7: 539.

220. Skjesol A, Aamo T, Hegseth MN, Robertsen B, Jørgensen JB (2009) The interplay between infectious pancreatic necrosis virus (IPNV) and the IFN system: IFN signalling is inhibited by IPNV infection. *Virus Research,* 143: 53-60.

221. Smith J, Sadeyen JR, Butter C, Kaiser P, Burt DW (2015) Analysis of the early immune response to infection by infectious bursal disease virus in chickens differing in their resistance to the disease. *Journal of Virology,* 89 (5): 2469-82.

222. Snyder, DB (1990) Changes in the field status of infectious bursal disease virus. *Avian Pathology*, 19 (3): 419-23.

223. Soubies SM, Courtillon C, Abed M, Amelot M, Keita A, Broadbent A, Härtle S, Kaspers B, Eteradossi N (2017) Propagation and titration of infectious bursal disease virus, including non-cell-culture-adapted strains, using ex vivo stimulated chicken bursal cells. *Avian Pathology,* 47 (2): 179-88.

224. Spackman E, Stephens CB, Pantin-Jackwood MJ (2018) The effect of infectious bursal disease virus-induced immunosuppression on vaccination against highly pathogenic avian influenza virus. *Avian Diseases,* 62 (1): 36-44.

225. Staeheli P, Puehler F, Schneider K, Göbel TW, Kaspers B (2001) Cytokines of Birds: Conserved Functions- A Largely Different Look. *Journal of Interferon & Cytokine Research,* 21 (12): 993-1010.

226. Staeheli, P (1990) Interferon-induced proteins and the antiviral state. *Advances in Virus Research,* 38: 147-200.

227. Staines K, Batra A, Mwangi W, Maier HJ, Van Borm S, Young JR, Fife M, Butter C (2016) A Versatile Panel of Reference Gene Assays for the Measurement of Chicken mRNA by Quantitative PCR. *PLoS One,* 11 (8): e0160173.

228. Subler KA, Mickael CS, Jackwood DJ (2006) Infectious bursal disease virus-induced immunosuppression exacerbates Campylobacter jejuni colonization and shedding in chickens. *Avian Diseases,* 50 (2): 179-84.

229. Tacken MGJ, Peeters BPH, Thomas AAM, Rottier PJM, Boot HJ (2002) Infectious bursal disease virus capsid protein VP3 interacts both with VP1, the RNA-dependent RNA polymerase, and the viral double-stranded RNA. *Journal of Virology,* 76 (22): 11301-11.

230. Takeda K, Akira S (2004) TLR signalling pathways. *Seminars in Immunology,* 16 (1): 3-9.

231. Terasaki K, Hirayama H, Kasanga CJ, Maw MT, Ohya K, Yamaguchi T, Fukushi H (2007) Chicken B Lymphoma DT40 Cells as a Useful Tool for *in vitro* Analysis of Pathogenic Infectious Bursal Disease Virus. *Virology,* 70 (4): 407-10.

232. The PyMOL Molecular Graphics System, Version 2.0 Schrödinger, LLC.

233. Thornton PK (2010) Livestock production: recent trends, future prospects. *Philosophical Transactions of the Royal Society of London. Series B, Biological Sciences,* 365 (1554): 2853-67.

234. Tippenhauer M, Heller DE, Weigend S, Rautenschlein S (2013) The host genotype influences infectious bursal disease virus pathogenesis in chickens by modulation of T cells responses and cytokine gene expression. *Developmental and Comparative Immunology,* 40 (1): 1-10.

235. Tregaskes CA, Glansbeek HL, Gill AC, Hunt LG, Burnside J, Young JR (2005) Conservation of biological properties of the CD40 ligand, CD154 in a non-mammalian vertebrate. *Developmental and Comparative Immunology,* 29 (4): 361-74.

236. Tsukamoto K, Kojima C, Komori Y, Tanimura N, Mase M, Yamaguchi S (1999) Protection of chickens against very virulent infectious bursal disease virus (IBDV) and Marek's disease virus (MDV) with a recombinant MDV expressing IBDV VP2. *Virology,* 257 (2): 352-62.

237. Tsukamoto K, Tanimura N, Hihara H, Shirai J, Imai K, Nakamura K, Maeda M (1992) Isolation of virulent infectious bursal disease virus from field outbreaks with high mortality in Japan. *Journal of Veterinary Medical Science,* 54 (1): 153-5.

238. Tsurumi A, Zhao C, Li WX (2017) Canonical and non-canonical JAK/STAT transcriptional targets may be involved in distinct and overlapping cellular processes. *BMC Genomics,* 18 (1): 718.

239. Uchikawa E, Lethier M, Malet H, Brunel J, Gerlier D, Cusack S (2016) Structural analysis of dsRNA binding to anti-viral pattern recognition receptors LGP2 and MDA5. *Molecular Cell,* 62 (4): 586-602.

240. Umareddy I, Tang KF, Vasudevan SG, Devi S, Hibberd ML, Gu F (2008) Dengue virus regulates type I interferon signalling in a strain-dependent manner in human cell lines. *Journal of General Virology,* 89 (12): 3052-62.

241. Valmas C, Grosch MN, Schümann M, Olejnik J, Martinez O, Best SM, Krähling V, Basler CF, Mühlberger E (2010) Marburg virus evades interferon responses by a mechanism distinct from ebola virus. *PLoS Pathogens,* 6 (1): e1000721.

242. van den Berg TP, Eterradossi N, Toquin D, Meulemans G (2000) Infectious bursal disease (Gumboro disease). *Revue Scientifique et Technique*, 19 (2): 509-43.

243. van den Berg TP, Gonze M, Meulemans G (1991) Acute infectious bursal disease in poultry: protection afforded by maternally derived antibodies and interference with live vaccination. *Avian Pathology,* 20 (3): 409-21.

244. van Loon AA, de Haas N, Zeyda I, Mundt E (2002) Alteration of amino acids in VP2 of very virulent infectious bursal disease virus results in tissue culture adaptation and attenuation in chickens. *Journal of General Virology,* 83 (1): 121-9.

245. Vandesompele J, De Preter K, Pattyn F, Poppe B, Van Roy N, De Paepe A, Speleman F (2002) Accurate normalization of real-time quantitative RT-PCR data by geometric averaging of multiple internal control genes. *Genome Biology,* 3 (7): research0034.1-0034.11

246. Verhelst J, Parthoens E, Schepens B, Fiers W, Saelens X (2012) Interferon-inducible protein Mx1 inhibits influenza virus by interfering with functional viral ribonucleoprotein complex assembly. *Journal in Virology,* 86 (24): 13445-55.

247. Vidy A, Chelbi-Alix M, Blondel D (2005) Rabies virus P protein interacts with STAT1 and inhibits interferon signal transduction pathways. *Journal of Virology,* 79 (22): 14411-20.

248. Vincze T, Posfai J, Roberts RJ (2003) NEBcutter: a program to cleave DNA with restriction enzymes. *Nucleic Acids Research,* 31 (13): 3688-91.

249. Wang D, Fang L, Shi Y, Zhang H, Gao L, Peng G, Chen H, Li K, Xiao S (2015a) Porcine Epidemic Diarrhea Virus 3C-Like Protease Regulates Its Interferon Antagonism by Cleaving NEMO. 90 (4): 2090-101.

250. Wang D, Zhou X, She R, Xiong J, Sun Q, Peng K, Liu L, Liu Y (2009a) Impaired intestinal mucosal immunity in specific-pathogen-free chickens after infection with very virulent infectious bursal disease virus. *Poultry Science,* 88 (8): 1623-8.

251. Wang N, Zhang L, Chen Y, Lu Z, Gao L, Wang Y, Gao Y, Gao H, Cui H, Li K, Liu C, Zhang Y, Qi X, Wang X (2015b) Cyclophilin A Interacts with Viral VP4 and Inhibits and Replication of Infectious Bursal Disease Virus. *Biomedical Research International,* 719454.

252. Wang Y, Wu X, Li H, Wu Y, Shi L, Zheng X, Luo M, Yan Y, Zhou J (2009b) Antibody to VP4 protein is an indicator discriminating pathogenic and nonpathogenic IBDV infection. *Molecular Immunology,* 46 (10): 1964-9.

253. Wark K. 'Expression and processing of infectious bursal diseases virus proteins'. PhD Thesis, University of Hertfordshire; 2000.

254. Wei L, Hou L, Zhu S, Wang J, Zhou J, Liu J (2011) Infectious bursal disease virus activates the phosphatidylinositol 3-kinase (PI3K)/ Akt signalling pathway by interaction of VP5 protein with the p85alpha subunit of PI3K. *Virology,* 417 (1): 211-20.

255. Whitfill CE, Haddad EE, Ricks CA, Skeeles JK, Newberry LA, Beasley JN, Andrews PD, Thoma JA, Wakenell PS (1995) Determination of optimum formulation of a novel infectious bursal disease virus (IBDV) vaccine constructed by mixing bursal disease antibody with IBDV. *Avian Diseases,* 39 (4): 687-99.

256. Wong RT, Hon CC, Zeng F, Leung FC (2007) Screening of differentially expressed transcripts in infectious bursal disease virus-induced apoptotic chicken embryonic fibroblasts by using cDNA microarrays. *Journal of General Virology,* 88 (6): 1785-96.

257. Wu HJ, Bondada S (2009) CD72, a coreceptor with both positive and negative effects on B lymphocyte development and function. *Journal of Clinical Immunology,* 29 (1): 12-21.

258. Xie J, Wang M, Cheng A, Zhao XX, Liu M, Zhu D, Chen S, Jia R, Yang Q, Wu Y, Zhang S, Liu Y, Yu Y, Zhang L, Chen X (2019) DAHV-1 inhibits type I interferon signalling to assist viral adaption by increasing the expression of SOCS3. *Frontiers in Immunology,* 10:731.

259. Xu J, Tang S, Yin B, Sun J, Bao E (2018) Co-enzyme Q10 upregulates Hsp70 and protects chicken primary myocardial cells under *in vitro* heat stress via PKC/MAPK. *Molecular and Cellular Biochemistry,* 449 (1-2): 195-206.

260. Xu L, Wang W, Peppenlenbosch MP, Pan Q (2017) Noncanonical antiviral mechanisms of ISGs: Dispensability of inducible interferons. *Trends in Immunology,* 38 (1):1-2.

261. Yamaguchi T, Ogawa M, Inoshima Y, Miyoshi M, Fukushi H, Hirai K (1996) Identification of sequence changes responsible for the attenuation of highly virulent infectious bursal disease virus. *Virology*, 223 (1): 219-23.

262. Yamamoto M, Sato S, Hemmi H, Hoshino K, Kaisho T, Sanjo H, Takeuchi O, Sugiyama M, Okabe M, Takeda K, Akira S (2003) Role of Adaptor TRIF in the DyD88-Independent Toll-Like Receptor Signaling Pathway. *Science,* 301 (5633): 640-43.

263. Yang X, Chen X, Bian G, Tu J, Xing Y, Wang Y, Chen Z (2014) Proteolytic processing, deubiquitinase and interferon antagonist activities of Middle East respiratory syndrome coronavirus papain-like protease. *Journal of General Virology,* 95 (3): 614-26.

264. Yao K, Goodwin MA, Vakharia VN (1998) Generation of a mutant infectious bursal disease virus that does not cause bursal lesions. *Journal of Virology,* 72 (4): 2647-54.

265. Yasmin AR, Yeap SK, Tan SW, Hair-Bejo M, Fakurazi S, Kaiser P, Omar AR (2015) *In vitro* characterization of chicken bone marrow-derived dendritic cells following infection with very virulent infectious bursal disease virus. *Avian Pathology,* 44 (6): 452-62.

266. Yasukawa H, Misawa H, Sakamoto H, Masuhara M, Sasaki A, Wakioka T, Ohtsuka S, Imaizumi T, Matsuda T, Ihle JN, Yoshimura A (1999) The JAK-binding protein JAB inhibits Januse tyrosine kinase activity through binding in the activation loop. *EMBO Journal,* 18 (5): 1309-20.

267. Ye C, Han X, Yu Z, Zhang E, Wang L, Liu H (2017) Infectious bursal disease virus activates c-Src to promote 4 1 integrin-dependent viral entry by modulating the downstream Akt-RhoA GTPase-actin rearrangement cascade. *Journal of Virology,* 91 (3): e01891-16.

268. Ye C, Jia L, Sun Y, Hu B, Wang L, Lu X, Zhou J (2014) Inhibition of antiviral innate immunity by birnavirus VP3 protein via blockage of viral double-stranded RNA binding to the host cytoplasmic RNA detector MDA5. *Journal of Virology,* 88 (19): 11154-65.

269. Ye C, Yu Z, Xiong Y, Wang Y, Ruan Y, Guo Y, Chen M, Luan S, Zhang E, Liu H (2019) STAU1 binds to IBDV genomic double-stranded RNA and promotes viral replication via attenuation of MDA5-dependent β interferon induction. *FASB Journal,* 33 (1): 286-300.

270. Yu F, Ren X, Wang Y, Qi X, Song J, Gao Y, Qin L, Gao H, Wang X (2013) A single amino acid V4I substitution in VP1 attenuates virulence of very virulent infectious bursal disease virus (vvIBDV) in SPF chickens and increase replication in CEF cells. *Virology,* 440 (2): 204-9.

271. Yu X, Rui L, Shao Q, Liu H, Lu Y, Zhang Y, Li Z (2015) Change of CD4+CD25+ cells ratio in immune organs from chickens challenged with infectious bursal disease virus strains with varying virulence. *Viruses,* 7 (3): 1357-72.

272. Yu Y, Cheng L, Li L, Zhang Y, Wang Q, Ou C, Xu Z, Wang Y, Ma J (2019) Effects of IBDV infection on expression of chTLRs in chicken bursa. *Microbial Pathogenesis,* 135: 103632.

273. Zhang B, Liu X, Chen W, Chen L (2013) IFIT5 potentiates anti-viral response through enhancing innate immune signalling pathways. *Acta Biochemica Biophysica Sinica,* 45 (10): 867-74.

274. Zhang D, Su C, Zheng C (2016) Herpes Simplex Virus 1 Serine Protease VP24 Blocks the DNA-Sensing Signal Pathway by Abrogating Activation of Interferon Regulatory Factor 3. *Journal of Virology,* 90 (12): 5824-9.

275. Zhang L, Li P, Liu R, Zheng M, Sun Y, Wu D, Hu Y, Wen J, Zhao G (2015) The identification of loci for immune traits in chickens using a genome-wide association study. *PLoS One,* 10 (3): e0117269.

276. Zhang MF, Huang GM, Qiao S (2002) Early stages of infectious bursal disease virus infection in chickens detected by in situ reverse transcriptase-polymerase chain reaction. *Avian Pathology,* 31 (6): 593-7.

277. Zhang Y, Yu Y, Ou C, Ma J, Wang Q, Du S, Xu Z, Li R, Guo F (2019) Alleviation of infectious-bursal-disease-virus-induced bursal injury by betaine is associated with DNA methylation in IL-6 and interferon regulatory factor 7 promoter. *Poultry Science,* pez280.

278. Zhao S, Jia Y, Han D, Ma H, Shah SZ, Ma Y, Teng K (2016) Influence of the structural development of bursa on the susceptibility of chickens to infectious bursal disease virus. *Poultry Science,* 95 (12): 2786-94.

279. Zheng C, Zheng Z, Zhang Z, Meng J, Liu Y, Ke X, Hu Q, Wang H (2015a) IFIT5 positively regulates NF-κB signalling through synergizing the recruitment of IκB kinase (IKK) to TGF-β-activated kinase 1 (TAK1). *Cell Signalling,* 27 (12): 2343-54.

280. Zheng X, Jia L, Hu B, Sun Y, Zhang Y, Gao X, Deng T, Bao S, Xu L, Zhou J (2015b) The C-terminal amyloidogenic peptide contributes to self assembly of Avibirnavirus viral protease. *Scientific Reports,* 5: 14794.

281. Zierenberg K, Raue R, Nieper H, Islam MR, Eterradossi N, Toquin D, Müller H (2004) Generation of serotype 1/serotype 2 reassortant viruses of the infectious bursal disease virus and their investigation *in vitro* and *in vivo*. *Virus Research,* 105 (1): 23-34.

282. Zou H, Su R, Ruan J, Shao H, Wian K, Ye J, Yao Y, Nair V, Qin A (2017) Double-stranded RNA induces chicken T-cell lymphoma apoptosis by TRIF and NF-κB. *Scientific Reports,* 7 (1): 7547.

8. Appendices

Appendix A: Clinical sign scoring system used to assess pathogenicity of IBDV strains *in vivo.*

(E) indicates the bird should be euthanized immediately.

Appearance:
This is done by accumulative scoring.

Normal appearance	0
Pale comb / watties	+1
Fluffed out feathers	+1
Eyes half shut	+1
Drooping wings / hunched / hangs head	+1
Laboured breathing	+1

Behaviour without provocation:
Select the score suited to the individual being assessed.

Normal posture	0
Crowds with group, but alert and social interactions with other birds evident, efforts made to seek water / feed in an independent manner.	1
Crowds within group, but lacking signs of normal social interaction / looking depressed, no efforts made to seek water / feed in an independent manner	2
Stands alone, depressed and no normal social interaction or independent action	3
Laid down alone, depressed and no normal social interaction or independent action	4
Collapsed with clear signs of severe distress	5 (E)

Provoked behaviour:
Select the score suited to the individual being assessed.

Normal (escapes capture by running)	0
Normal posture and attempts to avoid capture (escape attempted by walking)	1
Weak response to capture	2
No attempt to avoid capture but struggles when picked up	3
No attempt to avoid capture and lethargic when picked up	4
Fails to move when provoked	5 (E)

Handling:
This is done by accumulative scoring.

Feels normal	0
Fails to gain weight	+1
Evidence of weight loss	+1
Crop filled with water	+1
Soiled vent with classic white faecal material	+1

- Infected birds must be checked and weighed twice daily from the onset of clinical signs until after the infection has cleared and no more clinical signs are present. When no clinical signs are present, the birds can be checked once daily.
- Birds scoring 8-11 are classed as having moderate disease and must be checked every 8 hours
- Birds scoring 12-17 are classed as having have severe disease and must be checked every 3 hours
- Birds scoring 17 or E must be humanely culled.
- Birds scoring 12 for 3 days must be humanely culled.

-The End-